The CO2CRC Otway stage 2B residual saturation and dissolution test: test concept, implementation and data collected

Milestone report to ANLEC 2011

L. Paterson, C. Boreham, M. Bunch, J. Ennis-King, B. Freifeld,
R. Haese, C. Jenkins, M. Raab, R. Singh and L. Stalker

October 2011 | CO2CRC Report No: RPT11-3158

REPORT

STUDIES IN CCS

CO2CRC PARTICIPANTS

Core Research Participants

CSIRO
Curtin University
Geoscience Australia
GNS Science
Monash University
Simon Fraser University
University of Adelaide
University of Melbourne
University of New South Wales
University of Western Australia

Industry & Government Participants

Anglo American
ANLEC R&D
BG Group
BHP Billiton
BP Developments Australia
Brown Coal Innovation Australia
Chevron
Dept. of Primary Industries - Victoria
Ministry of Science and Innovation
INPEX
KIGAM
NSW Government Dept. Industry & Investment
Queensland Energy Resources Ltd
Queensland Government
Rio Tinto
SASOL
Shell
Solid Energy
Stanwell Corporation
Schlumberger
Total
Western Australia Dept. of Mines and Petroleum
Xstrata Coal

Supporting Participants

CANSYD Australia
Charles Darwin University
Government of South Australia
Lawrence Berkeley National Laboratory
Process Group
The Global CCS Institute
University of Queensland

An Australian Government Initiative

The CO2CRC Otway stage 2B residual saturation and dissolution test: test concept, implementation and data collected

Milestone report to ANLEC 2011

L. Paterson, C. Boreham, M. Bunch, J. Ennis-King, B. Freifeld, R. Haese, C. Jenkins, M. Raab, R. Singh and L. Stalker

October 2011

CO2CRC Report No: RPT11-3158

Acknowledgements

The authors wish to acknowledge financial assistance provided through Australian National Low Emissions Coal Research and Development (ANLEC R&D). ANLEC R&D is supported by Australian Coal Association Low Emissions Technology Limited and The Australian Government through the Clean Energy Initiative. We thank Rob Heath and Sandeep Sharma for providing a review of this report.

Cooperative Research Centre for Greenhouse Gas Technologies (CO2CRC)

GPO Box 463
14 – 16 Brisbane Avenue
Barton, Canberra, ACT
Phone: +61 2 6120 1600
Fax: +61 2 6273 7181
Email: info@co2crc.com.au
Web: www.co2crc.com.au

Reference: **L. Paterson, C. Boreham, M. Bunch, J. Ennis-King, B. Freifeld, R. Haese, C. Jenkins, M. Raab, R. Singh and L. Stalker**, 2011. *The CO2CRC Otway stage 2B residual saturation and dissolution test - Report to ANLEC 2011*. Cooperative Research Centre for Greenhouse Gas Technologies, Canberra, Australia, CO2CRC Publication Number: RPT11-3158. 68pp.

Table of contents

Table of figures

Tables

Executive summary

This report provides an account of the Otway Stage 2B residual saturation and dissolution test. This is the first field test of this nature in the world and its execution and summary of the data obtained from the field test are reported here.

Residual trapping can immobilise carbon dioxide within a reservoir preventing buoyant migration where structural traps are absent or if seal integrity is lost. Even for storage sites that are based on secure structural trapping, potentially a large component of the carbon dioxide can be retained by residual trapping. Hence estimation of the amount of residual trapping is a very important consideration in storage site evaluation. With this in mind, the goal of the CO2CRC Otway Stage 2B project was to measure large-scale residual trapping of CO_2 in an actual field project using five different methods, compare the methods and make recommendations. It was realised during design that substantial information would be collected on dissolution trapping also allowing for analysis of this mechanism.

Following a lengthy design period, the field test program for Stage 2B of the CO2CRC Otway Project commenced on 17 June 2011 and finished on 12 September 2011. All the planned components of the field test were completed including the five methods for measuring residual trapping. Extensive high quality data has been obtained throughout the program that allows detailed analysis within each method. The responses at each stage show that the injected CO_2 was driven to residual saturation and was detected by each of the five measurement methods.

In particular, the conclusions can be summarised as follows:

1. Excellent quality downhole pressure data were acquired throughout the field program from the permanent gauges. The high permeability of the injection interval did not cause problems with getting a sufficient pressure response to give a good signal to noise ratio.
2. Excellent downhole temperature data were also acquired. The instantaneous readout of downhole temperatures proved extremely useful in diagnosing operational issues at several stages.
3. All three RST logs were run as intended. Current interpretation has residual CO_2 saturation around 0.18 in the lower half of the perforated interval and around 0.23 (average) in the upper half.
4. Fluid sampling using the U-tubes was completed consistent with the test plan. The noble and organic tracers were added to the injection stream as planned and were measured during production stages at concentrations were more than sufficient for analysis.
5. The organic tracer test shows the partial breakdown of the three parent compounds as hoped.
6. Sampling for the dissolution test including the added methanol was performed as intended.
7. Although not primary objectives of Stage 2B, the test sequence provided the opportunity to further test microseismic monitoring and provide controlled releases of CO_2 for atmospheric monitoring.

Detailed analysis of the five tests is planned to be completed by July 2012, with reports on individual elements becoming available in the interim. Nevertheless at this time we can conclude from the test program that it is possible to implement all of the methods in practice and each method can give useful information in an appropriate context.

Objective

The CO2CRC Otway stage 2B project was undertaken to verify and quantify the residual and dissolution trapping mechanisms for injected CO_2 in an aquifer in the absence of an apparent structural closure. Injectivity, migration and containment of the CO_2 plume are controlled by relative permeability, permeability heterogeneity and anisotropy of the reservoir system. At the CO2CRC Otway site a planned test sequence was conducted to determine the residual gas saturation of CO_2 in the vicinity of CRC-2 drilled in February 2010. The chosen storage target is a reservoir interval within the Paaratte Formation, a lithologically heterogeneous deltaic succession typical of many prospective geological systems under consideration for future commercial-scale CO_2 storage.

Completion of the following were specified to define a successful test:

- Measurement of residual trapping, S_{gr}, by five independent techniques in the test (numbering indicates priority):
    1. History matching injection and production pressures and flow rates by developing a two-phase relative permeability test in a well, based on Zhang et al. (2011);
    2. Measure hydrogen index using a pulsed neutron log (RST);
    3. Measure the thermal conductivity of fluids in the formation by thermal logging;
    4. Reactive ester tracer partitioning according to residual saturation, based on the Tomich et al. (1973) method for residual oil;
    5. A dissolution test, based on the Bragg et al. (1976) method for residual gas (methane);
- Comparison of field and lab results;
- An assessment and evaluation of the uncertainties around the above determinations.

Introduction

Key risks for commercial-scale projects include uncertainties regarding storage capacity and CO_2 containment. The CO2CRC Otway stage 2B project addresses both these risks and also provides the basis for a cost-effective aquifer appraisal process.

Residual capillary trapping and dissolution trapping are important mechanisms in geological storage because they provide for secure containment without necessarily the need for an overlying seal rock according to the IPCC special report on carbon dioxide capture and storage (2005), (Figure 1). Residual gas saturation (the fraction of the pore space in which the non-wetting phase is trapped) is related to the CO_2-water relative permeability curve. The relative permeability of the reservoir therefore plays a dominant role in determining the migration distances and migration rates of injected carbon dioxide plumes. Dissolution trapping refers to the portion of CO_2 that dissolves into formation water.

The distribution of CO_2-water relative permeability and the degree of residual and dissolution trapping are major uncertainties in the development of carbon dioxide storage sites within aquifers; often the single greatest uncertainty in commercial CCS projects. There has been particular emphasis in recent years on the nature of relative permeability hysteresis and the role it plays in storing CO_2 by residual saturation trapping. This phenomenon can be exploited to increase trapping by co-injecting brine with carbon dioxide, or by injecting chase brine after the carbon dioxide. This affects both the amount of residual trapping and the rate of CO_2 dissolution into formation brine. The possibilities raised by these injection strategies make it imperative to obtain a reliable characterisation of relative permeability behaviour at sites being considered for underground storage within aquifers.

It is difficult to obtain core samples suitable for the laboratory determination of relative permeability. Samples are often oriented (are long enough) in the vertical direction whereas relative permeability measurements are also required in the horizontal direction. Even then, laboratory results from cores only represent a small part of the reservoir and may not be representative of larger scale heterogeneities and facies transitions.

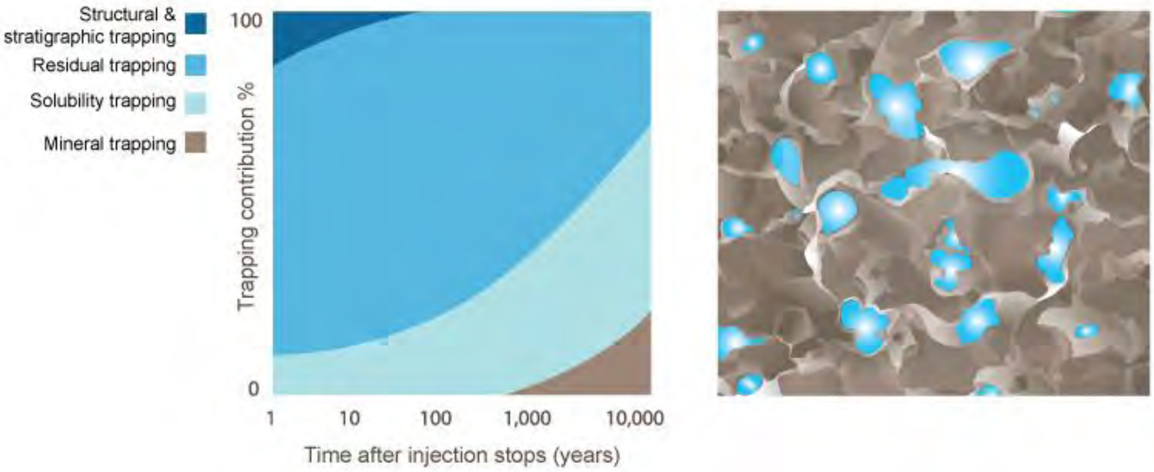

Figure 1. Trapping mechanisms of CO_2 (left). Concept of residual gas or capillary trapping of CO_2 (right).

There is great value in conducting a short-term test in the vicinity of an injection well prior to large-scale injection to obtain reliable estimates of reservoir-scale residual saturation that can be used to estimate reservoir-scale CO_2-water relative permeability, reducing risk and uncertainty in the modelled performance of a potential carbon dioxide storage site and thereby enhancing the “bankability” of a commercial project at an early stage.

Test concept

The Otway Stage 2B test was conceived around a single-well test that could be applied at commercial sites to reduce uncertainty in estimating large-scale residual trapping. Several methods already exist for single-well measurements of residual oil and non-aqueous phase liquids (NAPL-essentially petroleum contamination) but these have not yet been applied in the context of carbon dioxide. Carbon dioxide presents some particular challenges, mainly due to carbon dioxide’s high solubility compared to petroleum. Furthermore, the CO_2 residual saturation has to be established prior to measurement. For residual oil, the original oil in place commences with an accumulation that has stabilised under gravity whereas this is not the case for most situations with carbon dioxide. For the reasons there is value in comparing multiple approaches, especially when the incremental cost of each testing addition method is relatively minor. As a research site, the CO2CRC Otway site presents an ideal opportunity to test a variety of methods.

The methods for measuring residual saturation are listed below.

1. Pressure test (or hydraulic test). Essentially this is a multi-phase well test where numerical simulation is used to inverse model the reservoir response to derive the residual saturation. This method is described in detail in Zhang et al (2011). Further development of analytical methods may allow a formula to be derived and used similar to conventional well testing.
2. Measuring the hydrogen index using a pulsed neutron log (RST). Commercial RST logging is an established practice although experience with CO_2 is limited. The major drawback is that the pulsed neutron capture tool only penetrates about 20 cm, so this method samples the smallest volume of all the methods.
3. Thermal test. In the thermal test the borehole is heated and temperature is recorded using a fibre-optic distributed temperature sensor (DTS). The depth of penetration into the formation is 1-2 m, significantly greater than the pulsed neutron logging (Zhang et al 2011).
4. Organic tracer test. Organic reactive tracers have been used to measure residual oil (Tomich et. al 1973), however the reaction involving ethyl acetate that works for oil will not work with carbon dioxide. The application of this test requires identification of new tracers that perform the same role. Three tracers were identified and used in Otway Stage 2B. The lack of prior experience with these tracers means that there is a strong research component to this test.
5. Dissolution test. This test is based on a method for residual oil described by Bragg et al (1976). It is a relatively simple test involving the injection of water, dissolving residual fluid, and producing the water back to measure the dissolved fluid. It was easy to implement at Otway because of the stored water at the surface and the installed downhole fluid sampling. The downside of the test is that, unlike the other tests, it reduces the residual fluid removing the possibility of further testing.

Injection target

The formation top of the Paaratte Formation succession occurs at [1]1123 m MD (1119 m below ground level) and bottom at 1520 m MD (1516 m below ground level). The Paaratte formation well composite is displayed at the Appendix, showing well-log porosity, permeability, core porosity and lithology characterisation in terms of depositional-diagenetic facies associations (Figure 60).

Following core and well log interpretation, five potential CO_2 storage systems were identified within the lower part of the Paaratte Formation (1440 - 1520 m MD) formerly referred to as Zone 1. These five storage systems, labelled as options A to E, were assessed for homogeneity in the reservoir (injection) interval and sealing capability of any non-reservoir layers immediately above them (Figure 2).

The deepest option (Option A) has no sealing layer. This effect would make the test more difficult to interpret owing to likely vertical pressure communication and migration of CO_2. The aim is to reduce unknown effects on fluid movement in vertical and lateral directions due to the ratio of vertical and horizontal permeability, (k_v/k_h). A good sealing caprock is preferred to isolate the CO_2 plume migration so that it remains within the reservoir interval only.

Option B (above Option A in Figure 2) contains cemented layers and variable porosity and permeability, which make the test interval more heterogeneous. This would introduce uncertainty on the pressure response, which will be difficult to differentiate from possibly vertical migration of the CO_2. However, MCIP test results show a high potential to retain CO_2 (Figure 3).

Option E has no confirmed capping interval. A relatively thick cemented layer centred on 1472 m MD demonstrated poor sealing capacity. The risk of vertical migration would introduce uncertainty into interpretation of the pressure response.

Like Option B, Option D contains a thin cemented interval and a mixture of reservoir lithofacies. A thin sealing interval centred on 1457.5 m MD is unproven and was interpreted from well logs alone as core was not cut between 1449 – 1460 m MD.

The reservoir interval of the shallowest option, Option C (near the top in Figure 2) is the most homogenous when compared with the other options. Porosity (average ~28 %) and permeability (average ~2196 md) values from logs and cores are high and relatively consistent. Option C has a cemented interval and a thick non-reservoir lithofacies interval above with a high sealing capacity for withholding supercritical CO_2 (Figure 3).

For these reasons Option C was chosen as the injection interval for the new residual gas saturation and dissolution test. **Option C** has since been perforated for the test within the depth range: **1440 – 1447 m MD** (1436 – 1443 m below ground level).

---

[1] Note on depths: Unless otherwise specified, depths quoted in this report are measured depths in the CRC-2 well (MD), so that the perforations are at 1440 m - 1447 m MD, 1392.1 m - 1399.1 m TVD SS (sub mean sea level), or 1436.1 m – 1443.1 m below the surface (ground level) to the nearest 0.1 m. The datum for CRC-2 is 47.9 m above MSL.

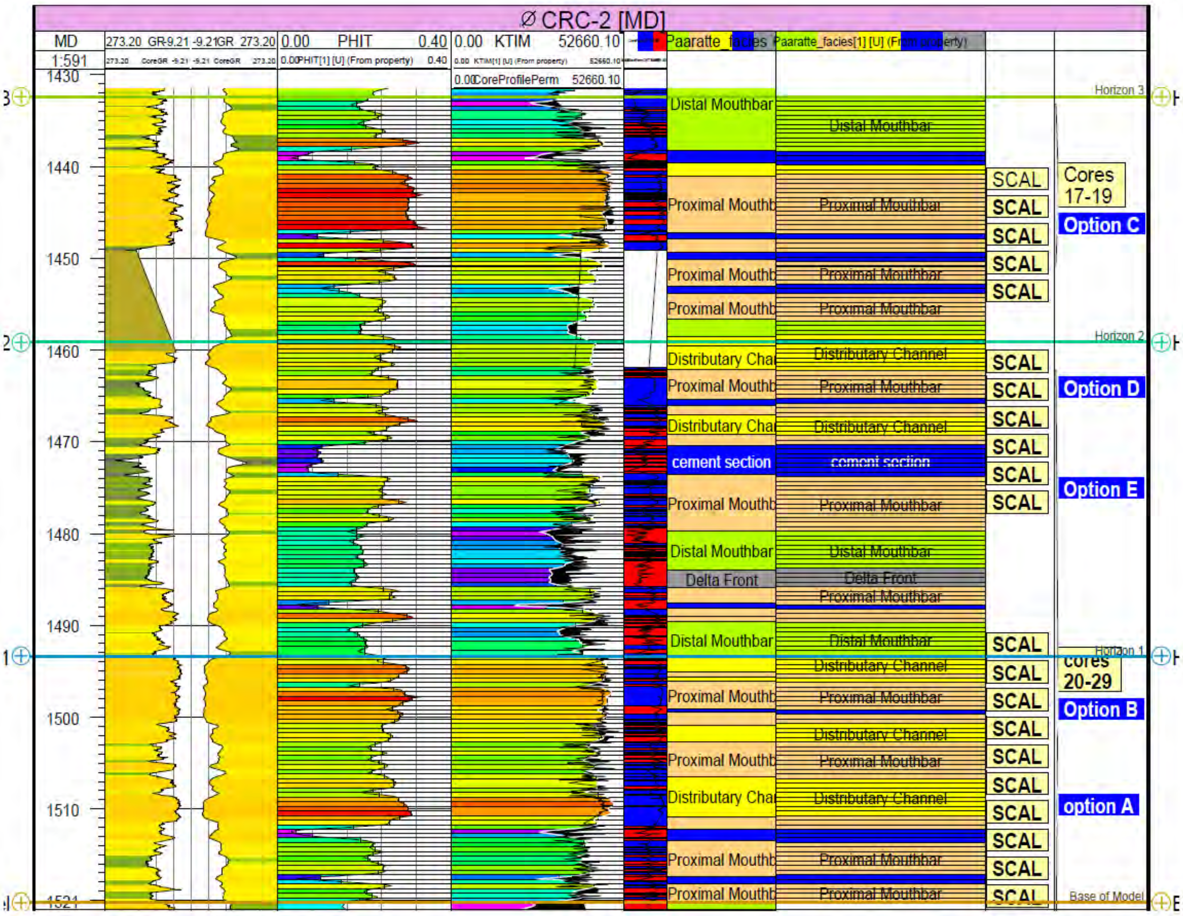

Figure 2. Log compilation of the lower part of the Paaratte formation. Division in 5 sections, labelled as option A to E.

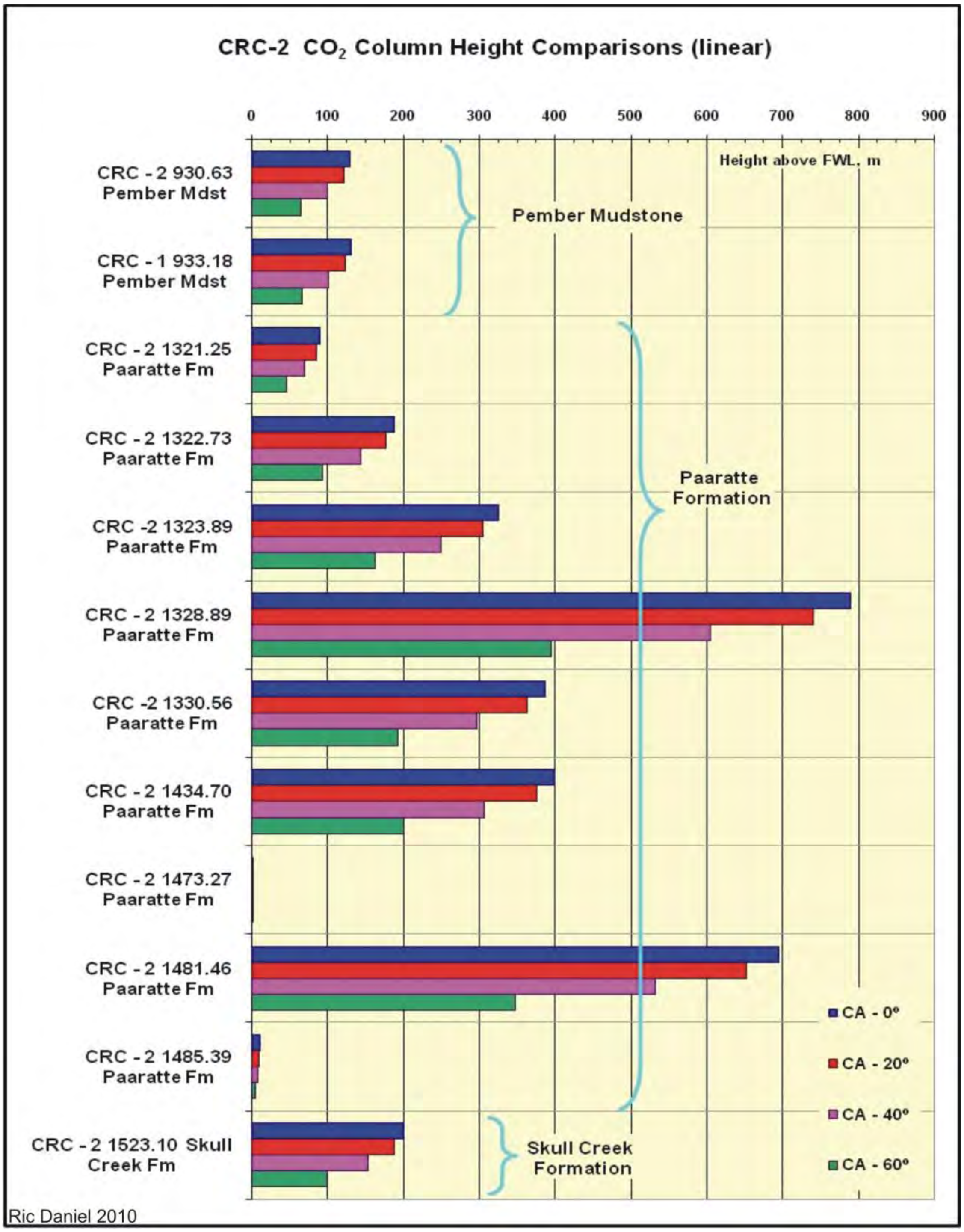

Figure 3. Seal Capacity column heights for CRC-2 top and intraformational seals priority samples from MCIP tests.

Downhole completion

The CRC-2 well is cased and 0.14 m (5½ inch) production casing runs from surface to the total depth of the well of 1565 m.

In the last two weeks of February 2011, the downhole completion was installed in the well after perforating the interval from 1440 to 1447 m (7m). The completion consists of a 2 3/8" Fox 13Cr80 tubing, an inflatable packer configuration, set to straddle the test zone and minimise the sump area, and several steel lines for gas lift, pressure gauges, Distributed Temperature Perturbation Sensor (DTPS), heating wire, and U-tube sampling (see Figure 5). Table 1 shows the various control lines at the wellhead. All lines are bare 316L stainless steel welded tubes. The seven steel lines housing the inline P/T gauge coax cables, DTS, heater lines, and U-tube samplers lines and packer inflate lines penetrate the top packer, which has been set at 1435.48 m. There are four real-time high-accuracy surface read-out P/T gauges on two TEC cables, U-tube, and DTPS measure fluid properties beneath the packer. The memory P/T gauge were located in X-nipples above the packer and below the gas lift mandrels in the tubing string, when required. The perforated interval is isolated from the bottom of the well by a lower packer set at 1449.55 m (see left diagram Figure 5).

Table 1. Control Lines in CRC-2 Completion

Control Line Description	Diameter	Termination Depth MD (m)
Packer inflate system	3/8“	1435 to below perforated interval
U-tube #1 and # 2	3/8“	1440
Gas injection mandrel	3/8“	846 with a 1/4“ orifice valve
Gas lift mandrel -	3/8“	996 with a 1/4“ orifice valve
DTS/heater	3/8“	1460
Panex TEC # 1	¼“	1439.8
Panex TEC # 2	¼“	1448.3

After the completion was installed, the well was flowed to retrieve a pristine formation sample for the baseline water geochemistry (salinity, type of dissolved solids, etc.) and microbial activity (original microbe content in formation water) of the Paaratte formation by swabbing. Preliminary analysis of the samples showed that the swabbing operation was not long enough and as such the completion fluid KCl brine and fluorescein was not fully retrieved. As the start of the water production phase the well was flowed till pristine formation water conditions were obtained, and this water was disposed of separately. Formation fluids from MDT sampling in CRC-2 also showed mud contamination (fluorescein). The perforated formation is at hydrostatic pressure and contains only formation water, the well will not flow by itself. To produce water, a gas lift method using Buttress gas was employed to lift the water column in CRC-2 via the casing annulus and up the 2 3/8" tubing. The Buttress gas entered the 2 3/8" tubing via an orifice valve located in the gas lift mandrel at 996.6m. The gas will lighten the water column in the well thus allowing flow to reach surface. The Buttress gas and water mixture from the gas lift was first flowed into a degassing tank where any excess gas that came out of solution was vented.

The well was initially flowed for 10 days, and subsequently for 3.4 days during the water reference test and 3.8 days at residual gas saturation to produce the injected tracers back to surface (see Table 2 and Figure 7).

Surface facilities were provided to catch the produced water on surface. A sampling protocol was established and the formation fluid contamination analysed in real-time via the U-tube while flowing the well. Some samples of pristine formation samples were taken using the U-tube system just at the perforation interval, while the fluid column was lifted to surface with the CO_2/CH_4 mixture from Buttress.

A second gas injection mandrel complete with a ¼” orifice valve located at 846m MD provided the inlet for pure CO_2 to be injected into the tubing for a later phase in the residual gas saturation test. The CO_2 was mixed with water for the “water injection with dissolved CO_2” activity after the pure CO_2 injection (day 46 to 49 in Phase 3 of 7). At 846 m the solubility of CO_2 into water is given according to Figure 4 at three different temperatures[2], assuming a hydrostatic pressure gradient that includes a pressure increase during injection, which is about 0.1 MPa for 1 Darcy rock, and about 1 MPa for 100 md rock. The distance from 846m to 1435 m was deemed adequate to dissolve the CO_2 before it reaches the perforated formation.

Four real-time P/T gauges and two retrievable memory gauges were located beneath the lower gas mandrel to confirm optimum mixing of CO_2 with water to prevent CO_2 under- or over-saturation (see right diagram Figure 5). The memory gauges were installed at 948 and 1095m MD and retrieved using Slickline. A set of mixing tables for water versus CO_2 rates were made available to the pump operator in order to ensure that the correct rate ratio was transmitted during injection.

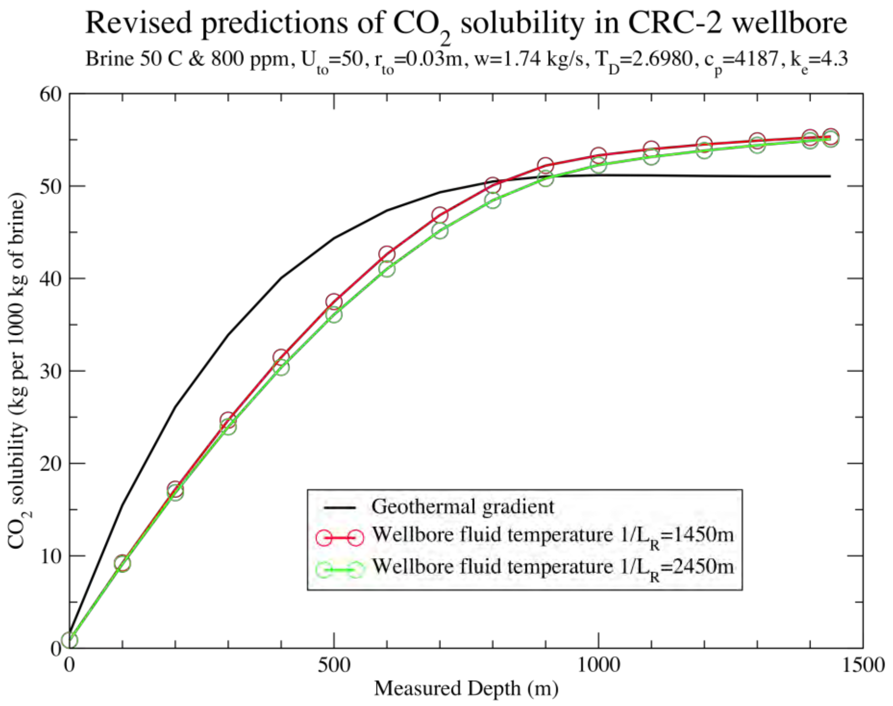

Figure 4. Solubility of CO_2 in water in the CRC-2 well.

---

[2] The first is in equilibrium with the geothermal gradient (an initial state, or at very low rates). The second assumes a steady state water injection over 5 days with the overall wellbore heat transfer coefficient set to 50 J/(s m^2 K) (a moderate to high value), giving a thermal equilibration length ($1/L_R$) of about 1000 m. The third case assumes a lower value of the overall wellbore heat transfer coefficient of 20 J/(s m^2 K).

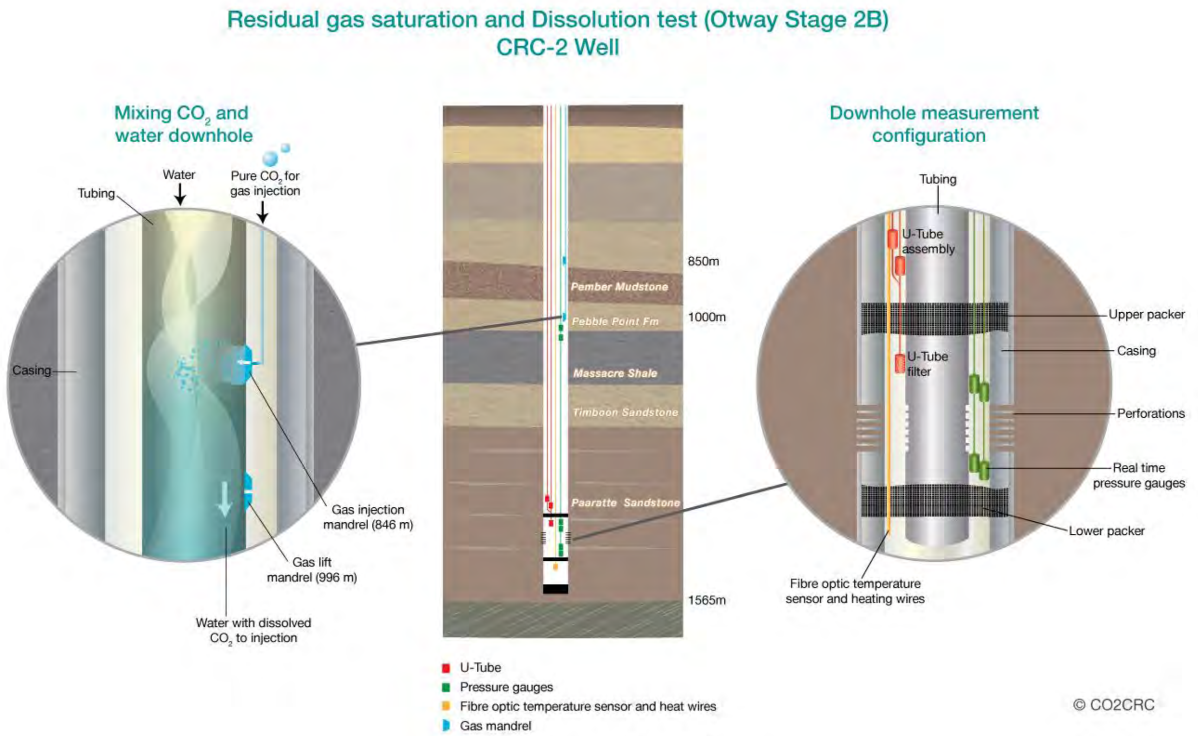

Figure 5. Downhole completion of CRC-2 for the residual gas saturation test. The diagram on the left shows the gas mandrel above the packer for mixing CO_2 and water downhole. The diagram on the right shows instruments below and above the packer.

Test sequence

The planned test sequence is shown in Figure 6, and the actual test sequence is shown in Figure 7. The main difference is due to operational delays, but otherwise all the activities in the original sequence were implemented. Following an initial water production phase, the residual gas saturation test sequence commenced on the 27th June 2011 and lasted for 76 days (see Figure 7 and Table 2). The initial water production phase comprised 10 days of water production, where 505 tonnes of water was produced. Three surface tanks were installed to handle the water storage. Since the gas lift method was employed with Buttress gas (CO_2/CH_4 mixture) via the bottom gas mandrel mounted on the tubing at 1000 m depth, provisions were to be made to safely vent the CO_2 that is both in free phase and ex-solved from the water and the free-phase CH_4.

The water was treated to prevent microbial activity using an ultraviolet system. Microbes can potentially grow at re-injection into the formation and block the entry pore space at the Paaratte injection zone. The produced water production provided a measure of the bulk permeability of water in the Paaratte formation, derived by the pressure draw down that is recorded by downhole pressure gauge measurements.

A maximum of 590 tonnes (590,000 litres) of formation water was produced from the reservoir. At various stages, portions of this water volume were reinjected and re-produced as shown in Figure 7. In total there was 1003 tonnes of pumping, both in and out. After the initial surface stock of 505 tonnes was established in Phase 1, 104 tonnes was injected in Phase 2 followed by 190 tonnes of production. This took the stored surface volume up to the maximum inventory of 590 tonnes.

In Phase 3, the largest water injection period (454 tonnes) was used to drive the CO_2 to residual saturation where the pressure should reach steady state. The remaining phases had four periods of production (104 t, 6 t, 75 t and 251 t final disposal) and three periods of production (182 t, 24 t and 131 t).

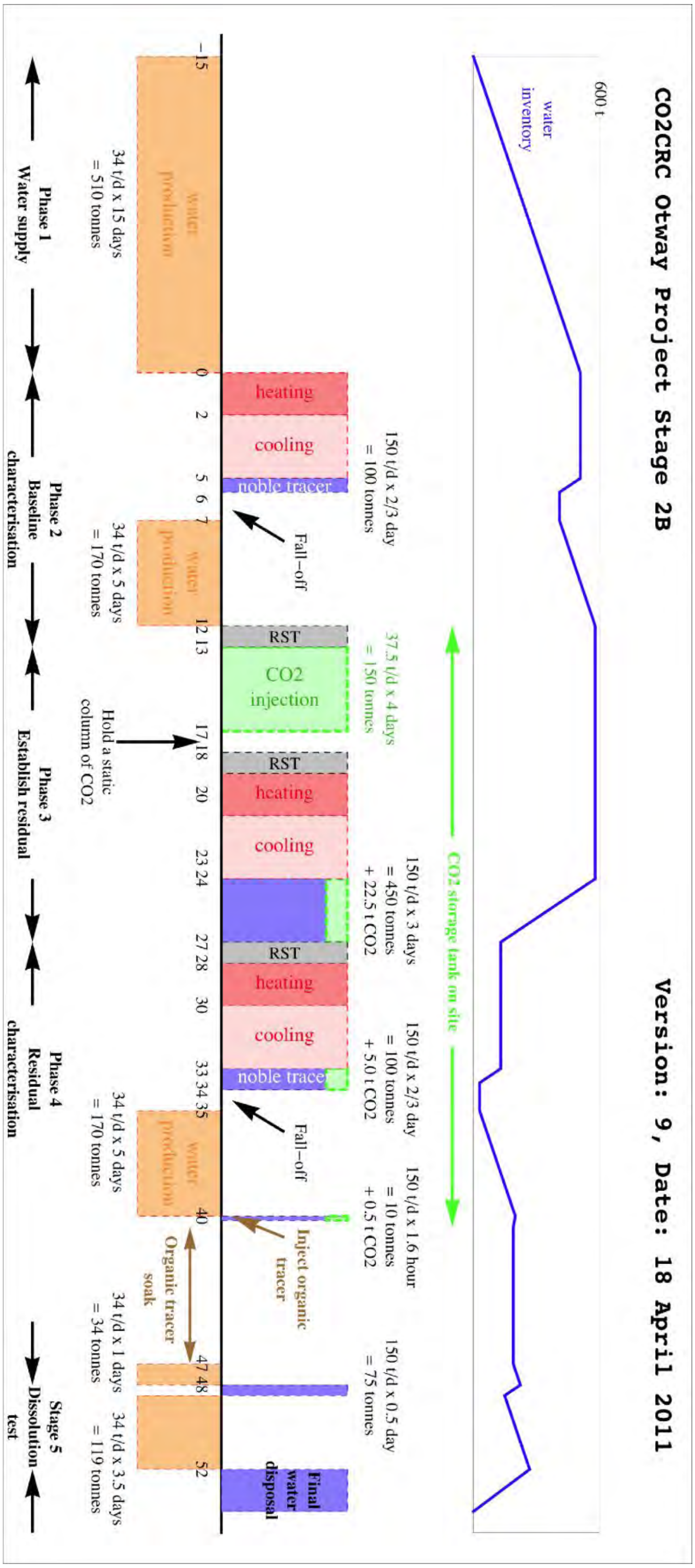

Figure 6. Planned residual gas saturation test sequence, 18 April 2011, prior to the field test.

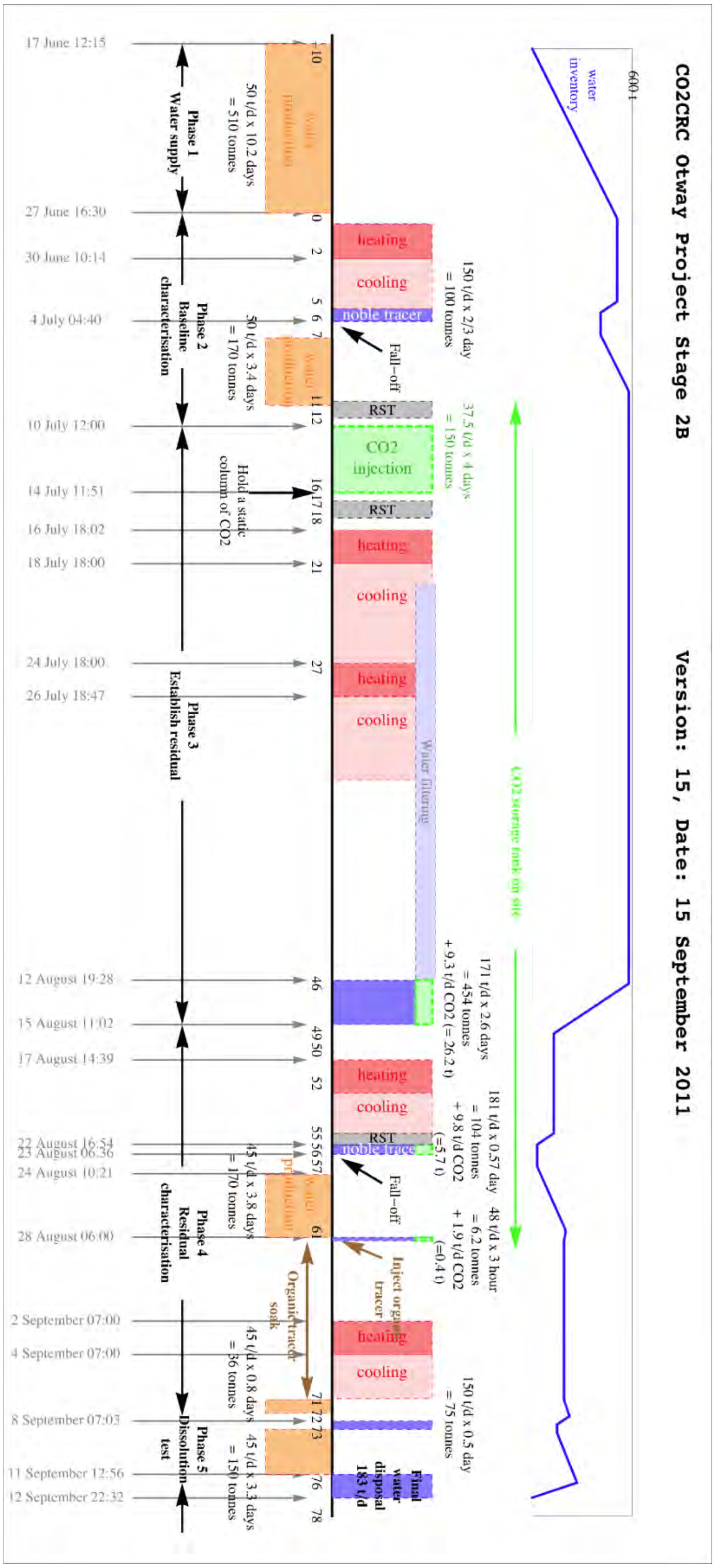

Figure 7. Actual residual gas saturation test sequence.

Phase 2 consisted of the baseline response tests when the system is in initial condition and water saturated (Figure 7). It began with the operation of the distributed thermal perturbation sensor (DTPS) to produce baseline thermal conductivity estimates. The formation was heated above 2°C of formation temperature within two days. The temperature fall off was recorded over a period of 3 days. During that period borehole remained unperturbed, no tools were to enter the well. The water saturated reference test was also conducted with tracers (krypton and xenon). This involved co-injecting 104 tonnes of water with 1200 litres of noble gases. They were injected at 5.0 l/min, 600 l of Kr and 600 l of Xe, maintaining a Kr:Xe ratio of 1. The downhole pressure increase was recorded for a pressure-buildup well test interpretation. Surface installations were provided that facilitated co-injection of gaseous tracer material with the water. The tracers were introduced in a discrete pulse at the start of injection to focus and concentrate the front so that the breakthrough curve was at its most concentrated on its return. Subsequently, 190 tonnes of the injected water and tracers were back produced over 3.4 days and samples were analysed for tracer concentration. At the end of Phase 2 the well was logged with pulsed neutron measurement (RST) to establish the baseline at fully water-saturated conditions.

Phase 3 commenced with injecting 37.5 tonnes of CO_2/day over a period of 4 days for a total of 150 tonnes injected. Carbon dioxide was brought into the stream by direct injection into the 2 3/8" tubing. The expected extent of the plume and gas saturation is illustrated in Figure 8.

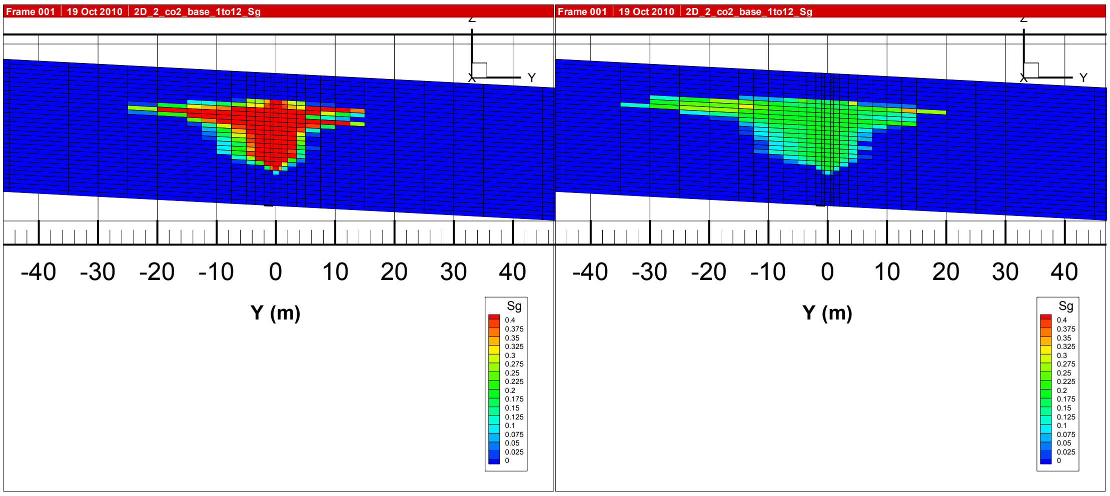

(a) (b)

Figure 8. Reservoir slice in dipping direction (2° dip) of contours of gas saturation (a) after gas injection and (b) after residual saturation (after drive to residual to S_{grmax}=20%).

The formation was left to equilibrate for 1 day. Another RST log was run in the well that showed CO_2 saturation close to the borehole averaged 30% in the lower part of the perforated interval and averaged 45% in the upper part. The DTPS measurement was then repeated, using changes of observed thermal conductivity as a proxy measurement for CO_2 saturation. Heating for 2 days followed by a quiescent cooling period of 3 days is used to measure thermal conductivity. After a delay, this was followed by an injection of 171 tonnes/day of water for 2.6 days at reservoir CO_2 saturation to drive the reservoir to residual gas saturation conditions. The pressure response and flow rate can be used to reconstruct the CO_2-water relative permeability curves based on the concepts of multiphase well testing. The relative permeability curve provides the residual gas saturation at zero gas mobility (see Figure 9), although this curve is for drainage (CO_2 displacing water) rather than imbibition (water displacing CO_2) and doesn't consider hysteresis.

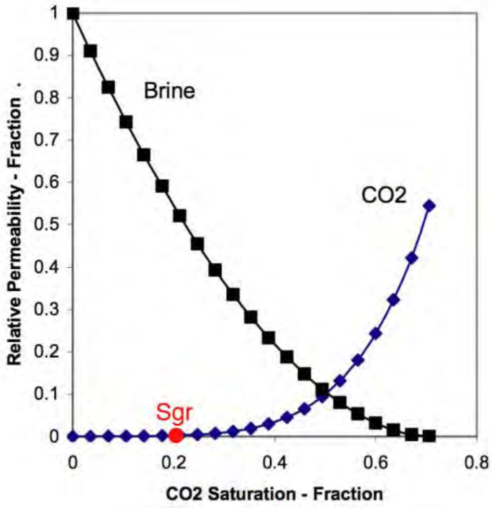

Figure 9. Relative permeability curve from Basal Cambrian sandstone drainage from tests by Bennion and Bachu (2005). S_{gr} = 20%

The injected water that drives the CO_2 to residual gas saturation was saturated with CO_2 to avoid dissolving the residual trapped CO_2. The water was mixed with pure CO_2 downhole, by pumping the CO_2 that had been vaporised and compressed through the upper gas injection mandrel at 846 m depth: 26.2 tonnes of CO_2 were used to saturate the 454 tonnes of water. Pressure was monitored throughout the CO_2 and CO_2-saturated water injection. The pressure response during the water injection period provided information about residual gas saturation for history matching with a flow simulator. Figure 10 shows the expected sensitivity of pressure to residual gas saturation, demonstrated for 10% and 20% S_{gr}. Note that the timeline of both plots, Figure 10 and Figure 11, only represents the CO_2 injection and subsequent creation of the residual gas saturation field.

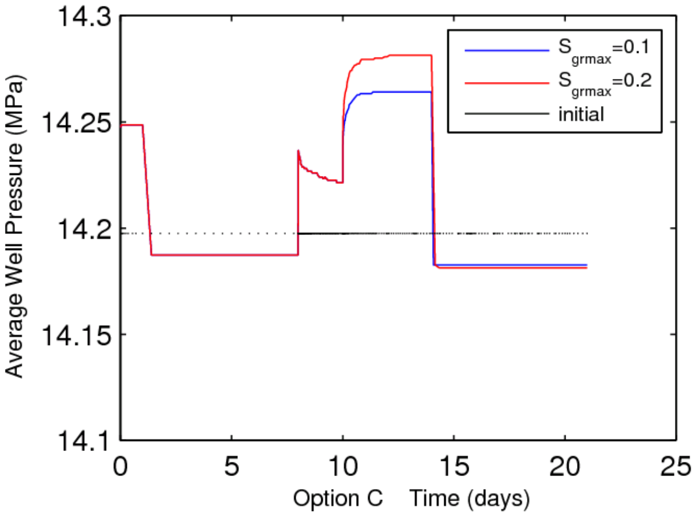

Figure 10. Pressure response and sensitivity to residual gas saturation.

Depending on the heterogeneity of the formation, the response will be more or less pronounced. This was tested and studied in several simulation runs (Figure 11).

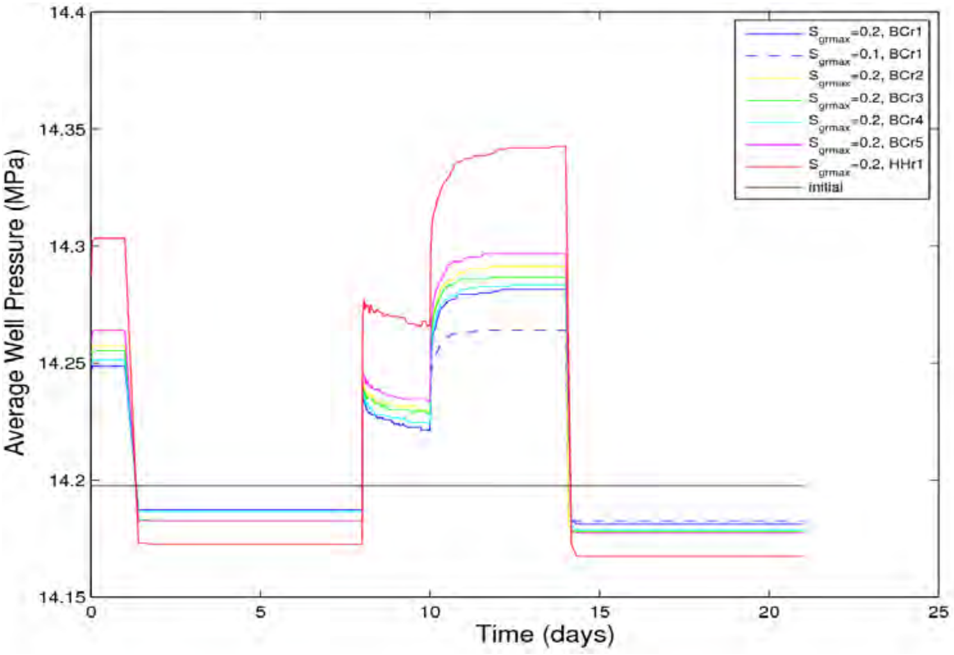

Figure 11. Pressure versus time for various geological models, BCr1 BCr2, BCr3, BCr3, BCr4, BCr5 , HHr1. Note 1: BC is base case heterogeneity HH is high heterogeneity (with shorter correlation length scale). Note 2: r1, r2 etc is realisation 1, 2, etc (which are all equally probably geological models).

After the creation of the residual gas field through water injection, the formation was left to equilibrate for one more day before thermal logging and the third and last RST log was run to establish an estimate of the residual gas saturation. The RST test can estimate the residual gas saturation close to the borehole, whereas the history matching interpretation of the residual gas saturation covers the extent of the CO_2 plume (~15 m radius). The combination of both history matching and RST provide complimentary information on the estimate of residual gas saturation.

Table 2. Injection and production amounts during the 5 phases of the residual saturation test

Description	Production	Injection
Initial water supply and pressure drawdown test	505 tonnes water.	
Noble tracer injection and Pressure Buildup test		104 tonnes water plus noble tracer.
Noble tracer analysis and additional water supply	190 tonnes water plus noble tracer.	
CO_2 injection		150 tonnes CO_2.
Water to push to residual saturation plus pressure response to analyse		454 tonnes water plus 26.2 tonnes CO_2 to prevent dissolution.
Noble tracer injection		104 tonnes water plus 5.4 tonnes CO_2 plus noble tracer.
Noble tracer analysis	182 tonnes water plus noble tracer.	
Organic tracer injection		12 kg of triacetin, 10 kg of propylene glycol diacetate and 8 kg of tripropionin by 8 tonnes water plus 0.3 tonnes CO_2.
Organic tracer analysis	23.7 tonnes water plus ester tracers and hydrolysis products.	
Dissolution test water		75 tonnes water without CO_2. Methanol was added in the water at a concentration of 1091 ppm.
Dissolution test analysis	131 tonnes water plus dissolved CO_2.	
Final water disposal		251 tonnes water.

A third DTPS data set was collected at the beginning of Phase 4 to further reduce the uncertainty of the residual gas saturation estimation. Six days after Phase 4 was commenced, the second tracer injection took place in an identical matter to Phase 2, where water is spiked with noble gas tracers, and saturated with CO_2. The noble gas tracers will partition according to the gas phase present, and the tracer recovered is inversely proportional to the gas saturation (residual gas saturation).

The reactive ester tracer partitioning test is based on the single-well tracer method to measure residual oil saturation described by Tomich, Dalton, Deans and Shallenberger (1973), except that different tracers were required for measuring residual carbon dioxide. Triacetin (12 kg) with formula $C_9H_{14}O_6$, tripropionin (8 kg) with formula $C_{12}H_{20}O_6$ and propylene glycol diacetate (10 kg) with formula $C_7H_{12}O_4$ are benign liquids (food grade products) and were added undiluted at the start of this section of testing followed by 6.2 tonnes of water saturated with 380 kg of CO_2 to prevent dissolution of the residual CO_2. The organic tracers were allowed to hydrolyse/soak for 10 days in the reservoir. Then 23.7 tonnes of water was produced and analysed for tracer composition and concentrations.

The last step was the dissolution test based on the Bragg-Shallenberger-Deans (1976) method described in SPE 6047. This involved injecting 75 tonnes of water, this time without any CO_2, and deliberately dissolving the residual CO_2. Approximately 78 litres of methanol was uniformly added to the injected water as a tracer (giving a concentration of 1091 ppm). Then 131 tonnes of this water was back produced from the formation and the CO_2 content was measured to calculate the residual saturation. Unlike the other methods this method dramatically alters the residual saturation hence was conducted last. CO_2 was brought back to surface in this final step. Provisions were made to safely vent the CO_2 that is both in free phase and ex-solved from the water.

Measurements

Instruments were installed downhole and at the surface. Table 3 lists the measurements and timing of those.

Table 3: Measurement types for formation fluid sampling and residual gas saturation test and timeline.

Surface	Measurement	Comments	Time
	Flow rate in	Rosemount 1700 series Coriolis flow meter for CO_2 injection. Rosemount 8732 Magnetic Flowmeter for water.	From day 15 onwards, with start of Phase 2
	Flow rate out	Rosemount 8732 Magnetic Flowmeter for water.	From day 1 of Phase 1
	Water Cut	No separator was required	From day 1 of Phase 1
	Wellhead pressure and temp at CRC-2	This was connected to the DCS providing a continuous record	From day 1 of Phase 1
Downhole	**Measurement**	**Comments**	**Time**
	Pressure and temperature (P/T)	Four (4) real-time surface read out Panex gauges across perforated interval.	Baseline recording for 2 days before day 1 of Phase 1, recording continuously until end of test. Realtime gauges were critical during the entire test.
	P/T in tubing	Two (2) Metrolog memory gauges below top gas mandrel and above top packer.	Memory gauges were only deployed when injecting water with saturated CO_2.

Downhole	Measurement	Comments	Time
	Formation gas & water & Tracer detection from test via U-tubes	At surface, sampling lab was installed at CRC-2 wellsite with LBNL mass spectrometer. GA Mobile field lab was equipped with 2 GC-MS wet chemistry equipment and DIC tester.	Baseline sampling for 2 days before day 1 of Phase 1 Sampling during back production in Phase 2, day 6 to 13, for tracers Sampling during CO_2 injection in Phase 3, day 14 to 18 Sampling during water with diss. CO_2 injection in Phase 3, day 24 to 27, to confirm mixing Sampling during back production in Phase 4, day 37 to 44, for tracers
	Distributed Thermal Perturbation Sensor (DTPS) and heating wires.	Standalone measurement	Heating formation and DTPS baseline recording for 2 days before day 1 of Phase 1 Continuous DTPS recording until the end of test Heating formation from day 18 to 20 in Phase 3 Heating formation from day 28 to 30 in Phase 4
	Pulsed neutron log	Logging tool, time lapse log	Evaluation of 100% water saturated conditions, day 12 Record near-borehole 100% CO_2 saturation, day 23 S_{gr} measured day 27

Surface data

The flow rates of fluids in and out of the well are the basic elements of the test, and of subsequent simulations. The rates recorded were for CO_2 injection and water injection, and the production of water, at one minute intervals. At some stages there was much short term variation in the rates, so for modelling purposes the rates have been approximated by a piecewise constant injection rate.

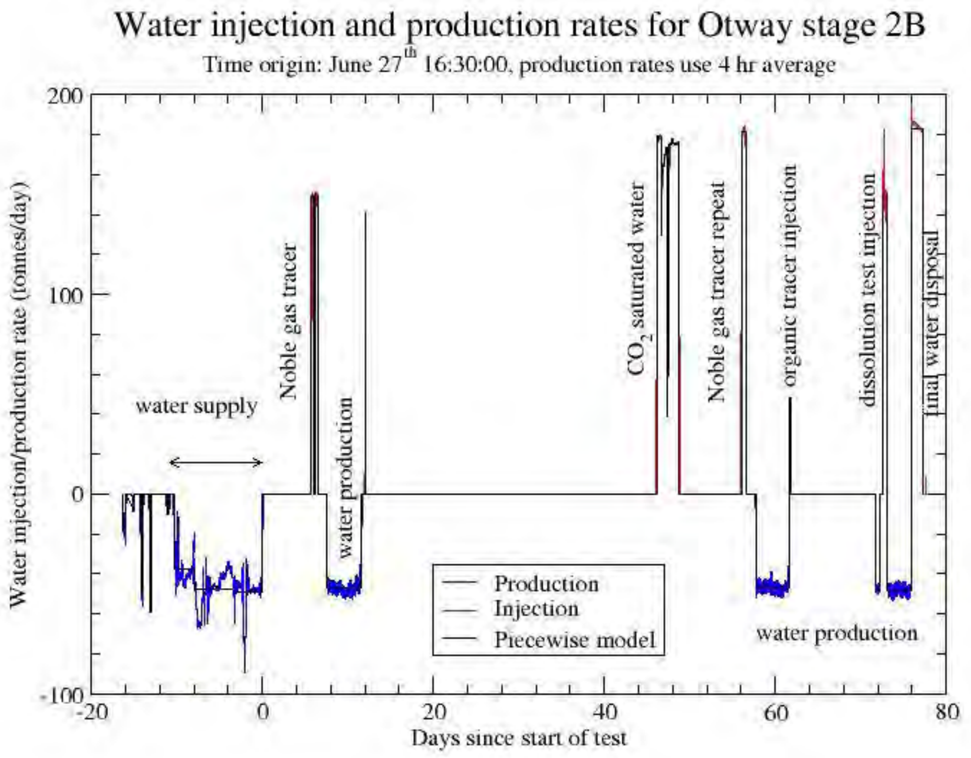

Figure 12: Water production rates (negative, blue lines) and water injection rates (positive, red lines) over the whole test. In black in shown the piecewise constant model for the injection rates. The water rate during the supply period (before the start of the test) has been adjusted as described in the text.

Figure 12 shows the water rates for injection and production throughout the test. Water injection could be carried out at 150-180 tonnes/day, whereas average water production rates, limited by gas lift, were around 50 tonnes/day. Thus by design the production periods were longer than the corresponding injection periods.

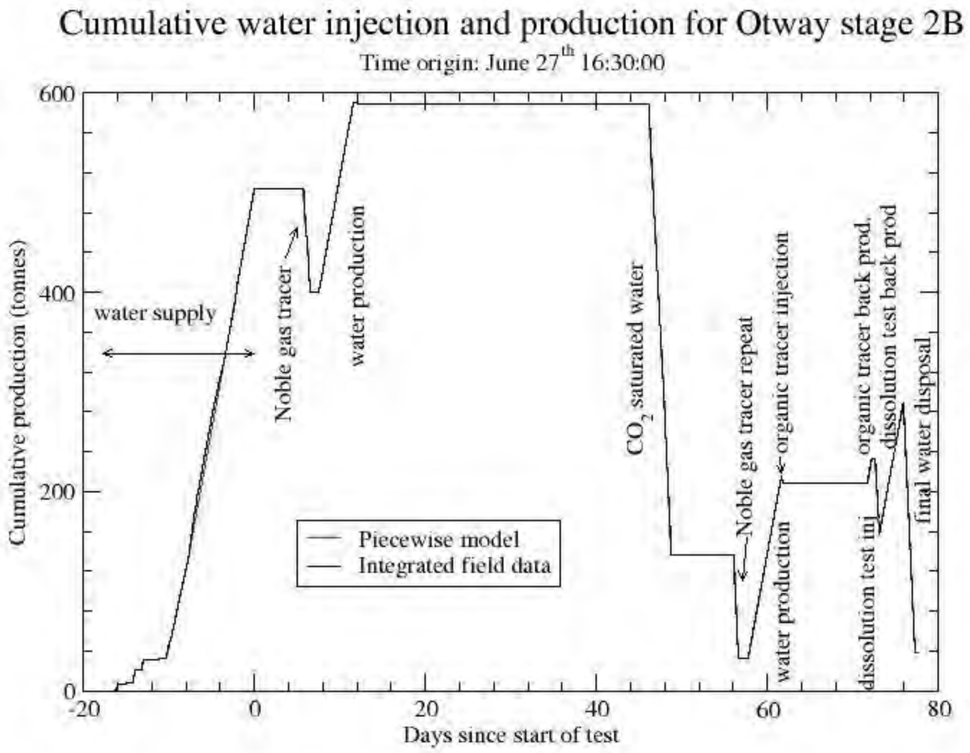

Figure 13: Cumulative water injection and production in tonnes, from the beginning of the gauge data. The time origin of the test is chosen as June 27th, 16:30. The water production during the supply phase (before the start of the test) has been adjusted as described in the text.

Figure 13 shows the cumulative sum of water production (here taken as positive) and water injection (here taken as negative) over the test cycle. At the end of the test there is still water in the tanks, although the reported total of 116 tonnes over the three tanks (T101 37 tonnes, T102 41 tonnes, T103 38 tonnes) does not match the endpoint of the figure, which was about 38 tonnes. On June 12th 10:00 Tank 102 was reported as being 18% full and tanks 102 and 103 as empty, corresponding to 43 tonnes of water. Clearly there was water production prior to this that was not metered - amounts of water disposal (by contractor) amounting to 44 tonnes are reported for Tank T101 from June 8th to June 9th. June 12th is very close to the beginning of the metered water production, and is taken as the initial level of the tanks. This resolves some of discrepancy in the integration of the field data, since from that initial level of 43 tonnes, it predicts 81 tonnes of water remaining in the tanks, compared to the observed 116 tonnes.

During the water supply phase (i.e. production using gas lift to provide water for the operation), a problem with the surface setup meant that there was additional flow through the surface gauges, leading to an overestimate of the production. This was corrected on June 24th at 10:30 (judging from the daily reports), so metered production before this time needs to be reduced proportionately to match the observed amounts in the tanks at the end of the water supply phase. On June 19th at 18:30 tanks T101 and T103 were reported empty, and T102 as 62% full, corresponding to 149 tonnes of water. On June 24th at 10:30 the integration of the field data gave 534 tonnes. On June 27th at 18:30 the tanks were reported as T101 33% full, T102 100% full and T103 88% full, corresponding to about 530 tonnes of water (240 tonnes per tank). On the other hand the integrated field data from water flow rates gave a figure of 694 tonnes. This data is summarised in Table 4.

Table 4: Water volumes in the storage tanks.

Time (days from midnight on June 1st 2011)	Tank volumes	Integrated gauge volume
11.416	43	0.0
18.770	149	201.3
23.4375		534.3
26.333	511	676.4
26.770	530	694.0

Assuming that the gauge data is accurate after June 24th at 10:30, one can infer that the tank volume at that point would be 370 tonnes. A two part correction was used, with the flow rate up to June 19th 18:30 being multiplied by 0.524, and the flow rate from June 19th 18:30 to June 24th 10:30 being multiplied by 0.665. The tank readings in the daily reports are no more than 1% accurate (about 2 tonnes), and possibly less. Thus the calibration of the early production is only approximate.

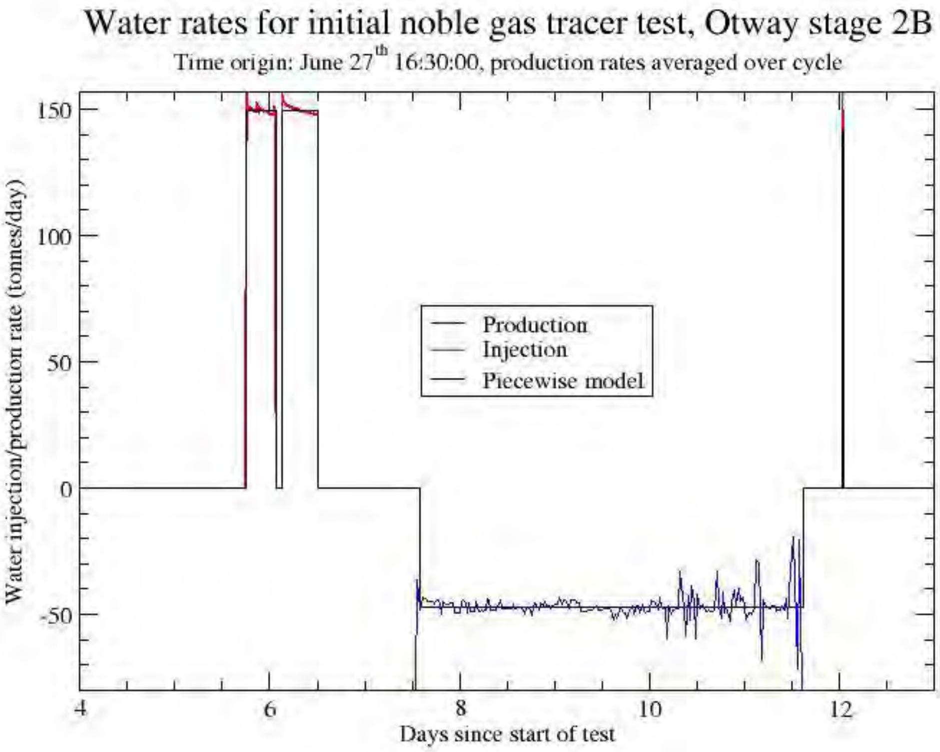

Figure 14: Water injection and production rates for the first noble gas tracer test.

The water flow rate during the initial noble gas tracer test are shown in Figure 14, along with the piecewise constant model for the simulations. The gap in the middle of the injection was due to a short power outage in the area. The gauge data for water production is complicated by the location of the flow gauge. A small tank is filled up, and when this reaches a certain level, the produced water is then pumped on to the large tanks. As a result, the gauge data shows a short burst of flow, followed by an interval of no flow. Figure 15 illustrates this for the start of the water production data during the initial noble gas tracer test. The open circles represent the average flow rate from the start of one pumping cycle to the start of the next.

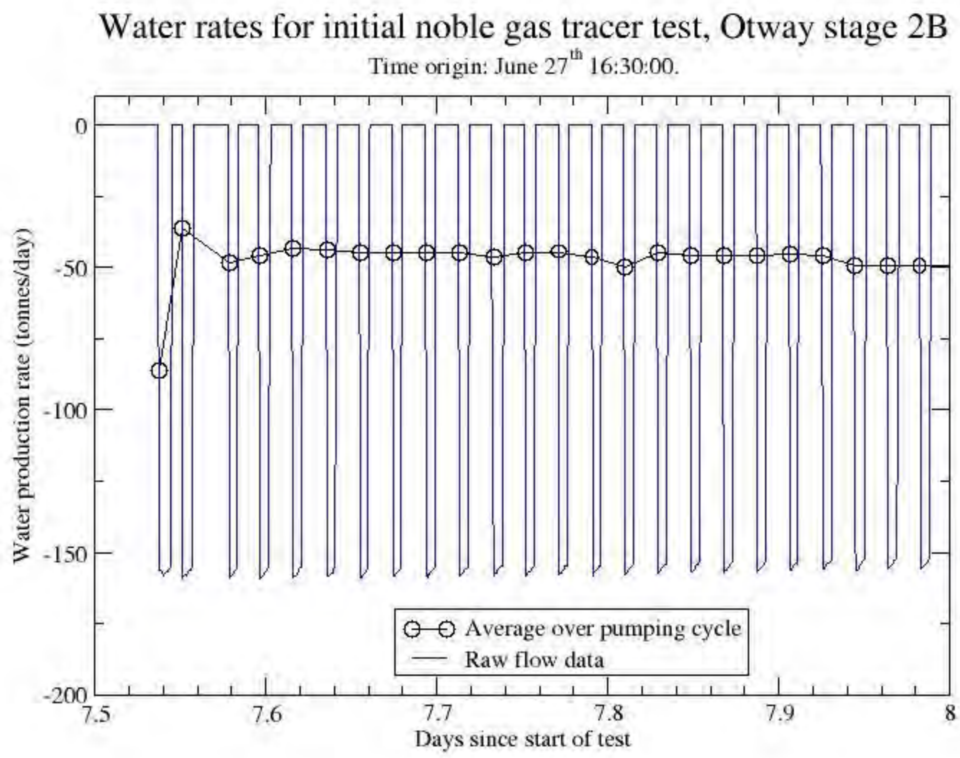

Figure 15: Comparison of raw flow data for water production with average rate over each cycle.

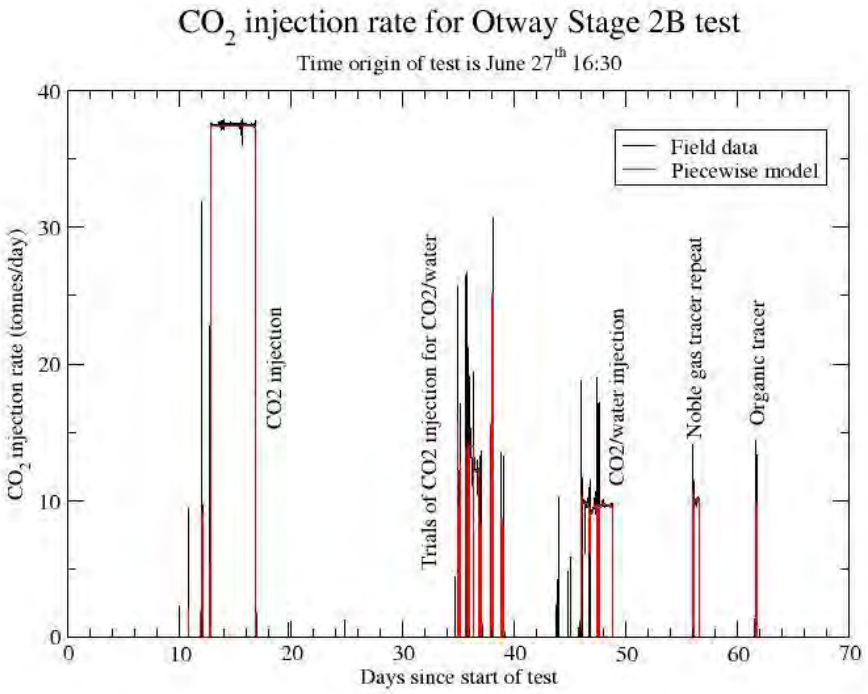

Figure 16: CO$_2$ injection rates over the whole test, compared to a piecewise constant model.

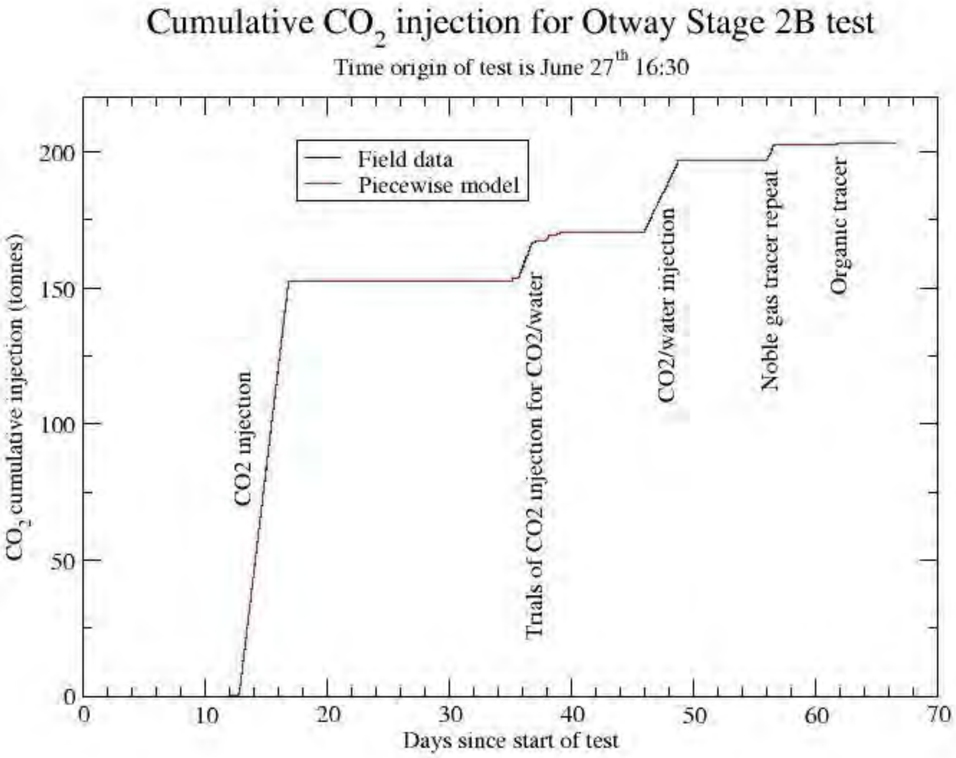

Figure 17: Cumulative CO$_2$ injection during the whole of the test. The piecewise constant simulation model is shown for comparison.

The CO_2 injection rates for the whole test are shown in Figure 16, along with a piecewise constant model for simulation purposes. Figure 17 shows the cumulative amount of CO_2 injection over the test. The main CO_2 injection was relatively straightforward. Figure 18 shows an enlargement of the rate for that period. Subsequent CO_2 injections had to be balanced with simultaneous injections of water to produce CO_2-saturated brine at bottomhole conditions. The design rate for these sections was 7.5 tonnes/day of CO_2, but this proved difficult to achieve without the CO_2 pump gassing up. After much experimentation with surface equipment (e.g. see the trials of CO_2 injection in the period 35-40 days in Figure 16, and the enlargement of this in Figure 19), a way was found to get a relatively stable rate of around 10 tonnes/day, balanced with a suitable water rate.

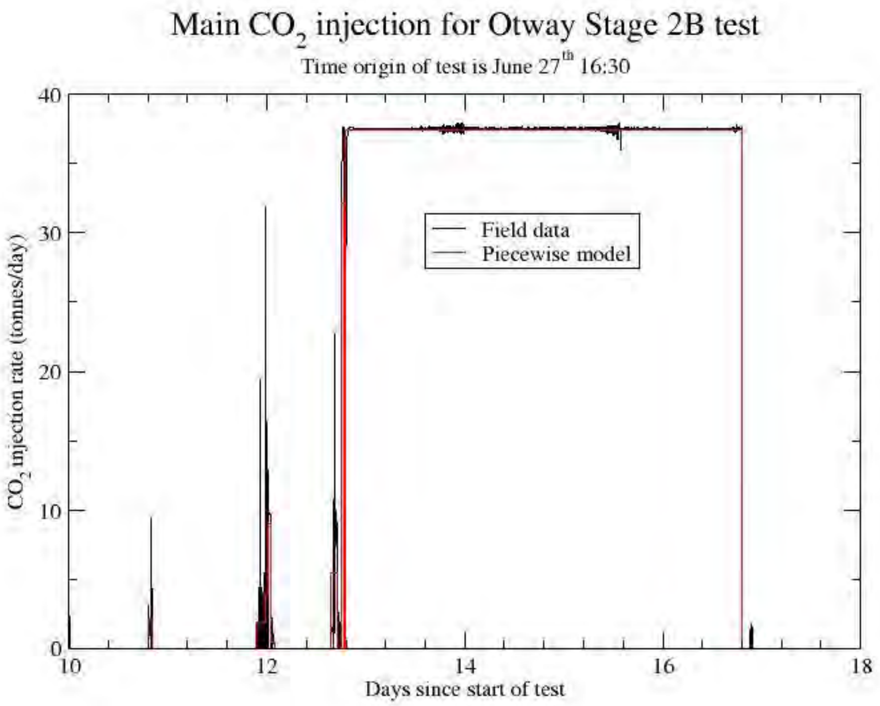

Figure 18: CO_2 injection rate during main injection phase to establish gas saturation near the well.

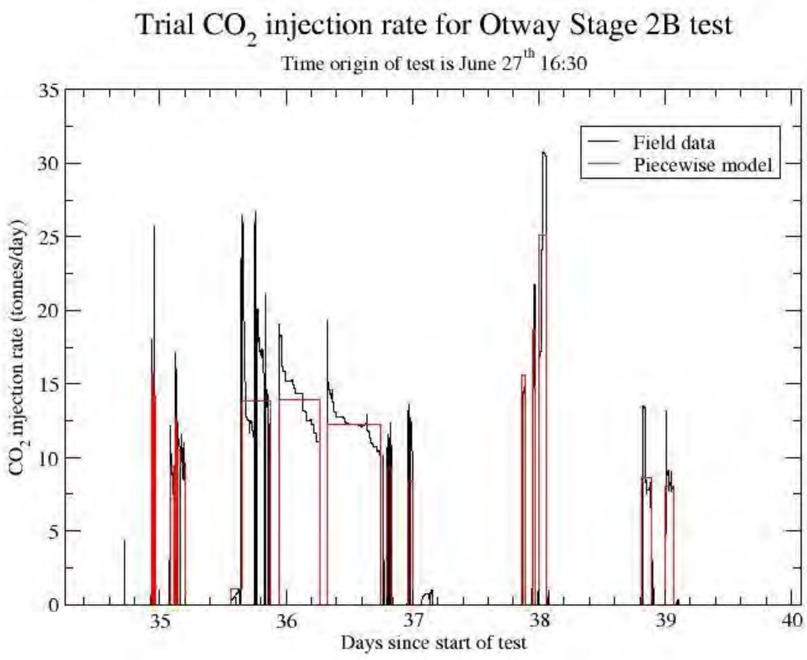

Figure 19: CO$_2$ injection rate during trial phase for adjusting surface equipment, compared to piecewise constant simulation model.

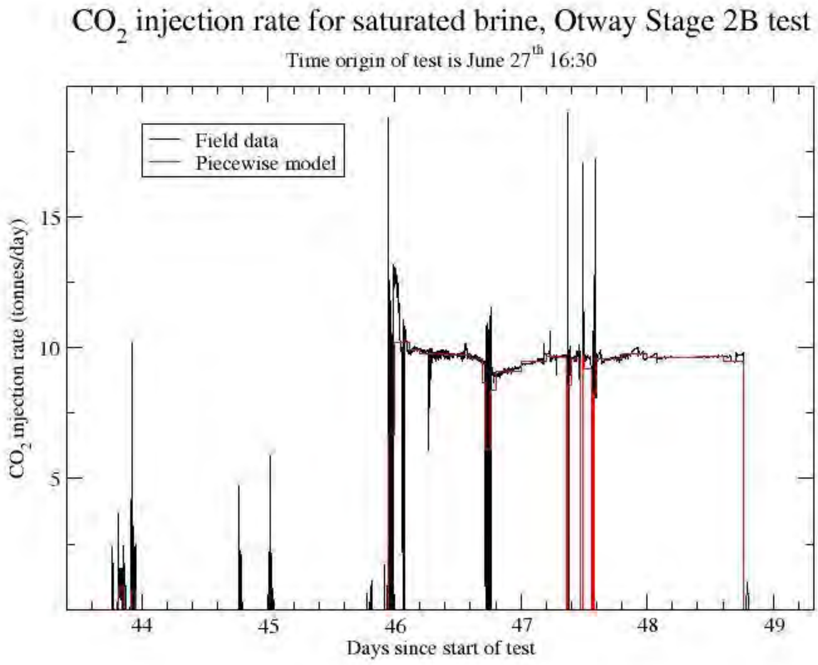

Figure 20: CO$_2$ injection rate for saturated brine injection during drive to residual saturation. The piecewise constant simulation model rate is shown for comparison.

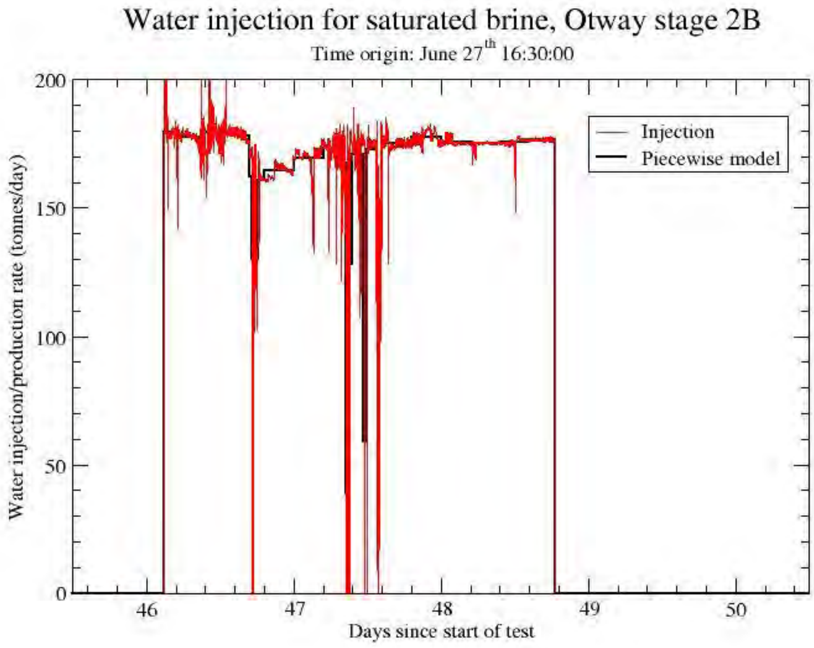

Figure 21: Water injection rate in the injection of saturated brine during the drive to residual saturation. The piecewise constant simulation model rate is shown for comparison.

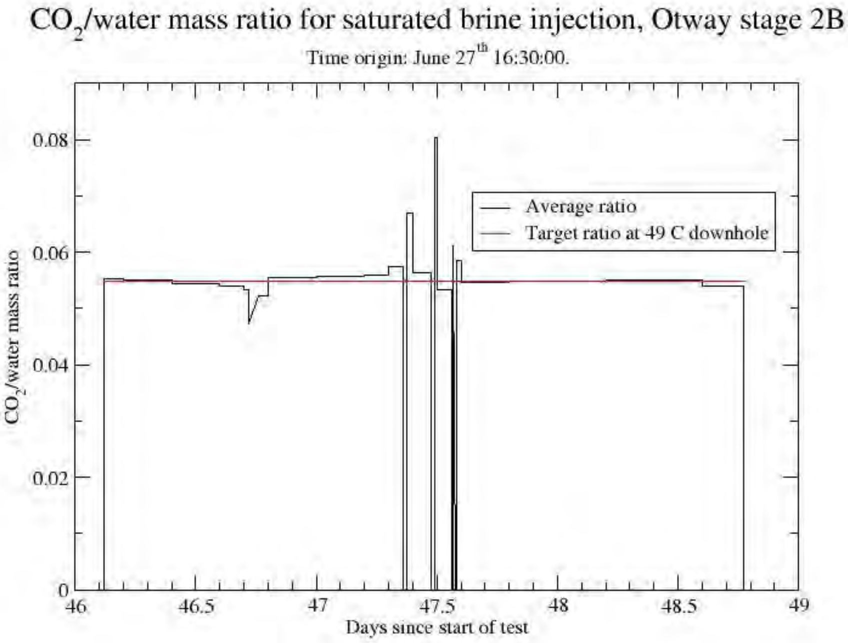

Figure 22: CO$_2$/water mass ratio during saturated brine injection for drive to residual saturation. The target mass ratio for a downhole temperature of 49° C is shown in red.

The CO_2 rate and the water rate during the injection of CO_2-saturated water (to drive the near-well environment to residual saturation) are shown in Figure 20 and Figure 21. The mass ratio of CO_2 to brine is shown in Figure 22. The overall mass ratio for this part of the test was 0.0578, whereas the target rate (shown in Figure 22 as the red line) was 0.0548. Design calculations were made based on CO_2 solubility in brine at downhole conditions (the mixing of the CO_2 and brine occurs at the check valve depth for the instrument tubing at about 840m depth). The aim was for the brine to be very slightly undersaturated at bottomhole conditions (to avoid introducing any further gas phase CO_2), and very slightly oversaturated far from the well. As will be seen elsewhere in this report, injection of brine lowers the downhole temperature to about 49 °C, so as one goes out from the well in the target formation, the temperature increases back to the formation temperature of 59 °C, while the pressure decreases. Given the high reservoir permeability, the pressure change is slight, so the temperature effect on solubility is much more important.

In operational practice, a table of target water rates was supplied to the operators, with rows for downhole temperature (to be read from the PANEX gauges) and columns for the CO_2 rate. When the CO_2 injection rate stabilised, the water rate was adjusted to match the desired number. In practice the water rate fluctuated by at least 2-3 tonnes/day, and sometimes more if there were problems with filters. Table 5 is a part of one of these tables, giving the water in tonnes/day. Given the size of the fluctuations, and the small changes in rate with downhole temperature, in most cases only a single line of the table was needed for the operation.

Table 5: Example of part of a table that was used for setting CO_2/water injection ratios.

CO_2 rate t/day		**9.7**	**9.8**	**9.9**	**10.0**	**10.1**	**10.2**	**10.3**	**10.4**
Temp(C)	CO_2/Water mass ratio								
48.0	0.055006	176.34	178.15	179.97	181.79	183.61	185.43	187.24	189.06
48.5	0.054915	176.65	178.47	180.30	182.12	183.94	185.76	187.58	189.40
49.0	0.054825	176.97	178.79	180.62	182.44	184.27	186.09	187.91	189.74

After the injection of the CO_2-saturated brine, that drives the near-well environment to residual gas saturation, tests are then conducted to characterise this residual saturation. The rates of CO_2 and water injection for the repeat of the noble gas tracer test (but this time with CO_2-saturated brine, to avoid dissolving the residual CO_2 near the well) are shown in Figure 23 and Figure 24. The average mass ratio of CO_2/brine in this part of the test is 0.0548, which agrees with the target ratio of 0.0548.

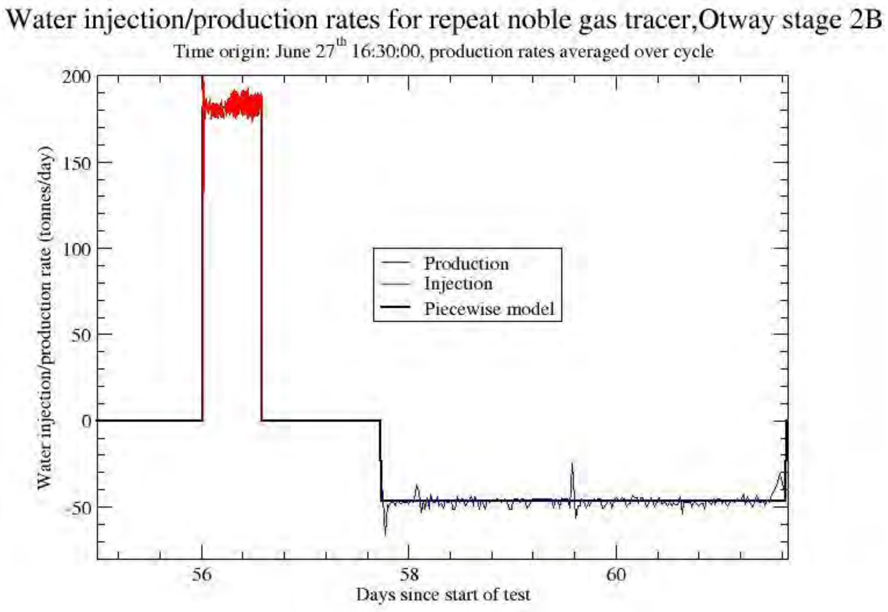

Figure 23: Water injection and production rates for the repeat noble gas tracer injection. The production data is averaged over one pumping cycle. The piecewise constant simulation model injection rate is shown for comparison.

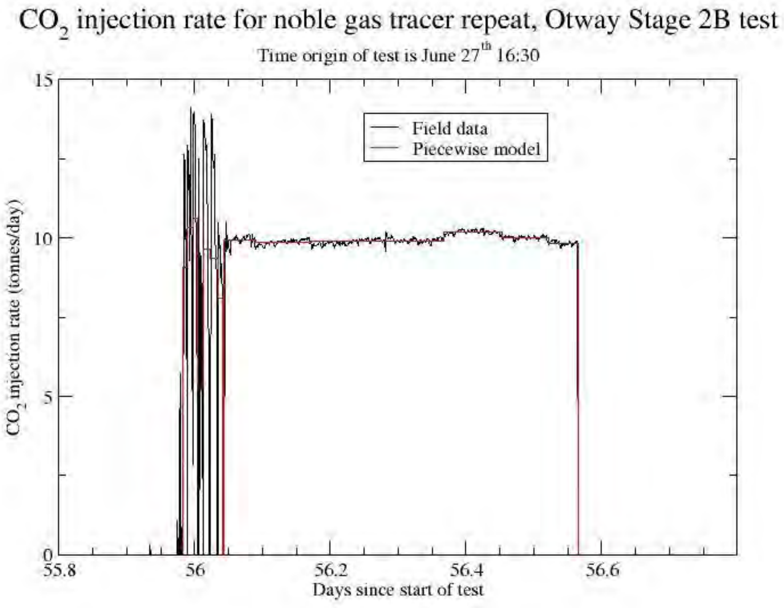

Figure 24: CO_2 injection rate for the repeat of the noble gas tracer injection. The piecewise constant simulation model rate is shown in red for comparison.

The organic tracer test similarly involves the injection of CO_2-saturated brine, but only a fairly small amount. Figure 25 and Figure 26 show the water and CO_2 injection rates for this test. The average CO_2/brine mass ratio for this test was 0.0616, which was slightly oversaturated compared to the target ratio. However the injected amount was relatively small. The water back production rate for the sampling part of the test is shown in Figure 27.

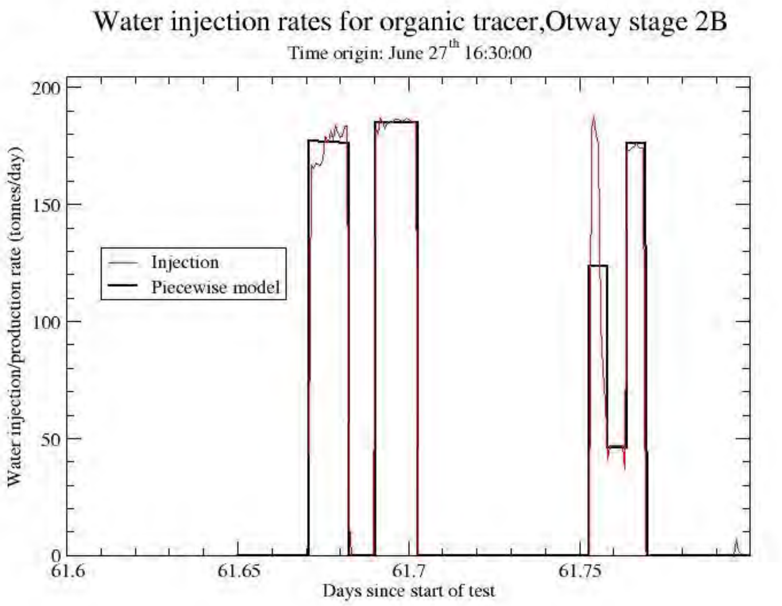

Figure 25: Water injection rate for the organic tracer test. The piecewise constant simulation model rate is shown for comparison.

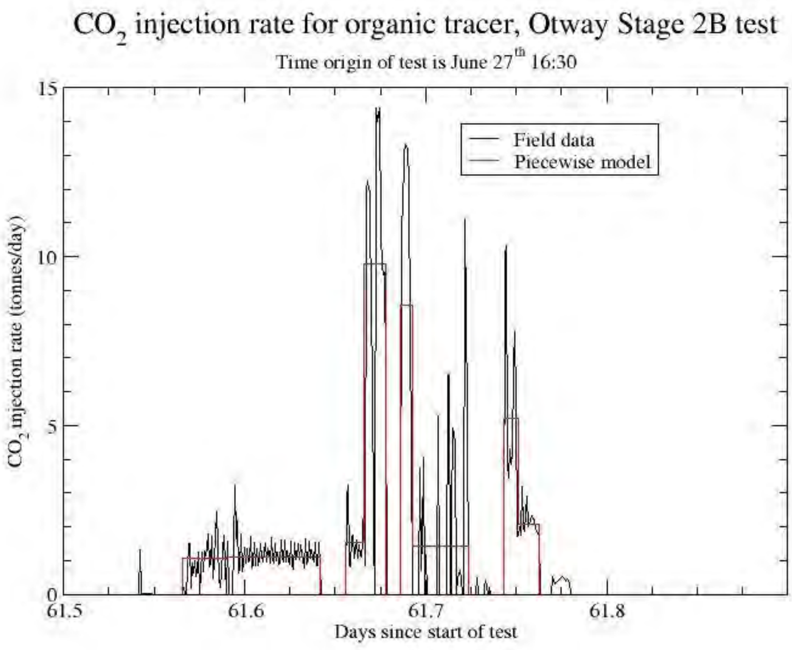

Figure 26: CO$_2$ injection rate for the organic tracer test. The piecewise constant simulation model rate is shown for comparison.

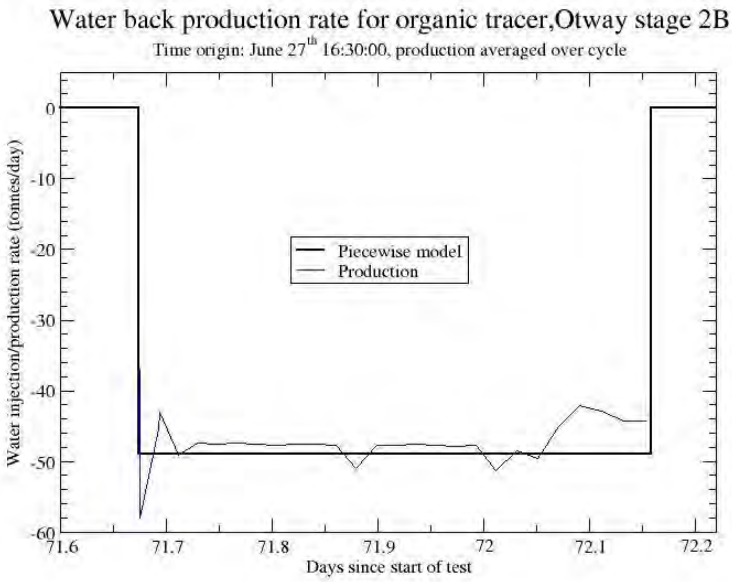

Figure 27: Water back production rate for the organic tracer test. The piecewise constant simulation model rate is shown for comparison.

The last residual characterisation test was the dissolution test, using unsaturated brine, where the explicit aim was to dissolve the residual gas, and monitor the dissolved CO_2 in the back-produced water. Figure 28 shows the water injection and production rates for this and also for the final water disposal.

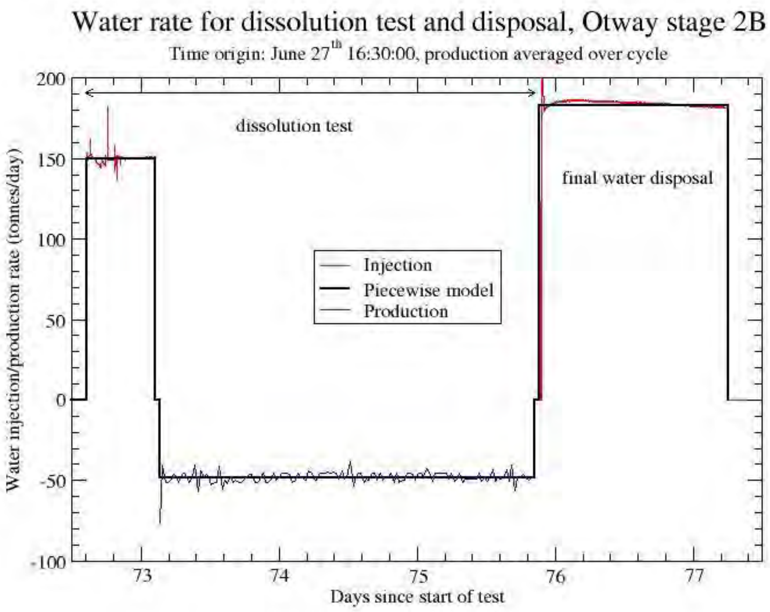

Figure 28: Water injection and production rates for the dissolution test and the final water disposal. The piecewise constant simulation model rate is shown for comparison.

The overall amounts injected and produced in each part of the test are summarised in Table 6 and Table 7, along with the average flow rates. In cases where there are many interruptions to injection, the latter average is not representative of the typical rates when flow was occurring. The above graphs show a more detailed piecewise constant model for the flow rates than is given in the tables. In the tables, the time origin of the test is taken as June 27th, 16:30.

Table 6: Summary of water injection and production.

Time (days since start of injection)	Purpose	Amount of water (tonnes) (+ for production, - for injection)	Average rate (tonnes/day) (+ for injection, - for production)
-16.358 – 0.000	Water supply	+504.4	-30.8
5.744 – 6.507	Initial noble gas tracer injection	-103.9	+136.2
7.538 – 11.623	Water back production for noble gas tracer	+190.2	-46.6
46.123 – 48.773	CO_2 saturated brine injection	- 453.7	+170.6
56.016 – 56.590	Repeat noble gas tracer injection	-104.1	+181.3

Time (days since start of injection)	Purpose	Amount of water (tonnes) (+ for production, - for injection)	Average rate (tonnes/day) (+ for injection, - for production)
57.740 – 61.641	Back production for repeat noble gas tracer	+182.4	-46.8
61.670 – 61.797	Organic tracer injection	-6.18	+48.4
71.674 – 72.158	Back production for organic tracer test	+23.7	-48.9
72.605 – 73.106	Dissolution test – injection	-75.0	+149.7
73.139 – 75.852	Back production for dissolution test	+130.86	-48.2
75.881 – 77.252	Final water disposal	-250.6	+182.8

Table 7: Summary of CO_2 injection.

Time (days since start of injection)	Purpose	Amount of CO_2 (tonnes)	Average rate (tonnes/day)
12.788 – 16.806	Main CO_2 injection to create gas saturation	150.5	37.4
34.940 – 39.071	Trial injection of CO_2 for pumping adjustment	18.3	4.4
45.948 – 48.763	CO_2 saturated water	26.2	9.3
55.983 – 56.564	Noble gas tracer repeat	5.7	9.8
61.566 – 61.763	Organic tracer test	0.38	1.93

Thermal logging

A Distributed Thermal Perturbation Sensor (DTPS) is an instrument which provides estimates of formation thermal parameters (Freifeld et al. 2008) and can infer hydrological properties and fluid phase saturation using changes in thermal properties as proxy measurements. The DTPS consists of a borehole length heater and a fiber-optic distributed temperature sensor (DTS). These distributed temperature sensors are commercially available temperature measurement devices, capable of high spatial resolution (~1m) with measurement precision as high as 0.01 °C. Typical operational accuracy is closer to ±0.1°C. Distributed temperature sensor systems operate using standard telecommunications grade multimode fiber-optics sensors as the sensing medium. To observe changes in thermal properties the heater is used to create a thermal pulse. The decay of the thermal pulse is then used to estimate a thermal diffusivity.

For the Otway Stage 2B residual saturation test, the DTPS was deployed to monitor changes in CO_2 saturation. Table 8 shows when the heating phase of DTPS testing was conducted. To observe changes in CO_2 saturation the heater creates a thermal pulse using fixed power input (30kW), and then after a fixed duration of heating, the thermal decay is monitored. A snapshot of the temperature profile along the borehole is recorded every 15 minutes. For CRC-2 testing, after two days of heating, cooling trends were monitored for an additional three days. Since supercritical CO_2 has a thermal conductivity roughly 20 times less than that of formation fluid, the temperature is hotter in CO_2 rich regions of the reservoir and the thermal decay is slower, as the CO_2 acts to reduce the formation thermal diffusivity.

Table 8: DTPS operational tests conducted.

Date (heating)	Comments	Acceptable for thermal analysis
27 – 29 June 2011	Baseline Dataset – fully water saturated formation	Yes
16 – 18 July 2011	Post-CO_2 Injection – large thermal background trends	No
24 – 26 July 2011	Post-CO_2 Injection – moderate background thermal trend	Yes
17 – 19 August 2011	Post-H_2O sweep – large thermal background trends	No
2 – 4 September 2011	Post-H_2O sweep – moderate background thermal trend	Yes

A thermal profile at the depth of the CRC-2 perforated interval is shown in Figure 29. It was acquired during heating, and pinpoints the locations of the straddle packer assembly. The packers stand out as local high temperatures because the rubber glands act as insulators. Figure 30 shows the baseline thermal profile. The small inflections in temperature reflect either changes in formation thermal conductivity. At a depth of approximately 20 m is the transition from a water filled borehole to an air filled borehole.

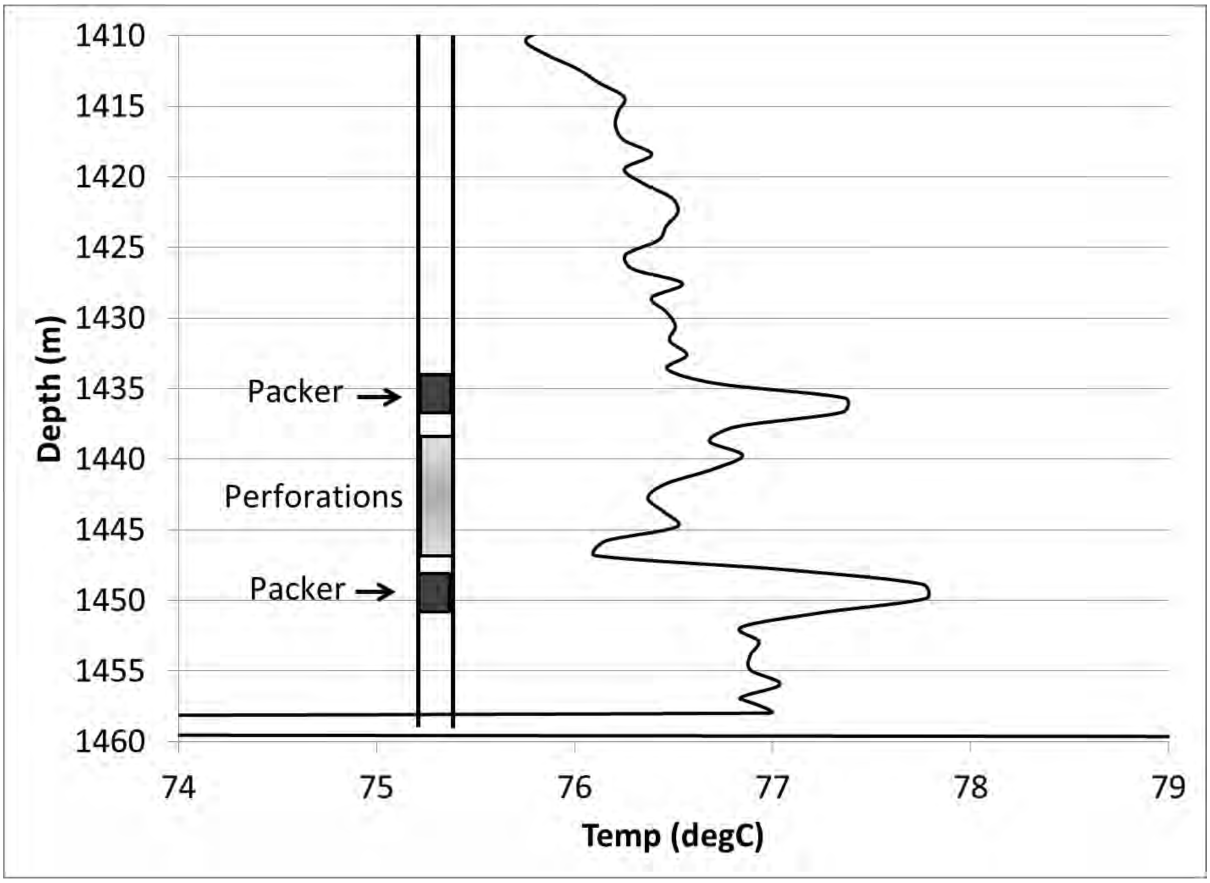

Figure 29: CRC-2 thermal profile acquired during heating (29 June 2011) showing the location of the two TAMCAP packers, which stand out because of the insulating capacity of the rubber packer glands. Between the straddle packer assembly is the 7 metre long perforated interval.

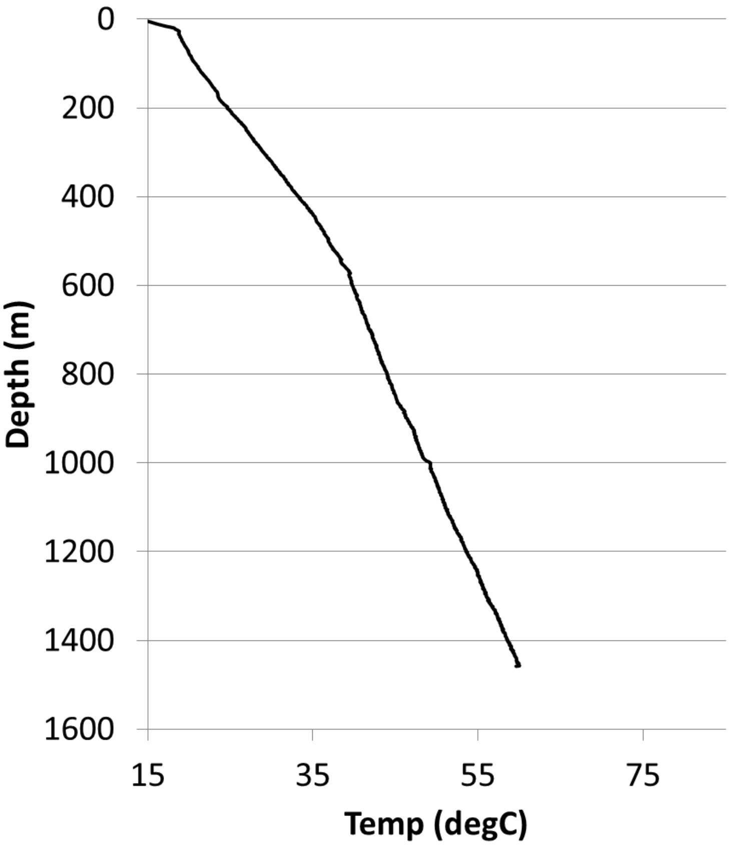

Figure 30: Baseline thermal profile of the CRC-2 well. The sharp change in the slope at a depth of 21 metres is the location of the fluid level in the borehole.

The baseline thermal test is shown in Figure 31. Borehole heating was conducted at 15.4 W/m for a period of two days. Post-heating thermal recovery was monitored for three days. The data collected using the DTS system is still being processed, but is similar to the PANEX temperature data – except at more locations. Figure 32 shows the thermal response post-CO_2 injection. The gradual increase in background temperature at the start of testing is from the thermal rebound from the cooler injected CO_2. A large change in the thermal response is noted for the deeper gauges – Gauge 1279 located at a depth of 1445.3 m and at Gauge 1274 located at 1447.3 m. Figure 32 shows the 24 – 26 July thermal test, conducted after the injection of CO_2 but before injecting brine to sweep the CO_2 to residual.

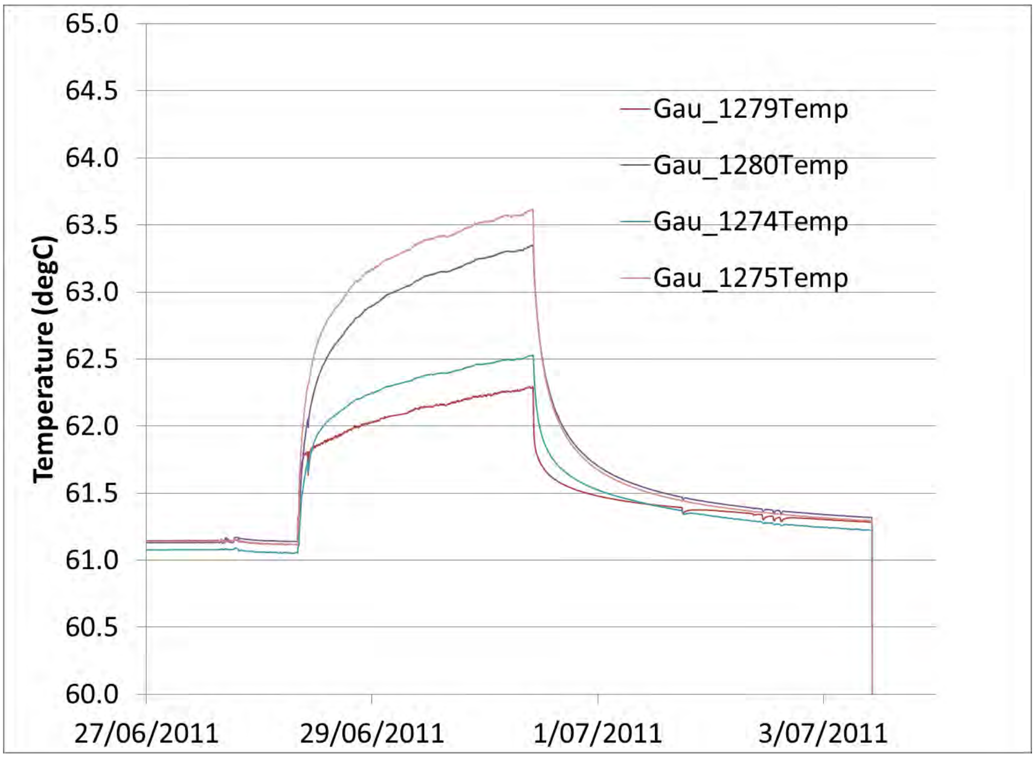

Figure 31: The heating and cooling profiles associated with the baseline thermal perturbation test, as recorded using the downhole PANEX pressure/temperature gauges.

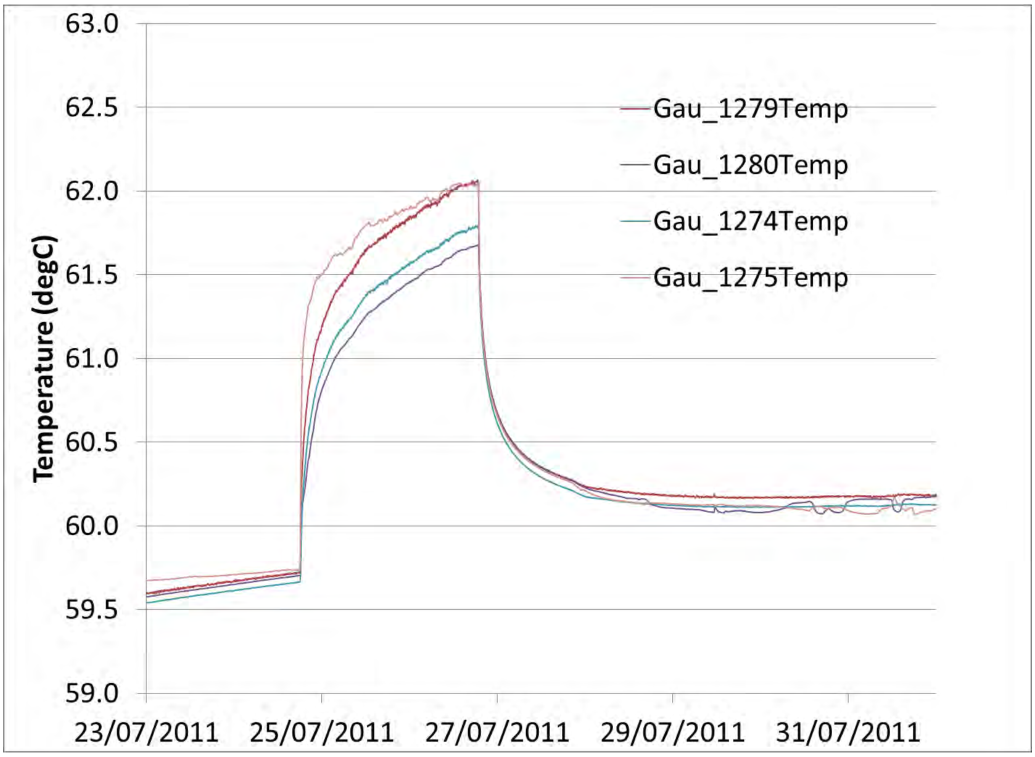

Figure 32: Post-CO_2 injection thermal profile. This thermal test was conducted after the injection of CO_2 but before injecting water to sweep the CO_2 to residual saturation.

During the residual saturation test there were approximately 7000 data files collected with the DTS at 15 minute intervals. Those files are currently being processed and calibrated using the PANEX temperature data as a calibration reference. The DTS heating and cooling curves will be fit using a thermal conduction model, and then changes in thermal conductivity will be used to estimate residual gas saturation. Thermal profiles above the injection interval can be used to indicate the contact point between $ScCO_2$ and formation fluid in the production tubing. Because thermal profiles below the injection interval should be constant over time, they are used to assist in the calibration and data qualification for shallower depths.

Noble gas tracer tests

The noble gases krypton (Kr) and xenon (Xe) were a critical component in the design of a single-well injection-withdrawal test in the Paaratte Formation sandstone reservoir. Their ability to partition between the mobile water phase and immobile gas phase was used to evaluate the extent of residual CO_2 phase trapping (Zhang et al 2011). To determine the residual gas saturation (S_{gr}) the noble gases were coinjected with water before the injection of CO_2 when the pore space was fully water saturated (reference test) and once again when the residual CO_2 field had been created (characterisation test). The push-pull partitioning of tracer in combination with the hydraulic and thermal tests should reduce the estimation uncertainty in the S_{gr} field (Zhang et al 2011). Furthermore, performing a reference test provides information on formation dispersivity, resulting in reduced parametric and geological uncertainty and helps constrain two-phase parameters used in the synthetic models (Zhang et al., 2011). Subsequent to the proposed simulated test sequence by Zhang et al (2011) an organic tracer test and a dissolution test were added, with the latter test also involving the analysis of recovered Kr and Xe. Figure 7 shows the test sequence as was performed during the CO2CRC Stage 2B field study.

To collect suitable fluid samples for analysis, the U-tube assembly (Figure 33) enables a pressurised water sample to be taken directly from the reservoir level and transferred to the surface into a 4.7 L high pressure stainless steel cylinder under reservoir conditions of 2030 psi. Subsequently, a 150 mL pressurised water sample was taken for wet chemical analysis (pH, alkalinity, electrical conductivity and salinity) in the purpose-built field laboratory. The controlled pressure release of the storage cylinder resulted in the exsolution of dissolved gas, which flowed to vent. An instantaneous gas sample was collected in both an isotube and gas-bag once the initial pressure had dropped by 700 psi. The gases were analysed in the field laboratory for Kr, Xe, CO_2, O_2, N_2 and CH_4 by gas chromatography and mass spectrometry.

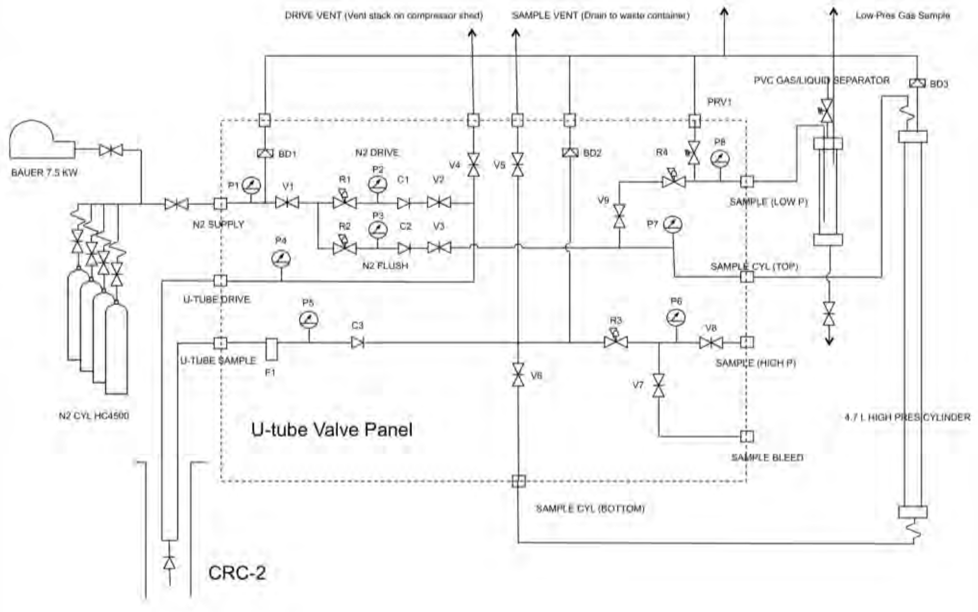

Figure 33: Schematic of U-tube surface assembly.

Phase 1 to initial Phase 2 – background test. Periodic collection of U-tube-derived gases showed baseline concentration of gases for Kr and Xe were below GC detection limits (< 1ppm) while CO_2 and CH_4 concentrations averaged 202 and 56 ppm, respectively. The balance of the gas was N_2 resulting from the initial 4.7 L N_2 in the SS storage cylinder at atmospheric pressure before filling with Paaratte water and its associated dissolved gases.

Phase 2 – Reference (baseline) Test. At the start of the water injection phase 2.46 kg of Kr (658 L @STP) and 3.62 kg of Xe (618 L @STP) were added at a constant flow rate over 120 minutes to the Paaratte formation water, which was being re-injected from the surface storage tanks at an average rate of ~136 tonnes/day. Water injection continued for another 14 hours (push) with the injection of 104 tonnes of water (Figure 7). After a further 24 hours, water production continued (pull) uninterrupted for another 3.4 days and 190 tonnes of water. Round-the-clock U-tube-sampling produced splits of derived water and gas at 90 minute intervals for near real-time aqueous and gas analysis.

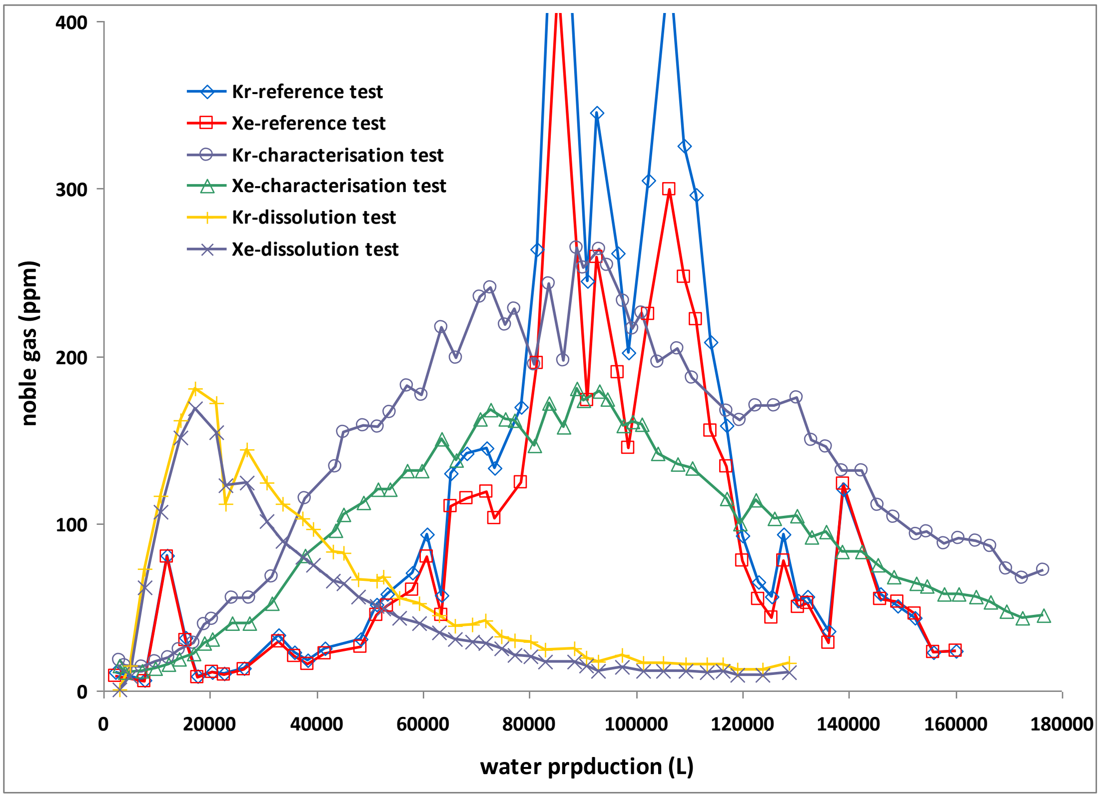

Figure 34: Breakthrough curve (BTC) with the concentration of Kr and Xe plotted against the cumulative water production for the reference test. The balance of the gas was N_2.

Phase 4 – Characterisation Test. At the start of the water injection phase 2.96 kg of Kr (791 L @STP) and 4.30 kg of Xe (734 L @STP) were co-inject at a constant flow rate over 100 minutes to the Paaratte formation with water being re-injected from the surface storage tanks at a flow rate of ~181 tonnes/day together. Carbon dioxide was injected through a 3/8" capillary line and mixed downhole with the water at a position high above the Paaratte Formation to maintain near CO_2-saturated water (~1 mol CO2/kg water) under reservoir conditions. Water and CO_2 injection continued for another 12 hours (push) with the injection of 104 tonnes of water (Figure 7). After a further 24 hours, continuous water production (pull) proceeded for close to 4 days and 182 tonnes of water. During this time, U-tube-derived water and gas samples were continuously sampled with a U-tube sampling period of ~90 minutes. Figure 34 shows the concentration of Kr and Xe plotted against the cumulative water production for the characterisation test. The balance of the gas was CO_2 and N_2 with an average CO_2/N_2 ratio of 5.65 ±1.17 σ.

Phase 5 – Dissolution Test. In this test CO_2-free formation water was injected into the Paaratte Formation resulting in dissolution of the residual CO_2 phase and remobilisation of the noble gas tracers back into the water phase. Subsequent water production and gas sampling produced the BTCs for Kr and Xe as displayed in the following section on the dissolution test.

In summary 1) the field laboratory provided real-time analytical results on gas composition and enabled sound operational decisions to be made (e.g. when to stop water production and sampling); 2) noble gas tracers were successfully injected, sampled and analysed; 3) noble gas tracer BTCs were observed in both the reference and characterisation tests; 4) the noble gas tracer BTCs are quite different with the characterisation test showing a much broader elution profile, in accord with tracer partitioning between the water and residual CO_2 phases – work continues on the conversion of the raw ‘ppm’ analytical results to the total tracer recovery yields and determination of S_{gr}; and 5) in the dissolution test, noble gas tracers that had partitioned into the residual CO_2 phase during the characterisation test are remobilised as a result of dissolution of the residual CO_2 phase with the injection of CO_2-free formation water. Again the shape of the BTC and concentration of the noble gases should allow refined estimates of S_{gr}.

Downhole data (memory gauges)

For part of the test pressure and temperature (P/T) memory gauges were run on battery and retrieved by slick line. These gauges were placed at 948 m and 1095 m. The memory gauges were run on August 5th, starting at around 16:10 for the bottom set bottom gauge, and 17:25 for the top set top gauge. They were retrieved on August 21st starting at 12:25 for the top set top gauge, and 13:20 for the bottom set bottom gauge. Correlating small events on the two pressure traces, it appears that the clock time differs by about 2384 second or 39.7 minutes, so the bottom gauge data have been shifted by this amount to match the top gauge. Relative to time origin of the test, the period of the memory gauges is from 38.98 – 54.83 days. The pressures are shown in Figure 35 and the temperatures in Figure 36. This covers the period after the trial CO_2 injection (when there were numerous attempts to stabilize the CO_2 rate at a suitable level) and covers the whole of the injection of CO_2-saturated brine, and the heating/cooling test immediately after that.

It is useful to analyse the implied fluid density difference between the two pressure gauges, using the pressure difference divided by g*h, where $g=9.80\ m/s^2$ is the acceleration due to gravity, and $h=147$ m is the vertical distance between the gauges. Experience indicates that slight differences in the pressure offsets between gauges may need to be corrected for if the densities are to be accurate. Under post-injection conditions, 50.6 days after the start of the test, the conditions at the top gauge are 9.106 MPa and 47.45 Cº, while at the bottom gauge the conditions are 10.605 MPa and 50.73 Cº. The density of the brine saturated with CO_2 should be around 1004.4-1004.9 kg/m^3, whereas the implied density difference from the difference in pressures is 1042.2 kg/m^3. If the pressure difference between the gauges is reduced by 0.0545 MPa, then the implied fluid density agrees with the theoretical calculation. This correction will be used in subsequent calculations with these gauges.

Figure 37 shows the implied fluid density information (with the correction). Initially the well is full of CO_2, due to the trial injection period, and the corrected density is around 558 kg/m^3. Theoretical calculations of the density of CO_2 at the location of the gauges give 566.4 kg/m^3 at the top gauge (11.24 MPa and 47.93 Cº) and 565.8 kg/m^3 at the bottom gauge (12.09 MPa and 51.57 Cº). When water injection begins, the fluid density quickly increases. At 48.0 days into the test, the implied fluid density (corrected) is 956.2 kg/m^3. At this time, the conditions at the top gauge were 9.357 MPa and 45.6 Cº, from which one can compute theoretically a CO_2 density of 377.5 kg/m^3 and an unsaturated brine density of 994.6 kg/m^3. The mass fraction of CO_2 in the injection stream was 0.0518 and of brine was 0.9482. If the CO_2 and brine were unmixed at that location, the density would be 917 kg/m^3. At the bottom gauge, the conditions at 48.0 days were 10.789 MPa and 46.6 Cº, from which one can compute theoretically a CO_2 density of 553.5 kg/m^3 and an unsaturated brine density of 994.8 kg/m^3. It’s clear that the CO_2 density is quite sensitive to pressure changes in this region. If the CO_2 and brine were unmixed at the bottom gauge location, then the fluid density would be 955 kg/m^3. Averaging the computed fluid density between the two locations (assuming the CO_2 is not dissolved in the brine) gives a density of 936 kg/m^3, which is lower than the implied fluid density from the pressure gauges of 956.2 kg/m^3.This is preliminary evidence that the CO_2 has partly dissolved in the brine between the time it enters the central tubing at the depth of the instrument tubing check value (853 mKB) to the time it reaches the gauge locations (948 mKB and 1095 mKB). An additional check would be to use the downhole gauge data near the perforations to infer the fluid density at that depth in order to see if the density reflects saturated brine only. This is important for ensuring that the brine is indeed saturated with CO_2 when it enters the reservoir, otherwise the CO_2 in the pore space might be dissolved rather than driven to residual values.

Another interesting feature is the drop in density just after injection ceases. At this stage there will be CO_2 not yet dissolved in the brine present in the tubing, and in a static situation this will rise due to buoyancy. This 'bubble' of rising CO_2 will cause a density drop at the gauge locations, before the CO_2-saturated brine fills that whole interval.

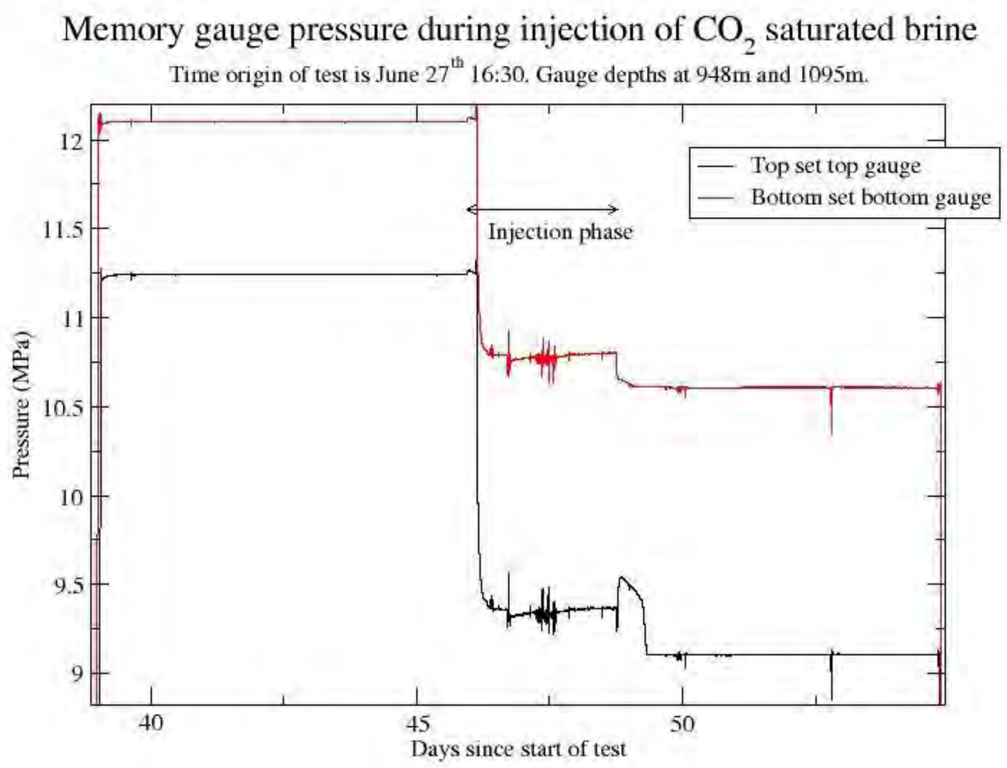

Figure 35: Memory gauge pressure during CO_2-saturated brine.

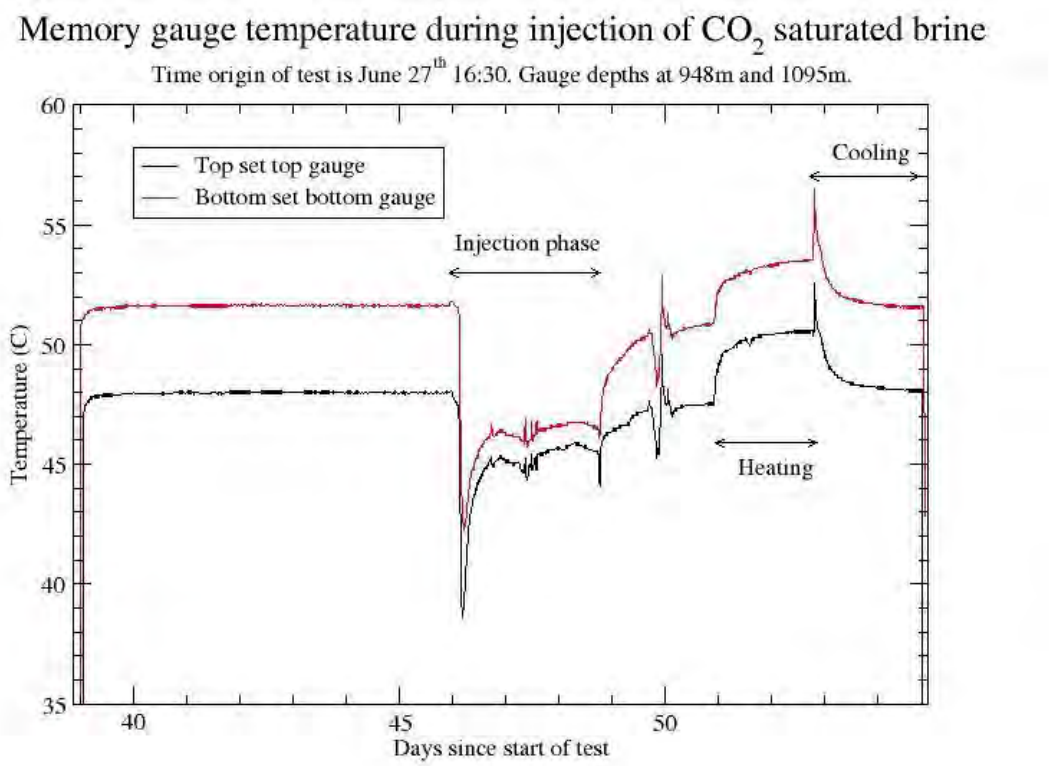

Figure 36: Memory gauge temperature during CO_2 saturated brine.

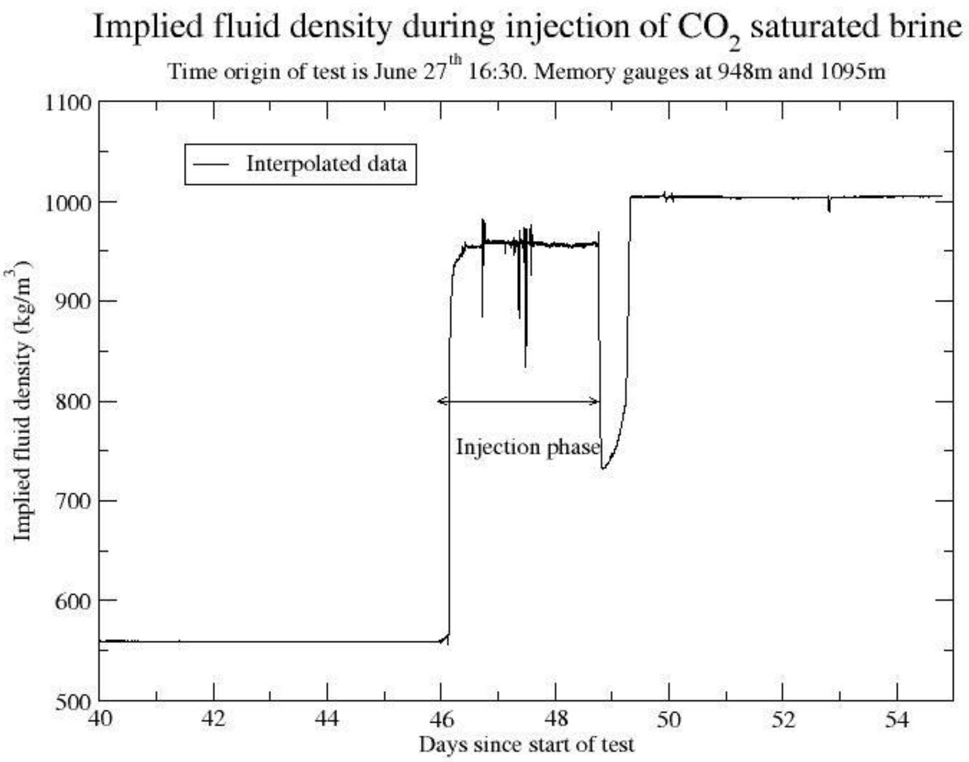

Figure 37: Implied fluid density during CO_2 saturated brine, corrected for the pressure offsets between the gauges.

Downhole data (permanent gauges)

Four real-time pressure and temperature (P/T) gauges were placed around the perforated interval, two above and two below. The entire sequence of measurements from these gauges is shown in Figure 38 and Figure 39. While the pressure measurements will primarily used as input to numerical history matching using reservoir simulation, there are parts to the test sequence that are amenable to standard well test analytical analysis. These pressure test data can be analysed using the methods described in Earlougher (1977) and Horne (1995). The first step in a simple semilog analysis is to produce a log-log plot of Δp vs t, shown in Figure 40. The next step is to determine the time at which the unit slope ends. To perform initial analysis the period with water injection containing noble tracers was chosen, along with the subsequent pressure decline. With measurements at 5 minute intervals it is difficult to find the unit slope, but from the swabbing analysis the orange line with unit slope in Figure 40 is consistent with 7 minutes. The semilog straight line can be expected to start 1.5 log cycles ahead of that point at around 3.7 hours. A Horner plot is shown in Figure 41 with the decline commencing Monday 4 July 2011 at 04:33:25. A 10.0 kPa/cycle slope for the solid line fit corresponds to

$$k = 0.183234 \frac{qB_w\mu_w}{mh} = 0.183234 \frac{(0.00174)(1)(0.48 \times 10^{-3})}{10.0 \times 10^3 \times 8} = 1.9 \text{ darcy}$$

This indicates the bulk permeability of the injection interval is about 2 darcy, consistent with the earlier estimate of 2.2 darcy when Option C was chosen as the injection interval.

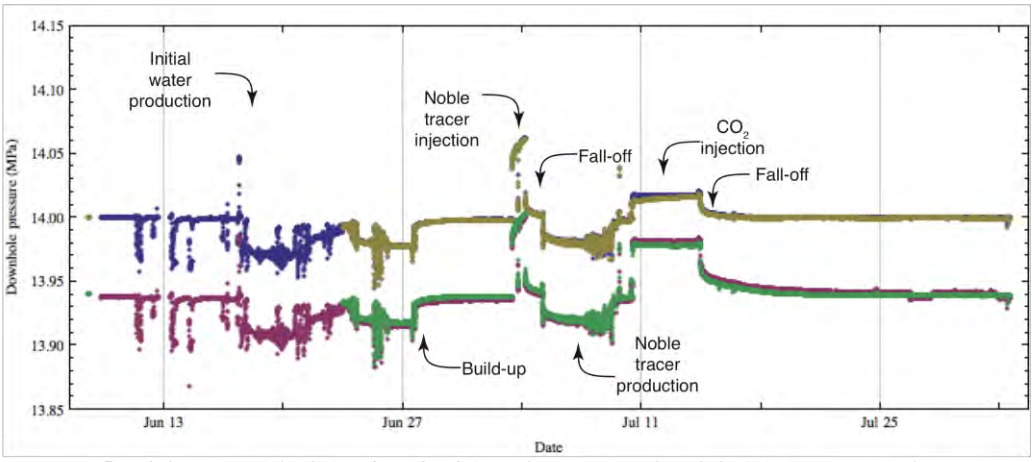

Downhole pressure 9 Jun (8:37am) to 1 Aug (14:57pm), average sample period = 309.52 sec = 5.159 min

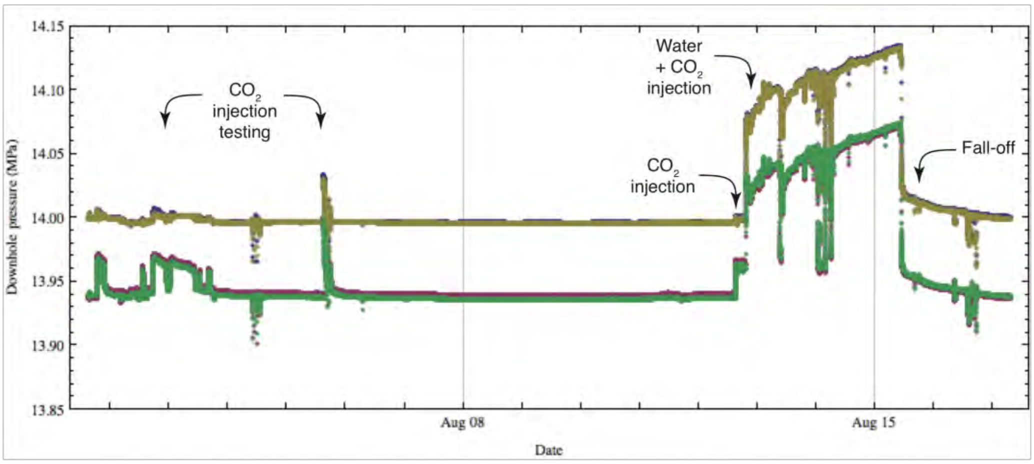

Downhole pressure 1 Aug (15:05pm) to 17 Aug (7:34am), average sample period = 15.213 sec = 0.2535 min

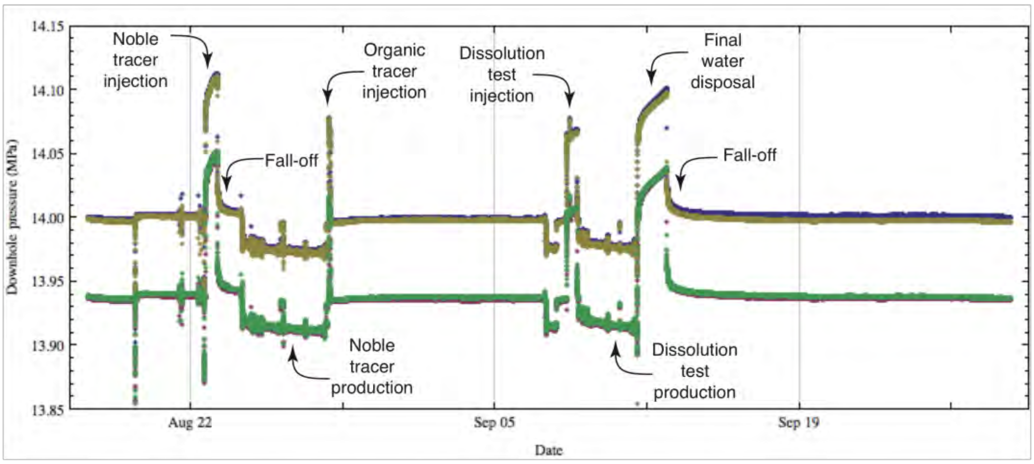

Downhole pressure 17 Aug (7:42am) to 28 Sep (16:46pm), average sample period = 60.24 sec = 1.004 min

Figure 38: Downhole pressure measured in the four permanent gauges.

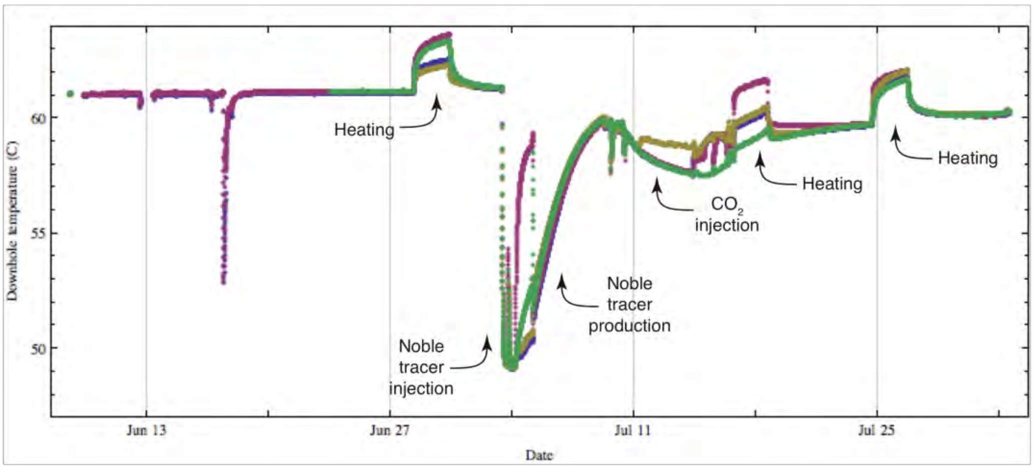

Downhole temperature 9 Jun (8:37am) to 1 Aug (14:57pm), average sample period = 309.52 sec = 5.159 min

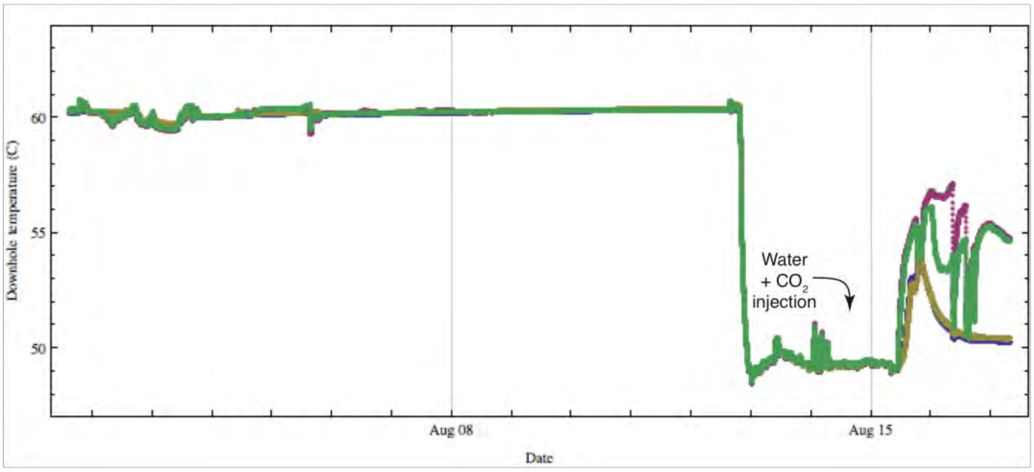

Downhole temperature 1 Aug (15:05pm) to 17 Aug (7:34am), average sample period = 15.213 sec = 0.2535 min

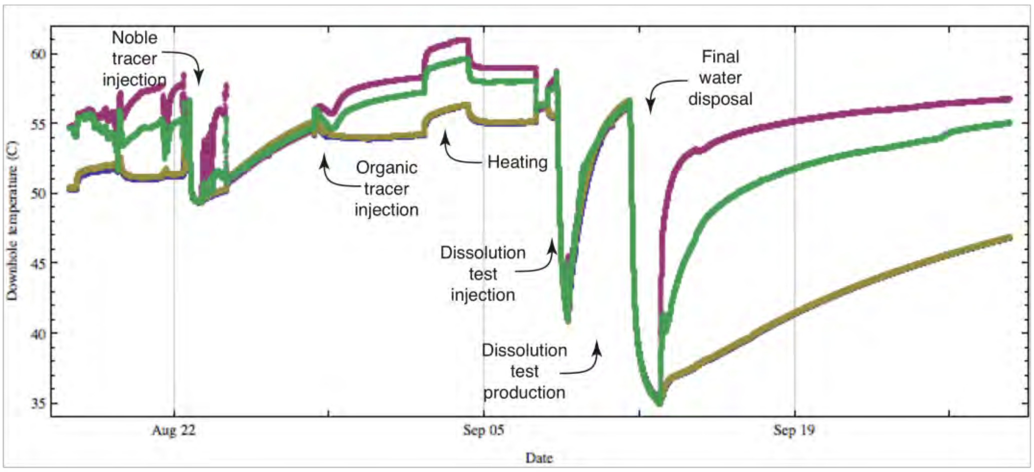

Downhole temperature 17 Aug (7:42am) to 28 Sep (16:46pm), average sample period = 60.24 sec = 1.004 min

Figure 39: Downhole temperature measured in the four permanent gauges.

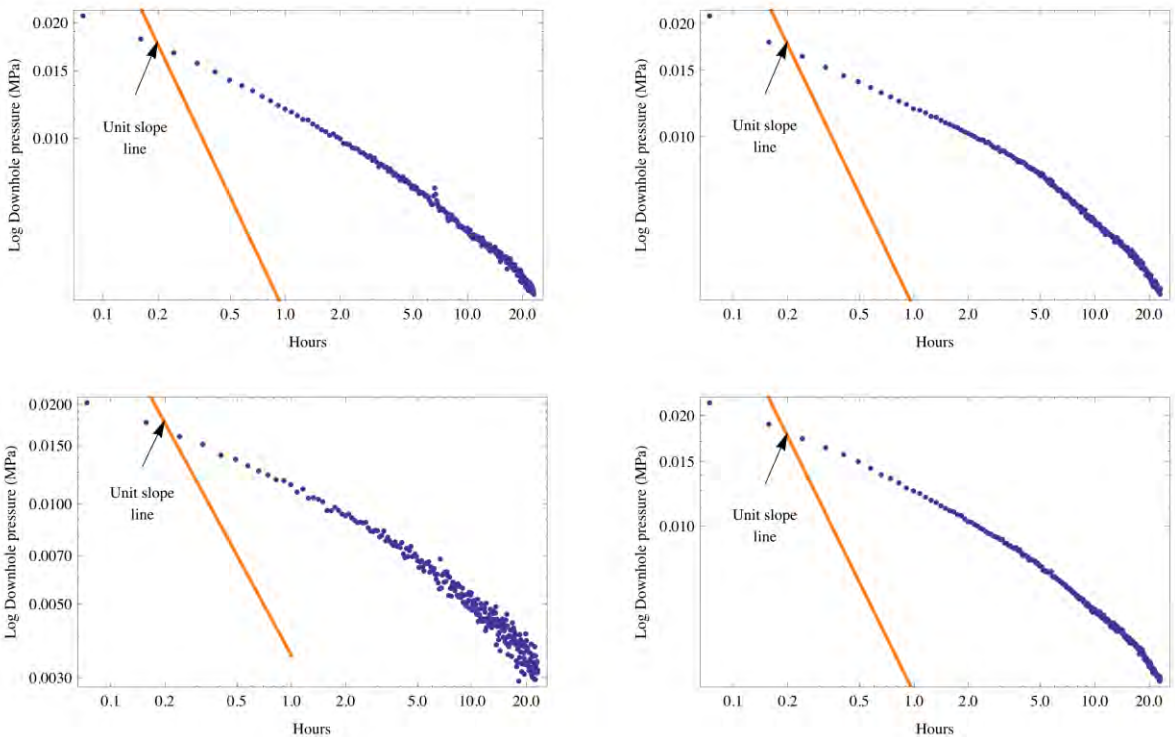

Figure 40: Log-log plot of ∆p vs. t after the first noble tracer injection for each of the four permanent gauges, see Horne (1995), Figure 2.11, page 25. This analysis confirms that the analysis is beyond wellbore storage effects.

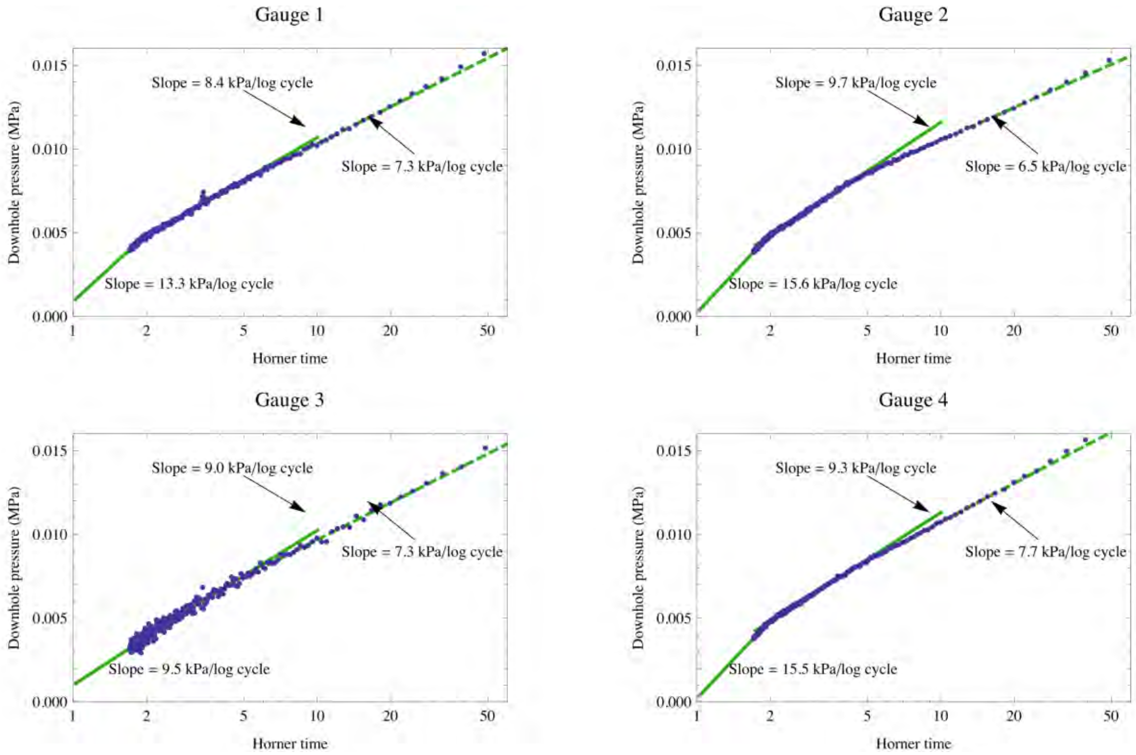

Figure 41: Horner plot of the pressure response during and after the first noble tracer injection period. Plots are for each of the four permanent gauges. The slope can be used to calculate permeability.

RST logging

Pulsed neutron RST (reservoir saturation tool) logs were run in CRC-2 on 7 July, 16 July and 22 August in the interval 1200m to 1455m MD. The tool was run from a Schlumberger logging truck (Figure 42) through the tubing (tool diameter: 43 mm = 1.71 inch) below the packer to measure the saturation in the 7 m perforated interval. Three measurement points were established, one at 100% water saturation, the second at 100% CO_2 saturation, and last at residual gas saturation. Prior to completion a baseline log was recorded in the cased borehole at 100% water saturation. This helps to analyse any variations caused by the completion. The tool's depth of investigation is 0.25 m (10 inch) and gives a detailed fluid saturation profile along the borehole, with 0.38 m (15 inch) vertical resolution. The tool was run in capture mode and at maximum logging speed of 183 m/hr (600 ft/hr) to log the hydrogen saturation accurately. Output from the three RST logs is summarised in Figure 43. In this figure, the blue shaded region is CO_2 saturation after CO_2 injection, the green shaded region is after water injection

Figure 42: (a) Schlumberger logging truck, and (b) the reservoir saturation tool (RST).

Three (3) RST runs were run in CRC-2 during this test. The first RST was run on 7th July 2011 to characterise the state of the water filled formation. As there was no pressure at the wellhead, this job was conducted using a standard packoff at surface. After the pure CO_2 was injected, a second RST run was conducted to log the CO_2 saturated formation. During this run, wellhead pressure was 2170 kPa and a lubricator with grease injection was rigged up for the job. This job incurred some 10 hrs of downtime due to rubber packing issues at the top of the lubricator that restricted free movement of the cable into the well. The job was successfully completed after rectification of the issue, but a significant amount of grease was introduced into the well system as a result of this run. A third RST run was completed on 22nd August 2011 to record the formation at residual state. A lubricator with grease injection was again used for this run due to the presence of 794 kPa wellhead pressure. The service company was requested to reduce the amount of grease they injected into the system.

In order to measure formation water saturation, the tool was run in sigma mode thus outputting formation neutron capture cross section, Sigma (SIGM) and thermal decay porosity (TPHI), which is a measure obtained from the ratio of the "Near to Far" detector capture count rates. The interpretation of the data is somewhat complicated by the fact that the TPHI computation from RST acquisition is well defined for conditions when fluid in the wellbore has a hydrogen index (HI) of ~1 but is not well defined for conditions when the fluid does not have a HI of 1. Although all efforts were made to ensure the presence of formation water around the tool between the dowhole packers, albeit a small dead zone in the annulus just below the top packer, for operational reasons this proved difficult to achieve and the post-CO_2 injection log was completed with CO_2 in the wellbore, which has a HI ≈ 0. Thus a shift was made to the TPHI log when CO_2 was in the borehole to account for the changed RST response in the near-tool region.

Due to the low salinity of the formation water (approx 800ppm), the TPHI output is used in preference to the SIGM output. Sigma and TPHI can both be used to invert for CO_2 saturation. Since the formation water is low (~ 800ppm), the change in Sigma could be prone to statistical errors. Thus TPHI is used for CO_2 saturation computation. Both outputs are however discussed below.

The results using the TPHI output are shown in Figure 43. The TPHI output responds to the hydrogen index in the formation. The log shows a small change in S_{gr}, within the perforation zone. It is noted that the formation is not 100% saturated after injection of pure CO_2 (blue curve) when driven to full saturation. It was observed that formation water re-entered the well pretty soon after the injection and this could be the reason why the saturation values are lower for the CO_2-saturated case. Residual state S_{gr} reads around 18% in the bottom half of the perforated interval and around 23% (average) in the top half.

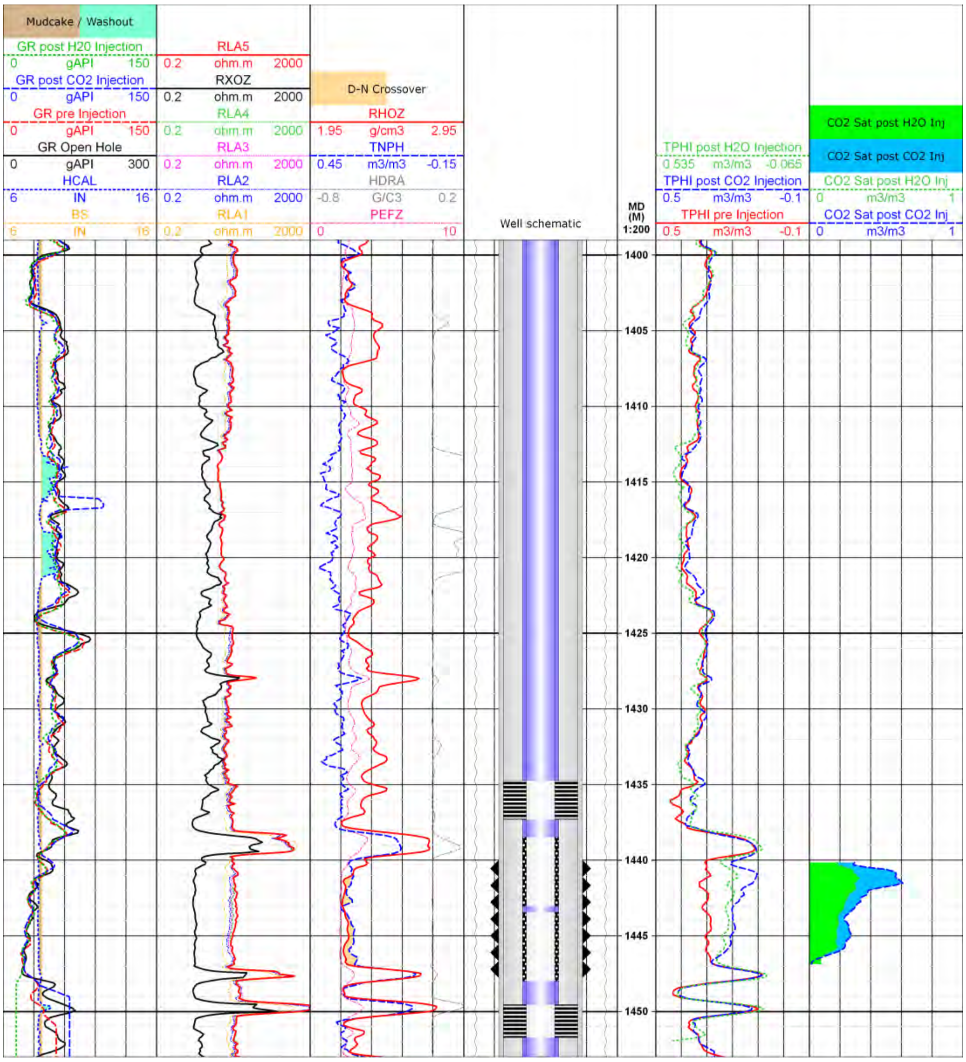

Figure 43: Comparing the three RST logs using TPHI output indicates that the CO_2 has displaced formation water over the interval from 1440 m to 1447 m. The blue shaded region is CO_2 saturation after CO_2 injection, the green shaded region is after water injection.

The results using SIGM output are shown in Figure 44. Residual S_{gr} reads around 20% on average in the perforated interval. As indicated earlier, due to the low salinity of the formation water, TPHI is preferred as a saturation measurement.

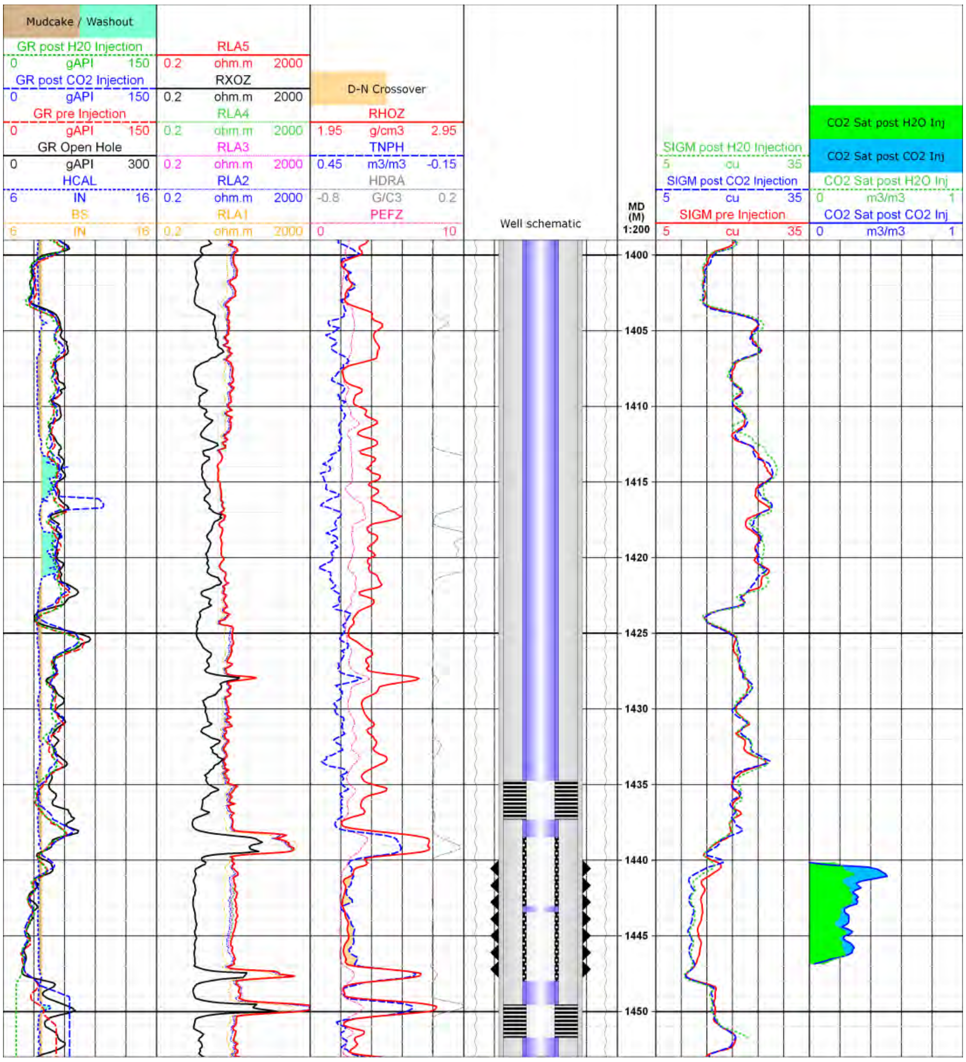

Figure 44: Comparing the three RST logs using SIGM output also indicates that the CO_2 has displaced formation water over the interval from 1440 m to 1447 m. The blue shaded region is CO_2 saturation after CO_2 injection, the green shaded region is after water injection.

The organic tracer test

Three reactive ester tracers (triacetin, tripropionin and propylene glycol diacetate) were identified and assessed in preliminary laboratory tests as potentially suitable for measuring residual saturation. This approach was pursued as there was concern that limited differences in the breakthrough profiles of the inert tracers would be observed (based on our general understanding of the chromatographic behaviour of krypton and xenon). This is further exacerbated by the difficulties in obtaining highly accurate and reproducible results from field experiments. The modelling of inert tracer behaviour is particularly sensitive to drift which may add further uncertainties to interpretation. The organic reactive tracers are designed to complement the other tests and the theory behind the reactive ester tracers is based on earlier work by Deans et al. (1971) who designed a series of experiments using ethyl acetate to determine from a single well test the residual oil saturation of an oil field. There are obvious similarities with their approach and our approach for the single well test at CRC-2.

All three ester tracers (30 kg total) are food grade liquids and were injected undiluted. The ester tracers were allowed to partially hydrolyse in the subsurface for 10 days. During water production 621 water samples (approx. 50-80 mL each) were collected and were immediately frozen on site using dry ice and were shipped to the National Measurements Institute in Perth for analysis. The initial results of the concentration breakthrough profiles for the parent tracers are given in Figure 45 and hydrolysis products of the parents tracer are given in Figure 46.

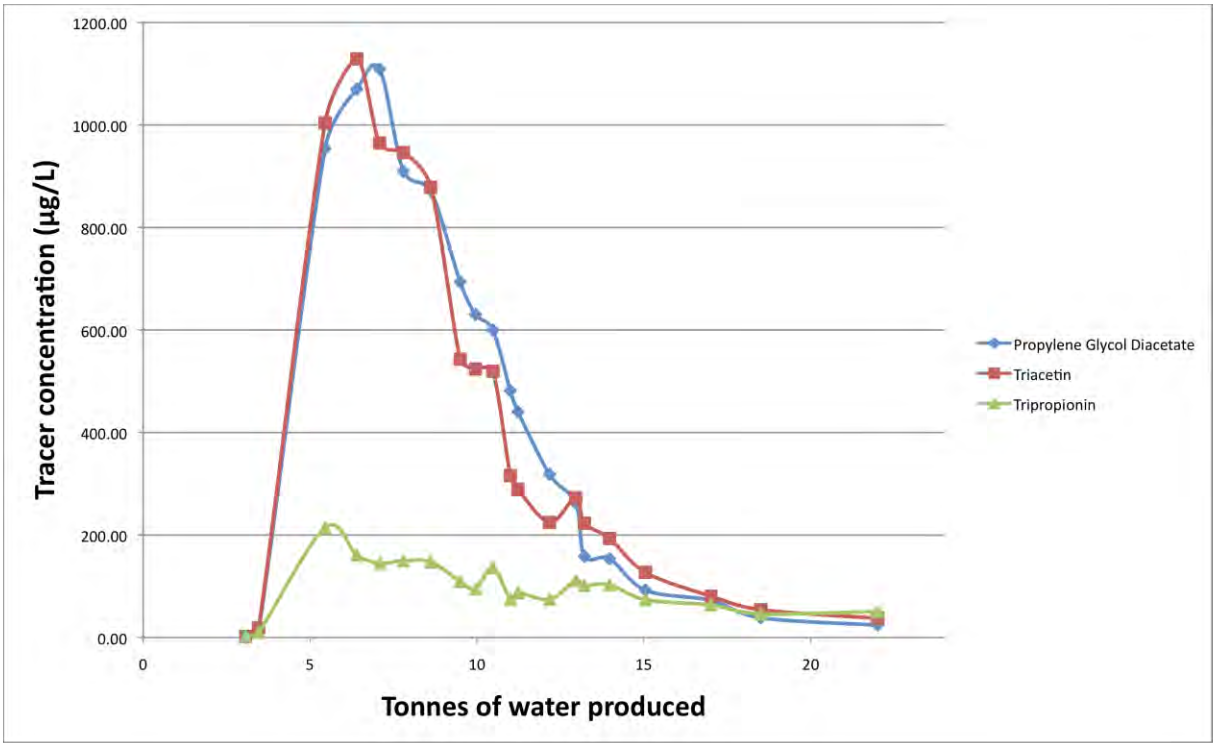

Figure 45: Parent tracer concentrations in the produced water during the organic tracer test.

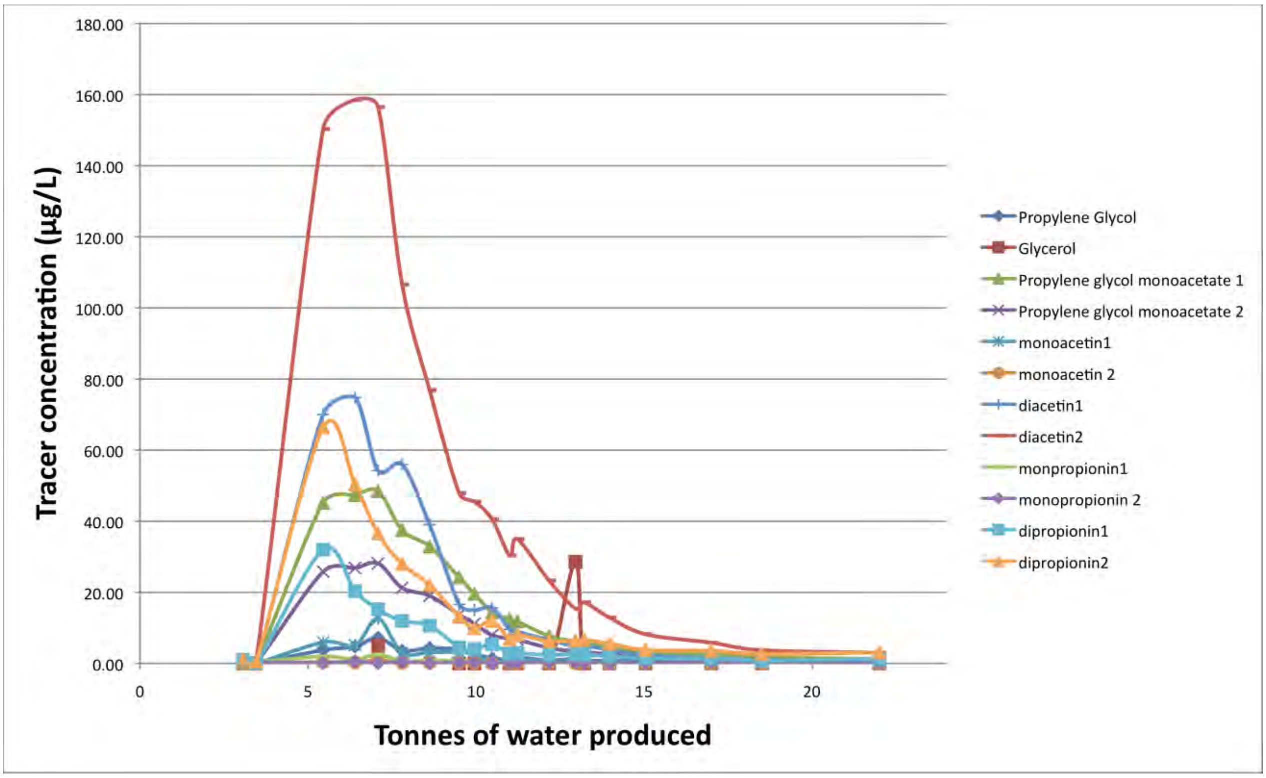

Figure 46: Products of the parent tracer concentrations in the produced water during the organic tracer test.

The analyses were conducted by a third party using standard chromatographic techniques explained in Myers et al. (submitted). The amounts of tracers in the samples were sufficiently high to be able to be analysed and in some cases required dilution. The results also confirmed the earlier calculations of kinetic behaviour where a 10-day soak period was preferred for an ideal mix of parent and daughter compounds proposed in Myers et al (submitted).

At this point, further samples were chosen to be analysed to fill in the early parts of the curves to better understand the arrival of the tracers at the start of water production. The results will be compared with our theoretical models that we have developed and presented in Myers et al. (submitted).

Using the data we will assess the best suite of compounds for calculating the residual CO_2 saturation for that part of the overall Stage 2B test.

The dissolution test

Following a period of injecting water without CO_2, the dissolution test measured the dissolved CO_2 during production. From the method in the original Bragg et al (1976) paper it was established that the measurement metric (XCO_2aq) had sensitivity primarily to one parameter: residual gas saturation, S_{gr}. Other parameters have only minor effect on the measured metric, as shown in Figure 47. It is estimated that the error associated with separating S_{gr} from other parameters is a value of 0.01 (absolute), as can be seen by observing the curves in Figure 48.

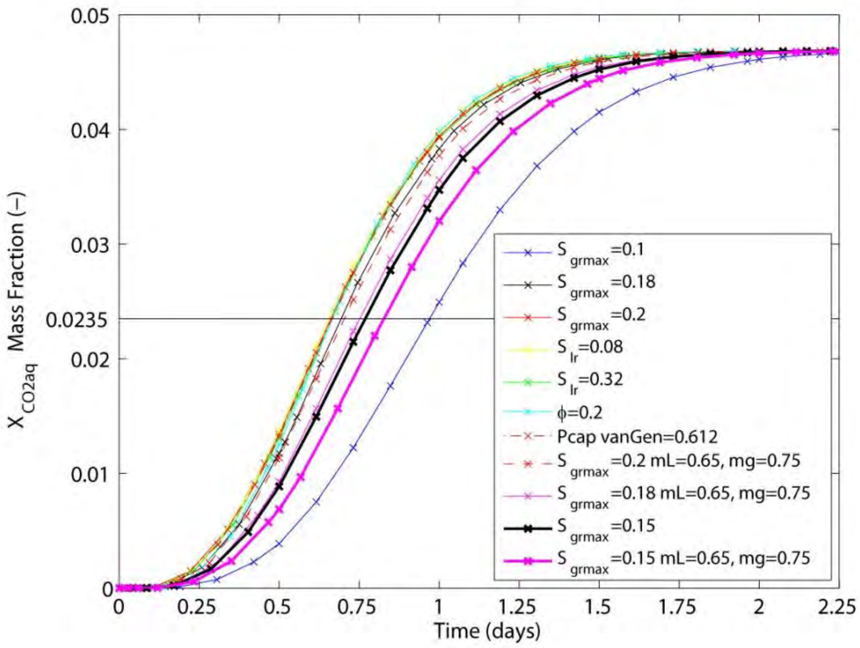

Figure 47: Mass fraction of dissolved CO_2 (XCO_2aq) versus production time, which is the data that will be used in the dissolution test. The sensitivity to various parameters is shown, and this indicates that S_{gr} is the parameter which has the greatest influence on XCO_2aq. The base case value of S_{gr} is 0.2. Note, a maximum mass fraction of 0.047 is equivalent to 1.07mol/L CO_2.

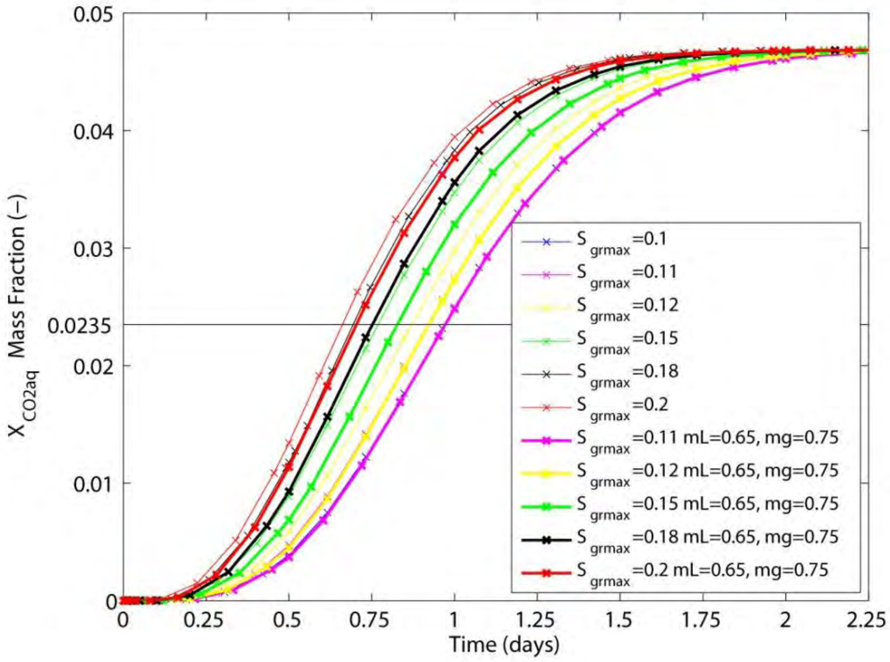

Figure 48: Curves as in Figure 47 except only selected cases are shown to indicate the error between two parameters S_{gr} and the van Genuchten parameter m. The error can be estimated at around 0.01, by comparing the S_{gr}=0.11 case which can be adjusted in other parameter m and overlap the case S_{gr}=0.11. The base case value of S_{gr} is 0.2.

For the test 75 tonnes of water without CO_2 were injected over 12 hours on the 9th of September 2011. Methanol was added to the injection water at a concentration of 0.1 vol% as a marker to estimate the aquifer drift during subsequent water production.

Formation water and its dissolved gas were sampled using the U-tube system, with (a) fluid samples taken under reservoir pressure (~140 bar) and (b) gas samples derived from the exsolved gas at reduced pressure (62 bar). U-tube samples were taken continuously approximately every 1.5 hours during the 62.5 hours of water production period leading to the collection of 40 samples. Water production commenced immediately after the injection of 75 tonnes of water and production was continuously at a rate of 49 tonnes per day (Figure 49).

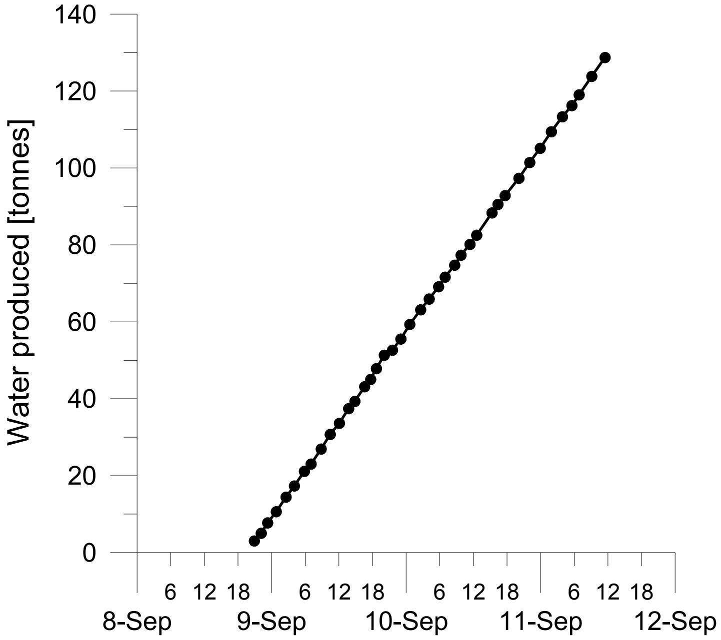

Figure 49: Water production and sampling times during the dissolution test.

Fluid samples were collected in two 150 ml stainless steel cylinders at reservoir pressure. One sample cylinder was used for the analysis of the dissolved inorganic carbon (DIC, DIC = ΣCO_2, HCO_3^-, CO_3^{2-}) concentration and its $\delta^{13}C$ and $\delta^{18}O$ isotopic composition. The other sample cylinder was used for general water properties (temperature, pH, salinity, alkalinity) analysed on site and for subsamples taken for the analysis of cations, anions and methanol at Geoscience Australia's laboratories.

The cylinder filled with formation water for DIC and isotopic analysis was connected to another cylinder filled with 100 ml of 0.5 M NaOH and valves were opened to allow the mixing of the two fluids. The aim was to make the sample fluid alkaline, so that all dissolved CO_2 is converted into CO_3^{2-}, which does not escape the fluid as CO_2 gas when pressure is reduced. The fluid from inside the two cylinders was collected over 15 to 20 minutes. DIC was analysed on site using the AS-C3 model by Apollo SciTech, which includes an infrared-based CO_2 detector (LiCor 7000). Carbonate was precipitated from solution by adding excess of SrCl leading to the formation of $SrCO_3$, which was filtered and dried in preparation for the carbon and oxygen isotopic analysis by isotope ratio mass spectrometry.

The second sample cylinder was opened and immediately depressurised. Temperature, pH and total dissolved solid concentration were measured by standard electrodes. Total alkalinity was determined by gran titration using 1 ml of sample, 0.02 M HCl as titration solution and a colour indicator. From every alternate cylinder, 4, 30 and 30 ml of fluid was subsampled for methanol, anion and cation analysis, respectively. The cation sample was acidified using 1 to 2 drops of concentrated HNO_3. Methanol was analysed by gas chromatography, anions by ion chromatography and cations were analysed by inductively coupled plasma optical emission spectrometry.

Gas samples were collected in Isotubes® and gas bags and analysed on site for CO_2, N_2, Kr and Xe on the gas chromatograph and quadrapole mass spectrometer (see Noble Gas section). Major ions, isotope and methanol sample analyses are still to be conducted, so only some preliminary analysis is reported here.

The dissolved inorganic carbon (DIC) concentrations show a clear pattern with a steep increase in concentration from the beginning to 26.9 tonnes of water production followed by relatively high concentrations to the end of the experiment (Figure 50). Concentrations range from 35 to 456 mmol / L DIC with significant variation from one sample to another suggesting variable loss of CO_2 during sampling despite the attempt to convert all CO_2 into CO_3^{2-}. The loss of CO_2 is also suggested by the difference between observed and predicted maximum CO_2 concentration. The CO_2 saturation concentration under reservoir conditions is close to 1000 mmol / L (see Fig. 46) and this concentration was expected once the plateau of high concentrations is reached. However, maximum measured concentrations of only ~450 mmol / L were achieved (Fig. 49). It appears the trend in DIC concentration follows the predicted pattern, but measured DIC concentrations underestimate the true value particularly in the high concentration range.

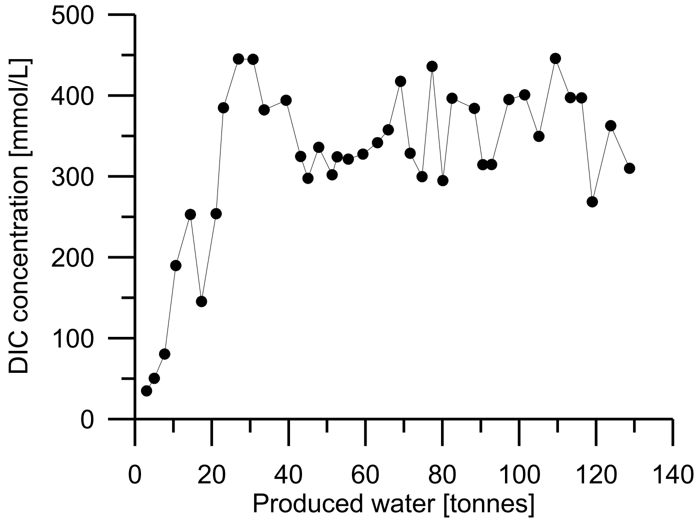

Figure 50: Measured dissolved inorganic carbon concentrations.

Total alkalinity is a measure for the buffering of excess positive charge resulting from the cation – anion balance in solution. Concentrations of HCO_{3-} (bicarbonate) and CO_3^{2-} (carbonate) usually determine total alkalinity and contribute to the DIC concentration. As the pH of the formation water of the Paaratte Formation water was consistently low with a value of approximately 5.6 (Figure 51), CO_3^{2-} would not stabilise. Consequently, total alkalinity represents the HCO_3^- concentration. Total alkalinity concentration shows an increase from 13 to 22 mmol / L during the course of water production (Figure 51). Such low concentrations demonstrate that HCO_3^- only contributes significantly to the DIC concentration at the beginning of the experiment.

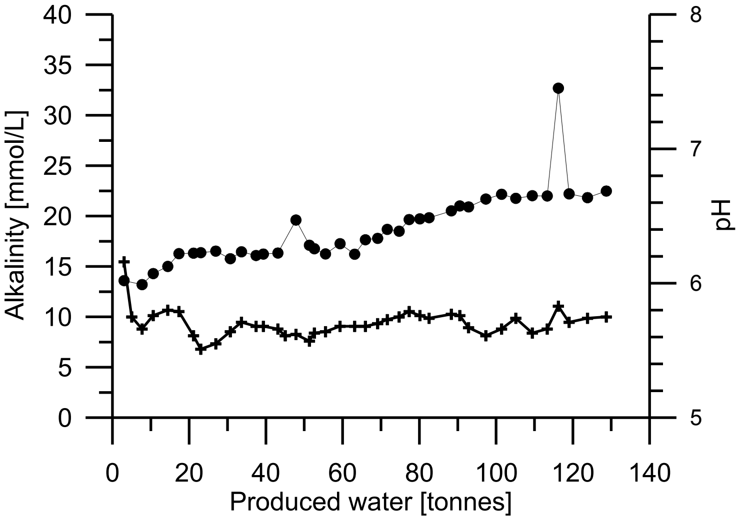

Figure 51: Measured pH (crosses) and total alkalinity concentrations (dots).

Exsolved CO_2 was collected at a pressure of 62 bar in a 4.7 litres stainless steel cylinder, which was initially filled with pure N_2. The gas mixture was sampled in an Isotube and the CO_2/N_2 ratio determined by gas chromatography. Similar to the DIC concentration curve, a steep increase in the CO_2/N_2 ratio is observed from the beginning to about 26.9 tonnes of water production followed by variable, but overall high values to the end of the experiment (Figure 52).

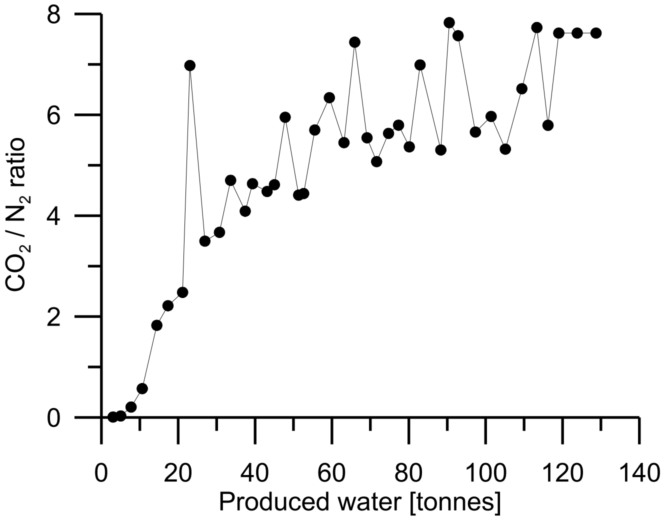

Figure 52: Measured CO_2/N_2 ratios after CO_2 exsolved from the fluid sample at 62 bar.

In order to quantify CO_2 concentrations in the gas and in the fluid phase from the observed CO_2/N_2 ratio in the gas, the following procedure was applied:

The initial N_2 amount in the stainless steel cylinder is 0.0446 mol/L (=$N2_{tot}$). As the N_2 solubility is << 0.0446 mol/L at 62 bar and 60 ^{0}C (formation water temperature), the $N2_{gas}$ concentration is calculated as

$$N2_{gas} = N2_{tot} - N2_{fluid}$$

with $N2_{fluid}$ being assumed to be the solubility concentration as calculated according to Mao and Duan (2006) and the N_2 partial pressure calculated as

$$pN2 = 62 \cdot \frac{N2}{CO2}$$

$CO2_{gas}$ can now be calculated from $N2_{gas}$ as

$$CO2_{gas} = N2_{gas} \cdot \left(\frac{CO2}{N2} \right)$$

$CO2_{fluid}$ can be calculated independently using Henry's law according to

$$CO2_{fluid} = \frac{pCO2}{k_H}$$

with pCO_2 being the CO_2 partial pressure and K_H being the Henry constant. As the latter is temperature dependent, K_H needs to be corrected according to

$$k_H(T) = k_H(T^0)\exp\left[-C\left(\frac{1}{T} - \frac{1}{T^0} \right) \right]$$

resulting in $K_H(60^0C) = 76.15$.

We know the solubility at reservoir conditions is at or just below 1 mol/L CO_2 (see Figure 47), which should equal the sum of $CO2_{gas}$ and $CO2_{fluid}$ in our calculations. This is indeed calculated for the period of overall high CO_2 concentrations starting at about 30 tonnes of produced water (Figure 53).

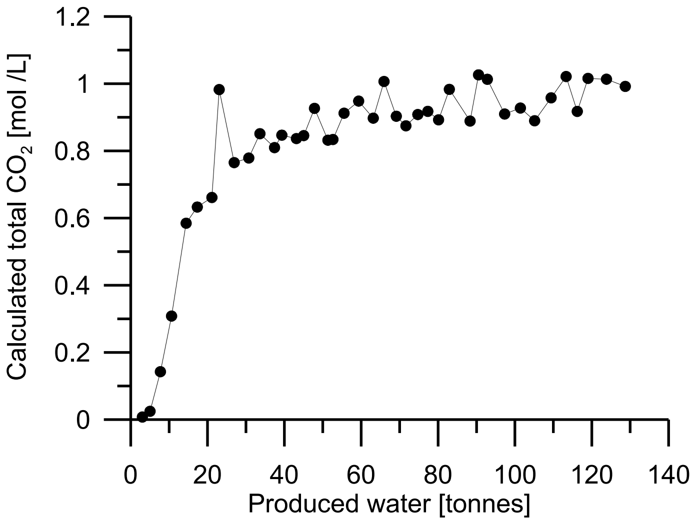

Figure 53: Calculated sum of CO_2-gas and CO_2-fluid concentrations.

The good match between theoretical and calculated values based on measurements is a promising result, yet, it is only preliminary as assumptions, eg a fluid-gas equilibration temperature of 60^0C, need to be tested and confirmed. The final total CO_2 concentration curve will then be used to estimate the residual gas saturation according to Bragg et al. (1976).

Laboratory core testing

As an adjunct to the field testing, a core sample from the injection interval in the CRC-2 well was provided to a team in the Department of Energy Resources Engineering, Stanford University, Stanford, California, USA (Krevor et al. 2011). This was from a vertical core cut from 1441.43 – 1441.53 mKB, so about 1.5m down from the top of the injection interval. They recorded that the sandstone sample is well sorted but otherwise texturally submature with no apparent cementing material and little clay. The sample had several low-porosity bedding planes perpendicular to the direction of flow in their experiments (equivalent to vertical flow in the reservoir). Outside of these zones, the porosity ranged between 0.28-0.29. They noted that the sample was similar in morphology and component composition to a Berea sandstone that was also included in their testing. They also tested two other rock types from different locations. The Stanford measurements are plotted in Figure 54.

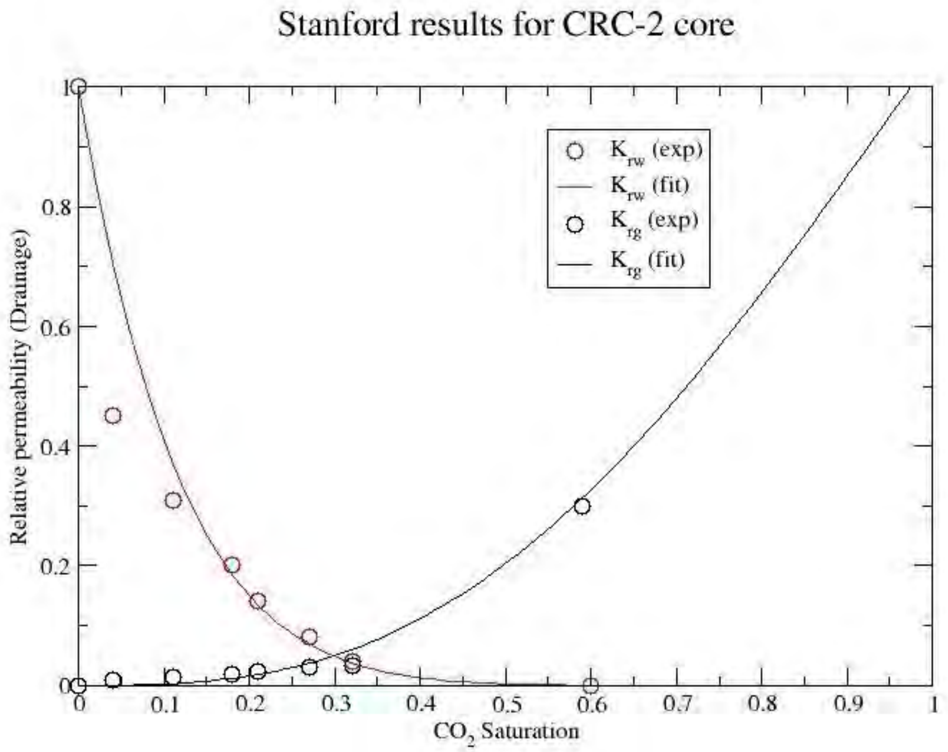

Figure 54: Drainage CO$_2$ (black circles) and water (red circles) relative permeability data for the CRC-2 sample. Solid lines are best-fit Brooks-Corey curves with best-fit parameters (Krevor et al. 2011).

The fitted functional forms for the relative permeability curves were as follows:

$$K_{r,w} = (S_w^*)^{N_w}$$

$$K_{r,CO2} = K_{r,CO2}(S_{wi})(1-S_w^*)^2(1-(S_w^*)^{N_{CO2}})$$

where

$$S_w^* = \frac{S_w - S_{wi}}{1 - S_{wi}}$$

S_w is the water saturation, $K_{r,w}$ is the relative permeability to water, $K_{r,CO2}$ is the relative permeability to CO_2, S_{wi} is the residual water saturation and N_w and N_{CO2} are numerical exponents. The fitted parameters were S_{wi}=0.05, $K_{r,CO2}(S_{wi})$=0.95, N_w=8 and N_{CO2}=2.

It was found that maximum saturation and permeability observed in this CO_2/water system should not be taken as endpoint unless a sufficiently high capillary pressure was obtained. Thus in the data shown from the core flood, the apparent maximum CO_2 saturation of 0.6 is not representative of reservoir conditions, and the fitted forms are used to extend the relative permeability curves to higher saturations.

Since the initial CO_2 saturation over the core varies due to heterogeneity, one can also plot the residual CO_2 saturation against the initial CO_2 saturation. Figure 55 shows the two curves that were fitted to the experimental data, which indicate that the residual CO_2 saturation can be low if the initial CO_2 saturation is also low. The Land curve is fitted to the functional form

$$S_{CO2,r} = \frac{S_{CO2,i}}{1 + CS_{CO2,i}}$$

where $S_{CO2,r}$ is the residual CO_2 saturation and $S_{CO2,i}$ is the initial CO_2 saturation. Here the fitted value for the Land coefficient C was 1.3. The other functional form due to Spiteri is

$$S_{CO2,r} = \alpha S_{CO2,i} - \beta S_{CO2,i}^2$$

where the fitted coefficients were α=0.86 and β=0.53.

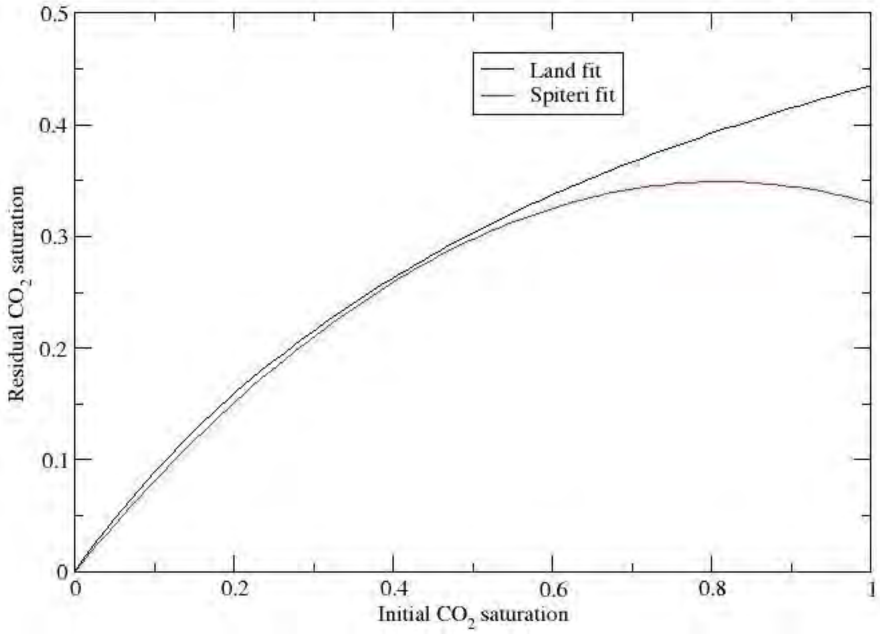

Figure 55: Two fitted functional forms for the relationship between initial CO_2 saturation and residual CO_2 saturation in the core flooding experiment, Red curve: Spiteri curve. Black curve: Land curve (for parameters see text).

Atmospheric monitoring

As part of the Otway Stage 1 monitoring, CSIRO has monitored atmospheric concentrations of CO_2 at a station some 700 m NNE of CRC-1. Fluxes of CO_2 were also measured at a separate instrument to the W of this station. As the instrumentation evolved, continuous measurements of CH_4 and $^{13}CO_2$ were added to the suite, all made with Picarro spectrometers. Flask samples were also taken at intervals and transported back to the laboratory for measurement of trace compounds, chiefly SF_6 which was added to the injection stream at CRC-1.

Some four years' worth of data has been accumulated but only one global calibration of the system was possible, based on emissions detected from the diesel engines used for the drilling of CRC-1. Originally it was expected that considerable amounts of Buttress gas would be vented during the water-lift phase of Stage 2B, and it was planned to use these emissions as a test of the sensitivity of the atmospheric monitoring to distant leaks of CO_2. In preparation for this, a second Picarro was installed at the Visitors' Centre at Otway, so that down-wind and up-wind measurements could be made during periods of SSW winds that would carry emissions from CRC2 towards the atmospheric monitoring tower.

Separately, a technique for localising CO_2 leaks has been developed by CO2CRC researchers, using an array of CO_2 sensors. The sensors used are of much lower quality than those used by CSIRO at Otway, but are cheaper. The array technique has been demonstrated at the CO2CRC test site at Ginninderra (developed by Geoscience Australia). The Ginninderra array was upgraded, which each sensor being made autonomous in power and communications, and deployed to Otway for the expected releases during Stage 2B.

Figure 57 shows the location of the CO_2 sensors used during these experiments. Figure 58 shows the CSIRO tower, in which the inlets for the sensors are located, and Figure 56 shows an example of an autonomous sensor from the array.

In the event, very little Buttress gas was needed for the water lift and this phase of Stage 2C did not provide the controlled release that was needed, either to calibrate the Stage 1 atmospheric monitoring or to test the array method. Accordingly a dedicated controlled release was carried out during the organic tracer soak test, 29th August – 5th September, at a rate of 9 tonnes per day. Since releases were only carried out during the working day, about 3 tonnes were released each day. Unfortunately this week was marked by sustained westerly winds, so that releases rarely reached the sensors. Based on wind forecasts, further more successful releases were carried out on the 18th (11am to 5pm) 23rd, 24th, 25th and 28th Sept from 8am to 5pm. In addition, emptying the pure CO_2 tank on site happened to coincide with southerly winds, adding a further datum. Figure 59 shows an example of released Buttress gas being detected at one of the array sensors. A considerable volume of data was collected, both continuous data from the fixed sensors and the arrays, and data from snapshot flask samples. This is now being worked up, in conjunction with the continuous meteorological data that are also gathered at the site. The overall carbon footprint of the exercise was approximately equivalent to 4 passenger-round-trips from Australia to Europe.

Figure 56: Autonomous CO_2 sensor deployed at Otway. The Stage 2B CO_2 tank is in the background. At times the cows provide a detectable source of methane.

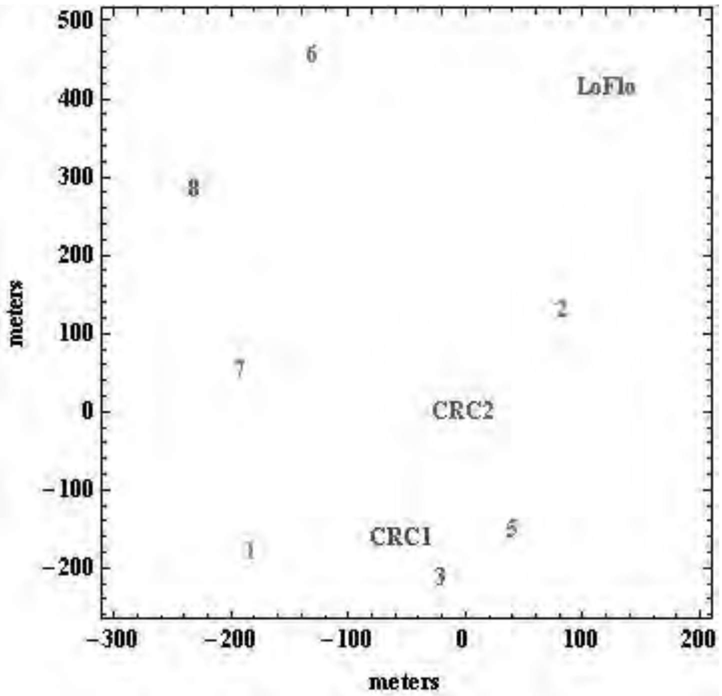

Figure 57: Map showing the location of the autonomous sensors (numbered). The “LoFlo” is the location of the permanent CSIRO sensor, and sensor 6 is located at the CSIRO flux tower.

Figure 58: The CSIRO flux tower; the LoFlo tower and its sea container are visible in the background at the end of the fence.

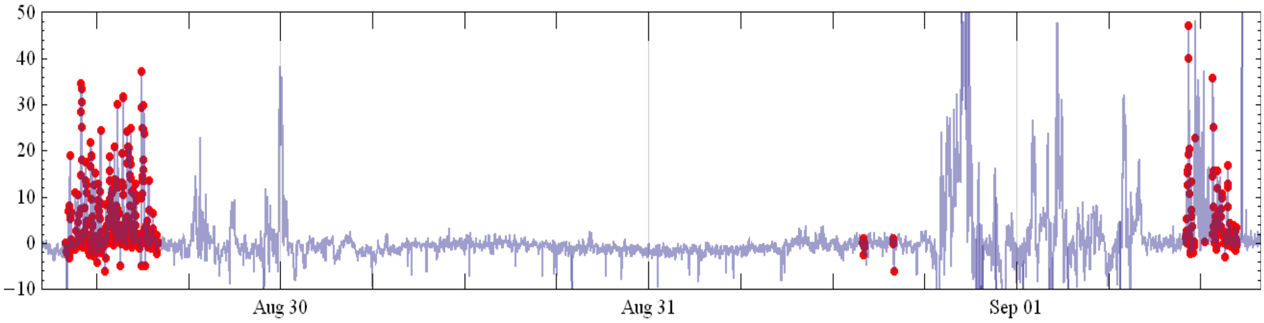

Figure 59: Data from autonomous sensor #3, located about 140 m from the release point. The continuous curve is the CO_2 concentration above background; red points mark times when the wind was in the correct direction to blow released gas to the sensor. There are large excursions around background at night-time (start-of-day on the time axis) because of light winds and ecosystem respiration.

Future work

This report has primarily been concerned with providing a description of the Otway Stage 2B field test conducted in 2011 and the data acquired during the testing. Further work is planned to provide a detailed analysis of the data and give recommendations on methods for field-scale residual saturation relevant to future large-scale commercial projects, especially those that have residual trapping as a major component of the storage volume.

The first stage of data analysis involves detailed quality control and compilation of the data. This includes examining noise and drift in the gauges, synchronising time records, labelling operational events and checking fluid sampling protocols. Units need to be standardised and calibration needs to be checked. For instance, gauge readings of water flow need to be checked for consistency with water volumes in the storage tanks. (Experience from Otway Stage 1 shows the pitfalls of premature reporting).

Uncertainties to be resolved are the region invaded by the injected carbon dioxide as it moved up under buoyancy and the effects of heterogeneity. Information on heterogeneity can be obtained from the initial inorganic tracer injection, and there are established methods in the literature to do this (Ronayne et al. 2010). Hence this will be an important initial part of the data analysis that will feed into the other components.

With the basic parameters established it will then be possible to analyse each of the independent test methods.

1. The pressure test will be modelled using the TOUGH2 and iTOUGH software based on Zhang et al. (2011).
2. Results from the hydrogen index using a pulsed neutron log (RST) are already available, but the calibration will be re-examined.
3. The thermal test will be analysed by plotting the temperature decay after heating using a Horner-style plot, the equivalent of pressure transient analysis in well testing, as well as fitting to non-isothermal simulation results. We will also use models for the effective thermal conductivity of two-phase systems (Xu and Desbrandes 1991, Ashworth 1992).
4. The organic tracer test analysis will be based on Tomich et. al (1973), Sheely (1978), Ptak et al (2004), Huang et al. (2010) and will be supplemented with numerical modelling.
5. The dissolution test analysis will be based on Bragg et al (1976), Sahloul et al. (2002), Parker and Park (2004) and Pan et al. (2007) and will be supplemented with numerical modelling.

Preliminary analysis of the data shows that wellbore volumes and phase movements will need to be included for a full analysis of the reservoir. Also thermal effects will need to be included in a complete analysis as the density of carbon dioxide depends on temperature.

It is planned to release the Final Report on Otway Stage 2B in July 2012, followed by conference and journal publication of various components in the manner of Otway Stage 1.

Conclusions

1. The field tests for Stage 2B of the CO2CRC Otway Project commenced on 17 June 2011 and finished on 12 September 2011, a total duration of 88 days. All the planned components of the field test were completed including the five methods for measuring residual trapping.

2. Excellent quality downhole pressure data were acquired throughout the field program from the permanent gauges. These gauges are more accurate than the excellent memory gauges used in the Stage 1 injection in the Waarre formation. The high permeability of the injection interval did not cause problems with getting a sufficient pressure response to give a good signal to noise ratio.

3. Excellent downhole temperature data were also acquired. The instantaneous readout of downhole temperatures proved extremely useful in diagnosing operational issues at several stages. Elements of the temperature records will take some effort to interpret due to persistent heat responses.

4. All three RST logs were run as intended. Two of the logs were run in a standard water environment, the other log was when CO_2 was in the tubing hence was run in a CO_2 environment. The latter log will require some additional considerations for a complete interpretation. Current interpretation has residual CO_2 saturation around 0.18 in the lower half of the perforated interval and around 0.23 (average) in the upper half.

5. Problems with the original gas-lift design where found when gas-lift was first attempted. This would have led to production flow rates that were too high leading to limitations on the number of fluid samples that could be obtained for the planned production volumes. The flow rate problem was solved by inserting an orifice plate at the surface. Resolving this problem caused a delay early in the test sequence.

6. Fluid sampling was completed consistent with the test plan. The noble and organic tracers were added to the injection stream as planned.

7. The reactive ester tracer test has not been conducted before in the field. The concentrations of ester tracers added were more than sufficient to be detected by standard chromatographic methods. The results to date show the partial breakdown of the three parent compounds (triacetin, tripropionin and propylene glycol diacetate). The 10-day soak period was a good fit with the theoretical breakdown kinetics. Further work will be done to fill in more data points and begin the interpretive stage of the work.

8. Sampling for the dissolution test including the added methanol was performed as intended.

9. BTEX above drinking water levels was found in the surface water. This was caused by the Buttress gas used in the gas-lift. The BTEX was removed through additional filtration although this led to a delay in the middle section of the test program.

10. Despite initial testing, it proved difficult to control the low CO_2 flow rates that were required when injecting water with dissolved CO_2. Modifications led to delays, and although the problem was largely controlled, difficulties did persist during the shorter injection intervals.

11. Experience with the Stage 2B testing shows that it would be helpful in future work to have a more detailed well model that takes into account two-phase flow movement within the casing. “Off-the-shelf” software may have problems correctly implementing CO_2 properties in the vicinity of the critical point, and a code comparison study of wellbore flow codes would be useful.

12. Although not primary objectives of Stage 2B, the test sequence provided the opportunity to further test microseismic monitoring and provide controlled releases of CO_2 for atmospheric monitoring. Both of these activities generated useful results. The test also provided experience with a column of CO_2 in the injection well as opposed to the CO_2-rich Buttress gas used in Otway Stage 1.

References

Ashworth, E. (1992) The variation of the thermal conductivity of tuff with moisture: Experimental results and proposed model, Proc 33rd US Symposium on Rock Mechanics, Santa Fe, 3–5 June, Balkema, Rotterdam, pp. 859–868.

Bennion, B. and Bachu, S. (2005) Relative permeability characteristics for supercritical CO_2 displacing water in a variety of potential sequestration zones in the Western Canada Sedimentary Basin, SPE 95547, SPE Annual Technical Conference and Exhibition held in Dallas, 9–12 October.

Bragg, J. R., Shallenberger, L. K. and Deans, H. A. (1976) In-situ determination of residual gas saturation by injection and production of brine, SPE 6047, 51st Annual Fall Technical Conference of the Society of Petroleum Engineers, New Orleans, 3–6 October.

Earlougher, R. J. (1977) Advances in Well Test Analysis. SPE, Richardson, Texas

Freifeld, B. M., Finsterle, S., Onstott, T. C., Toole, P. and Pratt, L. M. (2008) Ground surface temperature reconstructions: Using in situ estimates for thermal conductivity acquired with a fiber-optic distributed thermal perturbation sensor. Geophysical Research Letters, vol. 35, no. 14, article number L14309

Horne, R. N. (1995) Modern Well Test Analysis. Petroway, Palo Alto, California, 2 ed.

Huang, J., Christ, J. A. and Goltz, M. N. (2010) Analytical solutions for efficient interpretation of single-well push-pull tracer tests, Water Resources Research, vol. 46, W08538.

IPCC (2005) IPCC special report on carbon dioxide capture and storage: Special Report of the Intergovernmental Panel on Climate Change. Cambridge University Press, London.

Krevor, S. C. M., Pini, R., Zuo, L. and Benson, S. M. (2011) Relative permeability and trapping of CO_2 and water in sandstone rocks at reservoir conditions. Water Resources Research, submitted.

Mao, S. D. and Duan, Z. H. (2006) A thermodynamic model for calculating nitrogen solubility, gas phase composition and density of the H_2O-N_2-NaCl system. Fluid Phase Equilibria, vol. 248, no. 2, pp. 103-114. See also http://calc.geochem-model.org/Pages/Solubility.aspx

Pan, C. Dalla, E., Franzosi, D. and Miller, C.T. (2007) Pore-scale simulation of entrapped non-aqueous phase liquid dissolution," Advances in Water Resources, vol. 30, pp. 623–640.

Parker, J.C. and Park, E. (2004) Modeling field-scale dense nonaqueous phase liquid dissolution kinetics in heterogeneous aquifers, Water Resources Research, vol. 40, p. W05109.

Ptak, T., Piepenbrink, M. and Martac, E. (2004) Tracer tests for the investigation of heterogeneous porous media and stochastic modelling of flow and transport – a review of some recent developments, Journal of Hydrology, vol. 295, pp. 122–163.

Ronayne, M. J., Gorelick, S. M., and Zheng, C. (2010) Geological modeling of submeter scale heterogeneity and its influence on tracer transport in a fluvial aquifer, Water Resources Research, vol. 46, W10519.

Sahloul, N.A., Ioannidis, M.A. and Chatzis, I. (2002) "Dissolution of residual non-aqueous phase liquids in porous media: pore-scale mechanisms and mass transfer rates, Advances in Water Resources, vol. 25, pp. 33–49.

Sheely, C.Q. (1978) Description of field tests to determine residual oil saturation by single-well tracer methods, Journal of Petroleum Technology, vol. 30, pp. 194–202.

Tomich, J. F., Dalton Jr., R. L., Deans, H. A. and Shallenberger, L. K. (1973) Single-well tracer method to measure residual oil saturation, Journal of Petroleum Technology, vol. 25, no. 2, pp. 211–218, 1973.

Xu, H. and Desbrandes, R. (1991) Formation evaluation using in-situ measurements of formation thermal properties, The Log Analyst, vol. 32, no. 2, 144-157.

Zhang, Y., Freifeld, B., Finsterle, S., Leahy, M., Ennis-King, J., Paterson, L. and Dance, T. (2011) Single-well experimental design for studying residual trapping of supercritical carbon dioxide, International Journal of Greenhouse Gas Control, vol. 5, pp. 88–98.

Appendix

Figure 60. Paaratte formation well composite with log porosity, permeability, core porosity and lithology characterisation.

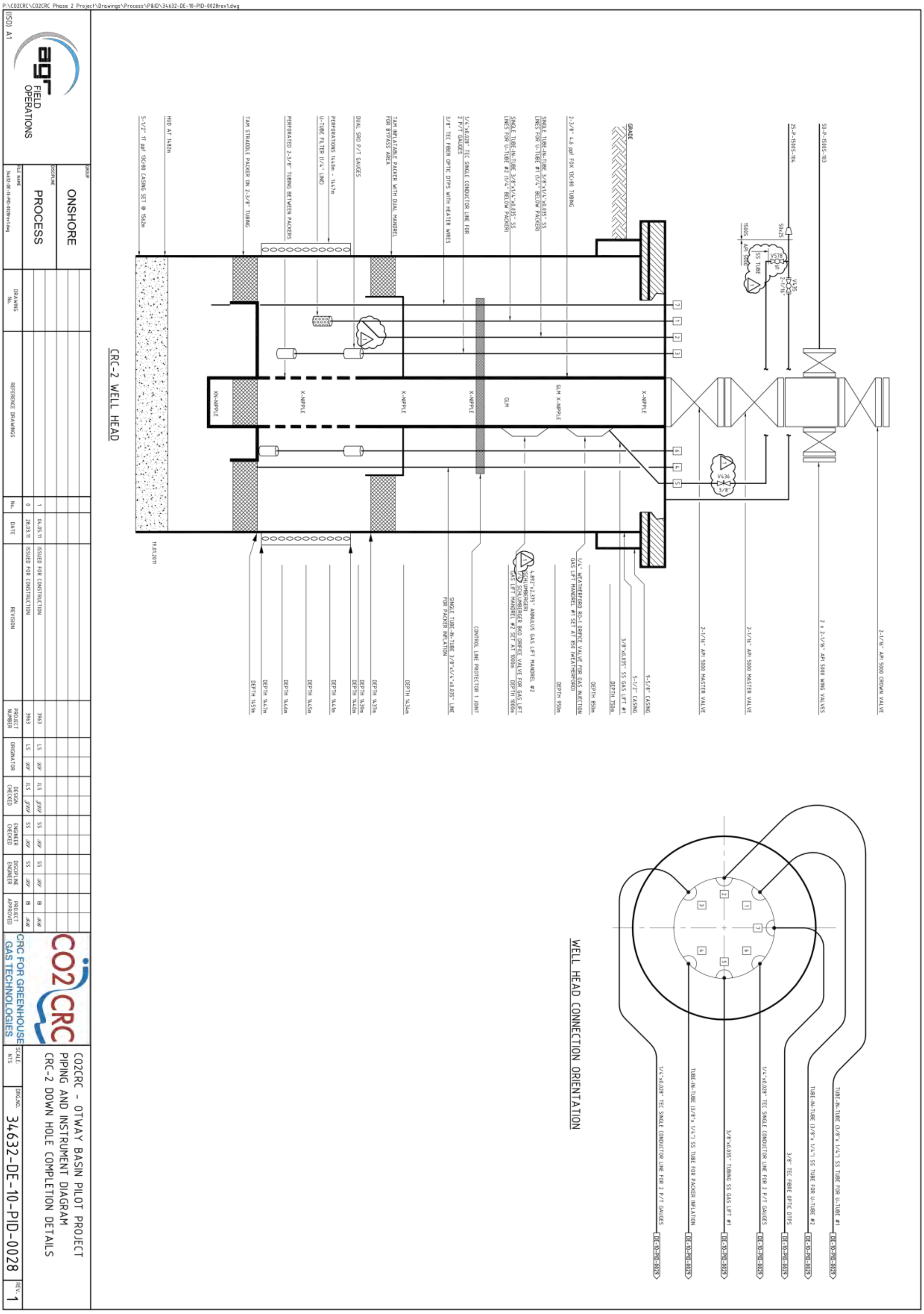

Figure 61. CRC-2 downhole completion details.

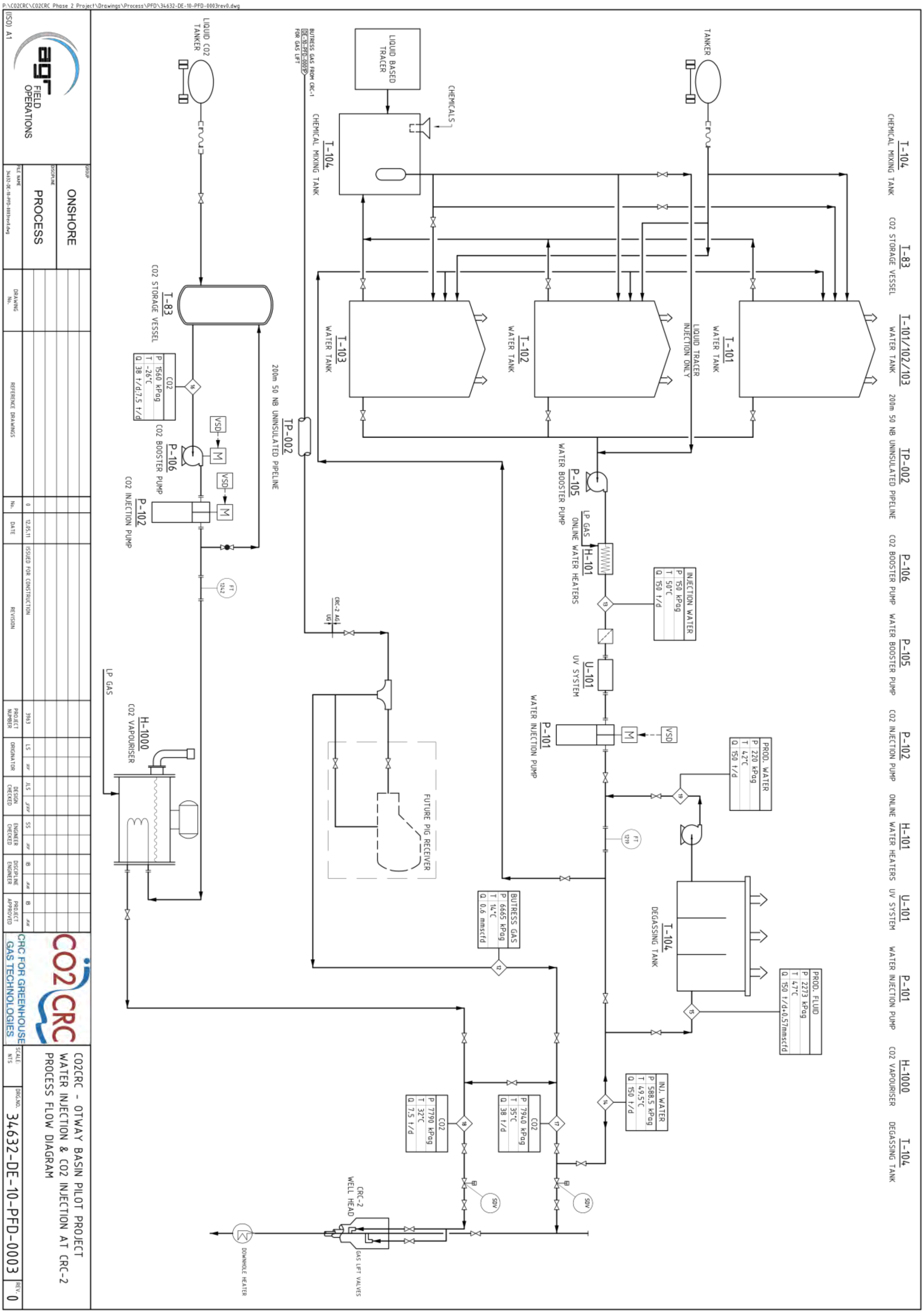

Figure 62. Water injection and CO$_2$ injection at CRC-2 process flow diagram.

Figure 63. Photograph of the CRC-2 site facility.

CONTACT US

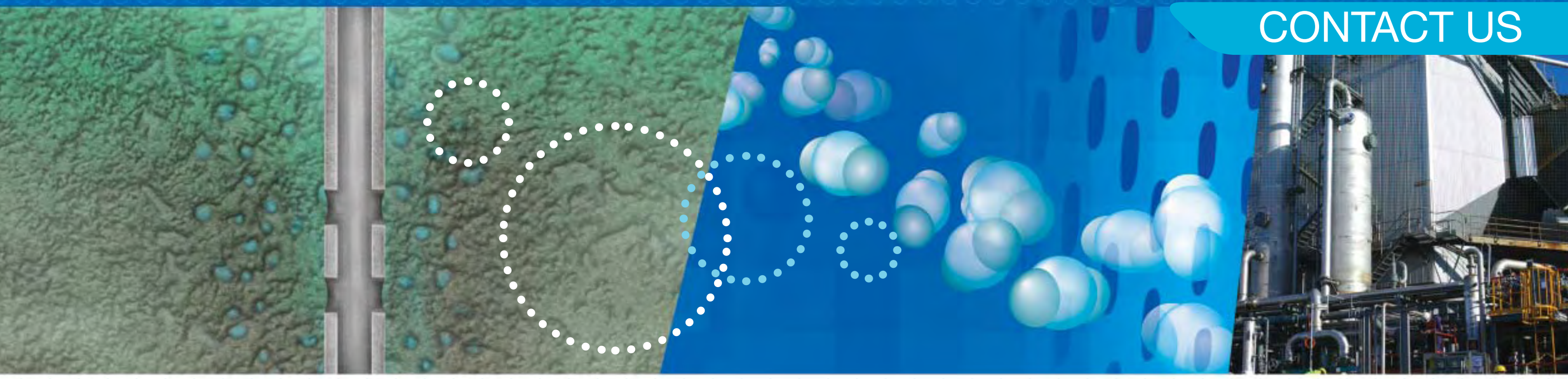

Canberra

Dr Richard Aldous
Chief Executive
GPO Box 463, Canberra, ACT 2601
Ph: + 61 2 6120 1600
Fax: + 61 2 6273 7181
Email: raldous@co2crc.com.au

Ms Carole Peacock
Business Manager
GPO Box 463, Canberra, ACT 2601
Ph: + 61 2 6120 1605
Fax: + 61 2 6273 7181
Email: cpeacock@co2crc.com.au

Melbourne

Dr Matthias Raab
Program Manager for CO_2 Storage
School of Earth Science
The University of Melbourne
VIC 3010
Ph: +61 3 8344 4309
Fax: +61 3 8344 7761
Email: mraab@co2crc.com.au

Mr Barry Hooper
Chief Technologist
Room 232/Level 2
School of Electrical & Electronic
Engineering, The University
of Melbourne, VIC 3010
Ph: + 61 3 8344 6622
Fax: + 61 3 9347 7438
Email: bhooper@co2crc.com.au

Mr Rajindar Singh
Otway Project Manager
School of Earth Science
The University of Melbourne
VIC 3010
Ph: + 61 3 8344 9007
Fax: + 61 3 8344 7761
Email: rssingh@co2crc.com.au

Sydney

Prof Dianne Wiley
Program Manager for CO_2 Capture
The University of New South Wales
UNSW Sydney, 2052
Ph: + 61 2 9385 4755
Email: dwiley@co2crc.com.au

Adelaide

Prof John Kaldi
Chief Scientist
Australian Schtool of Petroleum
The University of Adelaide, SA 5005
Ph: + 61 8 8303 4291
Fax: + 61 8 8303 4345
Email: jkaldi@co2crc.com.au

Perth

Mr David Hilditch
Commercial Manager (CO2TECH)
PO Box 1130, Bentley
Western Australia 6102
Ph: + 61 8 6436 8655
Fax: + 61 8 6436 8555
Email: dhilditch@co2crc.com.au

researching carbon capture and storage